University of Southern Queensland

Faculty of Engineering and Surveying

Effect of Epoxy Repairing on Girders Shear Strengthened with External Post Tensioning

A dissertation submitted by

Murshedul ALAM

In fulfillment of the requirements of

Courses ENG 4111 and ENG 4112 Research Project

Towards the degree of

Bachelor of Engineering (Civil)

Submitted: October 2004

ABSTRACT

Every year numerous concrete girder bridges are damaged by overweight vehicles. When this happens, bridge engineers are faced with numerous questions relative to the behavior and strength of the bridge. These questions must be answered, so decision can be made concerning traffic restrictions and future maintenance of the actions. External post-tensioning is an effective technology to upgrade and strengthen existing structures whereas epoxy resins usually are used as a treatment in a cracked structure. The focus of this work is on the behavior and effectiveness of external post-tensioning for shear strengthening of bridge girders with epoxy repairing.

This study examines four-point loading in four rectangular beams; one control beam and the others are constructed to simulate the effect of external post-tensioning repaired with epoxy resins on girders. Four beams are 2500 mm in length with supports of 2000 mm apart. Experimental studies are performed on four beams to develop basic understanding of the shear behavior. Tests are then extended on four girders and experimental results for the failure loads show different features.

This study first reviews failure mode including delamination with the use of external post-tensioning to rehabilitate various concrete structures and discusses methodologies used to characterize the failure processes of the system. Physical models of reinforced concrete beams are precracked, then retrofitted with epoxy and post tensioned and tested in an experimental program. Strengths are shown to increase with the strengthening technique of external post-tensioning and the addition of epoxy resin, the specimens are observed to fail through a similar type of mechanism. Parameters affecting these failure modes are discussed, and techniques used in the analysis of these modes are reviewed. Results of this review are used to make recommendations for future work in the understanding of shear strengthening by external post-tensioning with epoxy repairing of concrete structures.

.

University of Southern Queensland

Faculty of Engineering and Surveying

ENG4111 & ENG4112 *Research Project*

Limitations of Use

The Council of the University of Southern Queensland, its Faculty of Engineering and Surveying, and the staff of the University of Southern Queensland, do not accept any responsibility for the truth, accuracy or completeness of material contained within or associated with this dissertation.

Persons using all or any part of this material do so at their own risk, and not at the risk of the Council of the University of Southern Queensland, its Faculty of Engineering and Surveying or the staff of the University of Southern Queensland.

This dissertation reports an educational exercise and has no purpose or validity beyond this exercise. The sole purpose of the course pair entitled "Research Project" is to contribute to the overall education within the student's chosen degree program. This document, the associated hardware, software, drawings, and other material set out in the associated appendices should not be used for any other purpose: if they are so used, it is entirely at the risk of the user.

Prof G Baker
Dean
Faculty of Engineering and Surveying

CERTIFICATION

I certify that the ideas, design and experimental work, results, analyses and conclusions set out in this dissertation are entirely my own effort, except where otherwise indicated and acknowledged.

I further certify that the work is original and has not been previously submitted for assessment in any other course or institution, except where specifically stated.

Murshedul ALAM

Student No: 0050003605

Signature

Date

ACKNOWLEDGEMENTS

The author would like to express sincere thanks to Dr. Thiru Aravinthan, of the Faculty of Engineering and Surveying, University of Southern Queensland for his guidance throughout the duration of this project. Without his knowledge, experience and supervision, completion of this task would have been much more difficult.

Sincere appreciation is extended to Mr. Mohan Trada, Mr. Glen Bartkowski and Mr. Bernard Black for their invaluable technical and practical assistance during the construction and testing stage of this project.

Special thanks are also due to Mr. Mukit-Ur-Reza, Mr. Wong Chuan Mein and Mr. Evan Woods for their kind support and assistance throughout the course of this Project.

Table of Contents

Contents

1. Chapter One: Introduction

2. Chapter Two: Literature Review

3. Chapter Three: Design Methodology

4. Chapter Four: Experimental Methodology

5. Chapter Five: Test Results and Discussions

6. Chapter Six: Conclusion

Appendix I

LIST OF FIGURES

LIST OF TABLES

CHAPTER 1

INTRODUCTION

1.1 Background

Frequency of strengthening and repairing work of bridges has increased tremendously in recent years, and it has become part of a great economic opportunity, as well as a problem. So, it is urgent to find suitable procedures for strengthening or repairing concrete members. The most common delamination of concrete bridge girders is shearing of concrete. This may be the result of the ever-increasing traffic volume and loads, the deterioration of the structural members over time, inadequate maintenance or cracking of members leading to environmental contamination and the corrosion of steel reinforcement. The loading capacities of a structure such as bridge often lessen for the development of the shear and flexural cracks. This delaminated area is subject to chemical penetration from the surface and moisture which may attack the reinforcing bar which creates possibility of further delaminating and as a result the failure of the whole structure.

At present external post-tensioning seems to be a quite effective and promising tool for the rehabilitation or strengthening of old structural elements, mainly bridges. The adoption of a piecewise polygonal shape of the cables allows one to superimpose a new bending moment diagram opposite to the preexisting one (Pisani, 1999). Possibility to reduce crack widths under service loads, decreasing the deflection and increasing the load bearing capacity and serviceability can be achieved by applying the external post-tensioning.

Structural restoration of concrete by epoxy repairing has been proven a good treatment for existing cracks in concrete structures. It therefore results in large cost savings.

Injection protects the rebar and stops water leakage. It has been proved that the application of epoxy injection is suitable for concrete structures.

The applicability, suitability and effectiveness of epoxy repairing on girders shear strengthened with external post-tensioning will be tested and analysed during this project under the title-'Effect of epoxy repairing on girders shear strengthened with external post tensioning'. The investigations are being conducted in the Faculty of Engineering and Surveying of University of Southern Queensland, Australia.

1.2 Project aim and scopes

This project seeks to investigate the effectiveness of epoxy repairing on girders shear strengthened with post tensioning by performing experimental investigations using model beams. Moreover, the results will be compared with prediction made from existing design models.

To achieve this aim the following objectives must be met during the completion of the project.

- Research the background information relating applying the epoxy repairing on girders and shear strengthening of girders using external post-tensioning.
- Review the theory associated with the design and analysis of reinforced and post-tensioned concrete sections, and the shear behavior of these sections.
- Design and prepare model beams in order to conduct experimental investigations.
- Determine the transferring forces to the member section through end anchorages.
- Design of concrete beams with shear cracks and the installation of the external post-tensioning.
- Testing of model beams.
- Critically evaluate the data obtained as a result of specimen testing and analyze the data for future references.

- Obtain an outcome of the project, which will give a better understanding of the shear behaviour of beams after using epoxy repairing and shear strengthened with external post-tensioning.

1.3 Assessment of Consequential Effects

It is quite logical and reasonable to assume that any professional engineering activity should have some outcomes and therefore some consequential effects afterwards. As a professional, it is a huge responsibility to assess the foreseeable consequences, which might flow from ongoing project activities. Although the consequences of engineering and surveying technical activity will vary largely according to the nature of the activity, yet we might encounter three dimensions of consequential effects which are universal, namely sustainability, safety and ethical dimensions. While the safety and ethical responsibilities of engineers and surveyors have long been recognized, the dimension of sustainability is a relatively recent formal addition to the universal requirements of the engineering and surveying practice.

1.3.1 Aspects of Sustainability

Sustainable Development is ‘development which meets the needs of the present without compromising the ability of the future generations to meet their own needs’ (The Brundtland Report, World Commission on Environment and Development 1987). This can perhaps be rephrased as ‘development, which can continue to provide social and economic benefits, without significant environmental degradation, for as long as they are desired’ (I.E.Aust.Policy on Sustainable Development, July 1989). Economic and financial sustainability requires that the resources be used efficiently and that assets be maintained properly. Environmental and ecological sustainability requires the external effects of the project work, which might have an impact on the nature, and social sustainability requires that the benefits of the project reach all sections of the community.

One of the major problems faced in the transport industry today is the maintenance, repair and strengthening of deteriorating concrete bridges. Nearly 40% of all bridges in the U.S are in deteriorated stage due to several weathering conditions and continuous increase in the traffic volume (Klaiber et al. 1989). According to the Federal Highway Administration (FHWA), these bridges are classified as functionally deficient. When functional problems start to occur in bridges, two alternatives can be considered, such as either demolish and replace the existing bridge or use rehabilitation techniques to restore it. The later alternative involves either strengthening or repairing. In this regard, applying epoxy repairing in accordance with the external post-tensioning has the potential to be one of the most powerful techniques for the strengthening and rehabilitating existing concrete bridges.

Again in case of bridge engineering, the application of this technique may have some positive environmental impacts, which might flow from my research activity in the near future. It will save a lot of time for engineers to rebuild the infrastructures of solid and wastewater disposal system, traffic management system, etc. Hopefully, the implementation of the project outcomes will help not only developed countries but also the undeveloped and developing countries as well.

1.3.2 Aspects of ethical responsibility

From ethical point of view, it seems that the out come of my project work is deemed to comply with the 'code of ethics' outlined by Institute of engineers, Australia. Official guidelines (IEAust, 2000) specify that, in general compliance with the provisions of the Code of Ethics, members should work in conformity with accepted engineering and environmental standards and in a manner, which does not jeopardize the public welfare, health and safety. To the best of my knowledge, the consequences of my project work will result in considerable benefits to the community without violating anyone's right. The term 'community' should be interpreted in its widest context to comprise all groups in society including my own workplace. Since the application epoxy resin shear strengthened of external post-tensioning takes less time in strengthening a bridge

comparing to other techniques, it might be easier for the local community to continue their normal and regular traffic activity. Apart from that, it is my ethical responsibility to consider the afterward affects of my prepared specimens which are very heavy in weight. If proper care is not taken, it might cause substantial damage. Just after the completion of my testing of specimens in USQ laboratory, to the best of my knowledge, the beams will be taken away by a recycle concrete factory, which will reuse it for a cost effective production. It means the university authority and my laboratory colleagues need not to worry about the safety of the laboratory work place.

1.4 Definition of External Post-tensioning

External post-tensioning is a method in which tendons are installed outside a structural element, thereby enhancing its performance under loads. The forces exerted by the prestressing tendons are only transferred to the structure at the anchorages and at deviators. No bond is present between the cable and the structure, unless at anchorages or deviators bond is intentionally created.

1.5 External Post-tensioning Technology

External post-tensioning is a method in which post-tensioning tendons are placed on the outside of the structural member. It has become popular in the current construction trend due to its advantages such as:

(1) It adds little weight to the original structure;
(2) It allows the monitoring, re-stressing and replacement of tendons.

External post-tensioning is characterized by the features such as: the tension elements (post-tensioning tendons) are placed on the outside of the physical cross-section of the concrete. The forces exerted by the post-tensioning tendons are only transferred to the structure at the anchorages and at deviators. No bond is present between the cable and the structure, unless at anchorages or deviators bond is intentionally created. The application of external prestressing is indeed not bound to the use of the concrete, but it can be

combined with any construction material such as composite materials, steel, timber, steel and concrete combined and other modern plastic materials. As the tendons are outside of the structure, the tendons are more exposed to the environmental influences and the protection against these detrimental influences is therefore of special concern. Due to the exposure and accessibility of the tendons, surveillance and maintenance measures are facilitated compared to internal, bonded prestressing. Due to absence of bond, it is also possible to re stress distress and exchanges any external post-tensioning cable, provided that the structural detailing allows for these actions.

1.6 Application of External Post-tensioning

Typical applications of external post-tensioning are in repair work and strengthening of all kinds of structures, under slung structures; pre cast segmental construction, simple and continuous spans. Below figure 1.1 to 1.6 shows the application of external post-tensioning in different construction fields.

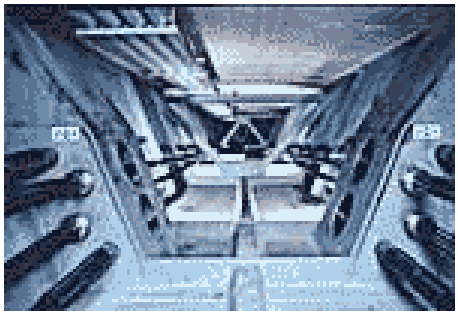

Figure 1.1: Bridges
(Source: VSL Strengthening Products, 2000)

Figure 1.2: Buildings
(Source: VSL Strengthening Products, 2000)

Figure 1.3: Industrial Structures
(Source: VSL Strengthening Products, 2000)

Figure 1.4: Parking Garages
(Source: VSL Strengthening Products, 2000)

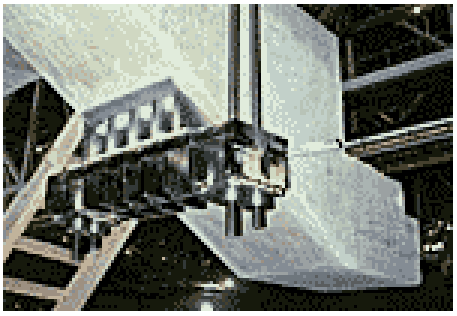

Figure 1.5: Stadium
(Source: VSL Strengthening Products, 2000)

Figure 1.6: Tank
(Source: VSL Strengthening Products, 2000)

1.7 Benefits and Limitations of External Post-tensioning

External post-tensioning has become popular due to its wide range of advantages. Major benefits of external post-tensioning are outlined below:

Compared to internal and bonded post-tensioning the external post-tensioning has the advantages of facilitating of concrete placing, improved condition of tendon placement, reduction of tendon placement, etc. Improvement of conditions for tendon installation is an advantage of post-tensioning which can take place independently from the concrete works.

External post-tensioning tendons can easily and without major cost implications are designed to be replaceable.
External post-tensioning reduces the friction loss, because the unintentional angular changes know as ‘wobble’ are practically eliminated.

On the contrary, external post-tensioning has some disadvantages. The tendons of external post-tensioning are more exposed to environmental influences (fire, vandalism, aggressive chemicals, etc) which increase the possibility of tendon deterioration. The statical height of the cross-section cannot be fully utilized, therefore requiring a greater depth or additional post-tensioning. Tendons are not bonded to the concrete the ultimate strength cannot be developed in ultimate design resulting in a higher prestressing steel consumption. The deviators and the anchorage plates are to be placed very carefully and accurately, which might sometimes be difficult. For certain cross-sections and construction procedures the handling of the tensioning devices may be more difficult.

1.8 Epoxy repairing

Epoxy repairing is a permanent crack repair method, which is applicable for both structural repair and structural preservation, keeping good concrete good. The material not only fills cracks, but also welds them together structurally with an epoxy that is forced through the crack under pressure and forms a bond that is stronger than the concrete itself. Injecting of epoxy is not limited to repairing cracks in concrete structures. Wood beams have been successfully injected, honeycombs and similar voids are also filled using injection techniques, floor overlays can be rebounded and loosened metal plates and bolts can be secured. This material is used for water proofing as well as structure repair.

Crack repairing by injecting epoxy is a system for welding cracks back together. This welding restores the original strength and loading originally designed into the concrete. Epoxy injection restores the structural qualities the concrete design intended. In other

words under most conditions it makes the concrete as good as new. It has become popular in the current construction trend due to its advantages such as:

1. Higher tensile strength and shear strength,
2. Wide range of strain to failure.
3. Various formulations can create epoxy with wide range of physical properties

1.9 Application of Epoxy Injection

Typical applications where epoxy injections are feasible, practical and economical are repair work and strengthening of all kinds of damaged structures, in the repair of concrete tie beams, slabs, columns, concrete areas of bridges and tunnels as well as swimming pool tanks.

Figure1.7: Application of epoxy in wall
(Source: Epoxy,2001)

Figure1.8: Application of epoxy in slab
(Source: Epoxy, 2001)

Figure1.9: Application of epoxy in tank (Source: Epoxy, 2001)

Figure1.10: Application of epoxy in Bridge Girder (Source: Epoxy,2001)

1.10 Benefits and Limitations of Epoxy

By applying epoxy injection, long and time costing method of repairing can be reduced. The substitution of epoxy injection in construction materials for other filament materials helps extend the lives of existing structure.

Epoxy injection currently offers the greatest potential in the field of restoring and repairing of concrete structure. The principal reasons for this are below;

1. The volumes of crack in bridges and in other structures arising are considerable,
2. The material can provide an end product with a variety of different construction uses.

Cost savings

By eliminating the cost of recovering the old concrete and in savings on existing structure costs, potential use of epoxy injections, and resisting potential bridge damage from transport of heavy vehicles, applying of epoxy injection has become more popular and proven effective.

The epoxy injection treatment process can be applied without stopping the traffic on bridges and without resisting other flows in other structure.

Physical advantages:

The physical advantages of epoxy injection are given below:

- Strong bond; epoxy is a powerful adhesive
- Works with a number of different materials
- Minimal shrinkage
- Can be implemented in cold or wet conditions
- Moisture tolerant

Other advantages*:*

Epoxy injection creates an impervious seal to air, water, chemicals, debris and other contamination. It has two purposes. First, it effectively seals the crack to prevent the damaging moisture entry. Secondly, it monolithically welds the structure together.

On the other hand the application of epoxy injection needs some careful considerations, as a matter of fact; these might be regarded as the limitations of epoxy injection. One of the major limitations of epoxy injection is that the health issue. The peel strength of epoxy is poor. It contains various harmful materials and can be proved injurious for health unless it is not operated carefully and professionally.

The other drawback is that it can weld concrete but it has no ability to resist new cracking of concrete structure. The main principal of epoxy injection is it makes bond with existing concrete which helps to weld existing cracking but it is unable to make any positive contribution to resist new cracking as it does not give strength to the structure.

1.11 Dissertation Overview

It should be mentioned that, there is few or no researches have been done on the combination of external post-tensioning and epoxy repairing on concrete structures. But researches on the effect of external post-tensioning and epoxy repairing have been done separately. Therefore, this project seeks to investigate the combined effects of external post-tensioning and epoxy repairing on the concrete girders.

Therefore, this dissertation is planned to submit the project activities in a comprehensive manner.

Chapter 2 of this dissertation contains a brief review of External Prestressing and Epoxy resins and their applications in the structural engineering field in the past and research programs conducted to investigate the shear strength performance and as well as repairing of crack using epoxy resin.

Chapter 3 contains the design of specimen and gives a brief idea about developing project methodology. This chapter also describes the design approach for calculating shear capacity of the strengthened beam.

Chapter 4 deals with the description of the experimental program. The constituent materials, the beam specimen and installation of external prestressing tendons are presented. A brief description of test set up and procedure is given.

Chapter 5 contains the test result and discussion. The observed crack patterns and modes of failure are reported. In addition, comparisons among test results to address factors affecting shear strength.

Chapter 6 provides the summary of this research program, and conclusions emerged from it. Recommendations for future research are also presented.

After the conclusion the project specification sheet, trial calculations for determining shear ligature size, design calculation of the thickness of the plate used during post-tensioning, placement of steel and concrete strain gauges, design of wooden block for supporting plates, sample calculation for concrete test results, risk assessment and management during testing and the tested data obtained from system five thousand machine are given in Appendixes.

CHAPTER 2

LITERATURE REVIEW

2.1 General Overview of the Problem and Possible Solution Mechanism:

Figure 2.1: Crack in Girder

(Source: Taiwaneq report, 1998)

The deterioration of existing bridges due to increased traffic loading, progressive structural aging, and reinforcement corrosion from severe weathering conditions has become a major problem around the world. The number of heavy trucks and the traffic volume on these bridges has both risen to a level exceeding the values used at the time of their design, as a result of which may of these bridges suffering cracking and are therefore in urgent need of strengthening and repair. (M. Harajli, N. Khairallah, and H.Nassif)

More than 40% of the bridges in Canada were built in the fifties and sixties, and most of these are in urgent need of rehabilitation (Neale, 1997). In the USA, over 200,000 bridges worth $78 billion are in critical need of repair (Klaiber et al. 1987, Munley 1994). $5.2 billion per year in maintenance would merely maintain in the status quo. Exact numbers for Canada are not available. These bridges are classified as functionally deficient according to the Federal Highway Administration (FHWA). The expansion of corrosion

products induces excess forces on the surrounding concrete that can be as high as 69 MPa (USDOT, FHWA, 1996). These forces cause delaminations and spalling, which along with the section loss of the reinforcing steel significantly decrease the serviceability of the structure. Post-tensioned concrete bridges may also exhibit loss in pre-stress overtime, resulting in drop in load carrying capacities of the affected members.

One of the first sign of structure deterioration is cracking. Most of the structural repair and retrofitting techniques for ordinary reinforced concrete are applicable to reinforced concrete bridges as well. Structural repair techniques include crack injection with low viscosity epoxy and patch repair using an approved material such as polymer modified mortar or non-shrink grout.

External prestressing is considered one of the most powerful techniques used for strengthening or rehabilitation of existing structures and ad grown recently to occupy a significant share of the construction market. And because external prestressing system is simpler to construct and easier to inspect and maintain as compared with the internal tendon system, it has been proposed recently in the design and construction of new segmental bridges. (Rabbat and Sowlat 1987; MacGregor et al. 1989; Miyamoto and Nakamura 1997).

Below the repair picture of a bridge with epoxy adhesive and strengthening of a deteriorated bridge with external prestressing have been shown:

Fig 2.2: Strengthening with external post-tensioning
(Source: D S Brown Company, 2004)

2.2 Historical Development:

2.2.1 Historical Development of External Post-tensioning:

The idea of external post-tensioning, a product of the twentieth century, announced the single most significant new direction in structural engineering of any period in history. It put into the hands of the designer an ability to control structural behavior at the same time as it enabled him or her- or forced him or her- to think more deeply about construction (David P. Billingtong, 2004).

The first bridge worldwide with external prestressing was built in Aue, Saxony, Germany 1935 to 1937 according to the concept of Dischinger. Dichinger granted his patent DRP 727,429 in 1934. It was a haunch beam with three spans (25.2 m - 69.0 m – 23.4 m) with a drop in girder in the mid pan. In this case, external tendons consist of smooth bars with yield strength of 520 N/mm^2 and a diameter of 70 mm. for the determination of the magnitude of prestressing, he proposed the concept of concordant prestressing, which later became known as the “load balancing”. (VSL Report Series, 1999)

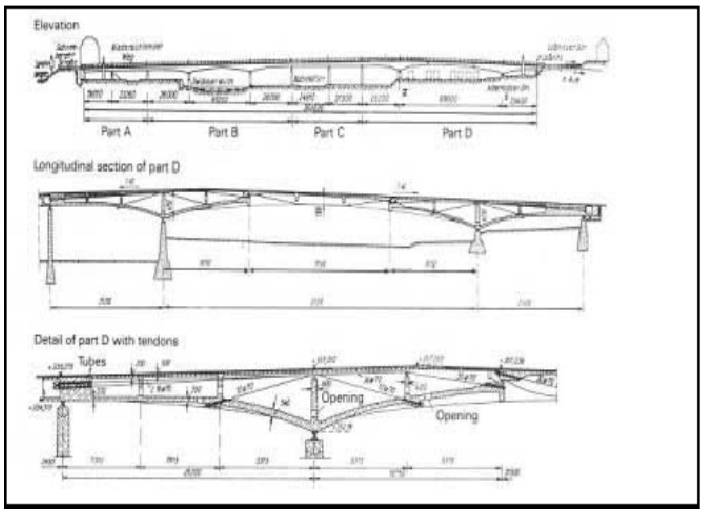

Figure 2.3: First prestressed concrete bridge: Bridge over valley basin and railway at Aue. Germany. (Source: VSL report series, 1999)

Figure 2.4: Bridge at Aue: External Prestressed bars of the drop-in span
(Source: VSL report series, 1999)

Based on Freyssinet's ideas, Wayss & Preytag AG designed and constructed in 1938 the bridge over the Dortmond-Hannover Autobahn in Oelde, FRG, was for the first time high tensile prestressing steel arranged inside the concrete section was used for 4 simply supported girders of 33 m span. The prestensioning method was applied and the prestressing steel was therefore bonded to the structure. This was actually the first bridge in what is now called conventional prestressed concrete. (VSL Report Series, 1999)

In the years 1938 to 1943, Haggbohm designed and built the Klockestrand Bridge (Fig 2.3), near Stockholm, Sweden. For the main spans (40.50 – 71.50 – 40.50 m) the Dischinger concept was applied. The main span superstructure was prestressed with a total of 48 bars of ∅30 mm having yield strength of 520 N/mm^2. (VSL Report Series, 1999).

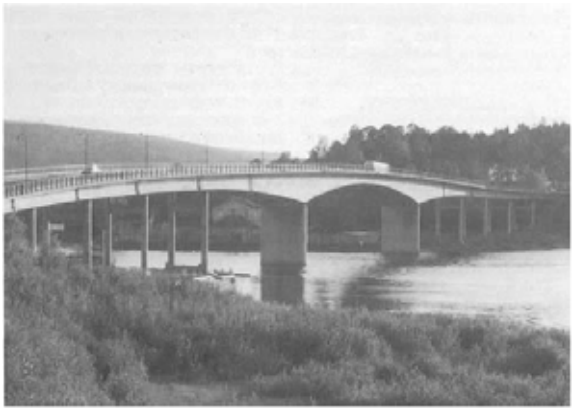

Fig 2.5: Klockestrand Bridge near Stockholm, Sweden
(Source: VSL report series, 1999)

The first application of external tendons for the strengthening of existing structures can be found during this period. And early example is the two span steel truss bridge (48 – 48m) over the River Aare at Aarwangen, Switzerland (Fig 2.6). This bridge was built in 1889 and was no longer capable of supporting modern traffic loads. In 1967 the bridge was strengthened with two locked-coil strands Φ63 mm having an ultimate strength of 1,370 N/mm^2. (VSL Report Series, 1999).

Fig 2.6: Bridge over River Aare at Aarwangen, Switzerland
(Source: VSL report series, 1999)

External prestressing was virtually discarded in the early 1960's due to the reputation it received after the closure of Can Bia Bridge in France. This bridge, along with many others of similar design suffered from major corrosion of the steel tendons due to insufficient protection from extreme environmental conditions.

A rebirth of external post-tensioning can be observed from the mid-seventies onward. Freeman Fox and Partners designed the Exe and Exmister Viaducts in England using external tendons each consisting of a bundle of 19 greased and plastic sheathed strands Φ13mm. The prime objective was to minimize the weight of the superstructure to overcome difficult soil conditions. (VSL Report Series, 1999)

The main developments certainly came from French engineers. In 1978/79 Muller introduced external post-tensioning in the United States, for the Key Bridges in Florida (Fig 2.7). His main goals were speed of construction and economy. Many other important structures followed. Since 1980, many bridges have been designed and built in France under the auspices of Virlogeux of SETRA (State design office of highway authority) using either external tendons or a combination of internal and external tendons.

Fig 2.7: Key Bridges in Florida (Source: VSL volume 1, 1999)

2.2.2 Historical Development in Epoxy Adhesive:

The application of epoxy injection on concrete structures can be considered to be an effective, viable, lucrative method of repairing and rehabilitating damaged structures due to overloading and progressive structural aging. Over the years not many researches have been carried out on the application of epoxy injection on structures strengthened with post tensioning.

Interest in the use of sealers dates as far back as the 1930s. As the awareness of the severity of corrosion problems has grown since 1960s, the interest in the use of sealers has grown exponentially. To follow the interest in the use of sealers, the number of manufactures and number of products available has also grows. Cady (Cady, 1994) identified 409 concrete sealers in approximate two dozen categories, produced by 169 manufactures.

The rapid growth in the industry was accompanied by lack of consensus of acceptable test methods to evaluate the performance of the sealers, and conflicting performance reports are common.

The New Jersey Highway Authority (Goldberg, 1961) used epoxy as a bridge deck sealer on several structures early as 1959 and 1960. The initial application procedures, two structures were treated in 1960 using more mechanized procedures to reduce application costs. Two component spray equipment was used to apply the material at a thickness of 0.25 mm to 0.38 mm. This involved a coverage rate of approximately 2.45m2/l. After the application of the epoxy material, a layer of crushed emery was spread on the fresh epoxy to create a skid resistant surface. It should be rated that the application rates and procedures developed in 1961 are similar to those in use today. There is minimal information available as to the effectiveness of the material used to seal the decks or the longevity of the treatment.

2.3 Previous Investigation

In past, numerous researches were conducted relating flexural strengthening of concrete structures both experimentally and analytically. No researches has been done relating epoxy repaired shear strengthening of concrete structures with external post tensioning in past. In fact, a very few researches have been done focussing on the strengthening of shear capacity of concrete structures adopting external post-tensioning. The reason for this low level of research activity in this field is that in recent year's pre stress with un bonded tendons has been used primarily for concrete structures with relatively low shear structures (Muller, 1980). It is also mentionable that, quite a few works have been carried out on the strengthening of shear capacity of concrete structures using Fiber Reinforced Polymer sheets, mesh and resins. For the above reasons, I have categorized this section into two broad subjects, external post-tensioning and namely epoxy repairing. As there is not direct researches have been done relating this project anything relating or relevance of these subjects has been included.

2.3.1 External Post-Tensioning

In recent years several studies have been conducted to study the flexural strengthening of RC members, however, few have concentrated on shear strengthening (Khalifa, 1998). Although little information is available relating to shear strengthening by external post-tensioning but some specific researches have given informative ideas and characteristics about shear strengthening of concrete structures external post-tensioning.

Tan and Naaman (1993) proposed a model based on the strut-and-tie method to predict the shear strength of simply supported, externally post-tensioned beams subjected to midspan concentrated load. The model defined a safe domain within which the beam would not collapse under the applied load. It predicts four possible modes of failure, which may be broadly classified into shear type failure and flexure type failure. Shear type of failure is due to the crushing of the diagonal compressive concrete strut or the yielding of web reinforcement, while the flexure type failure is due to the yielding of the internal longitudinal reinforcement or the yielding of the external post-tensioning tendons. The model is able to predict the main events leading to the failure of externally post-tensioned concrete beams.

Harajli and Hijazi (1991) proposed that shear deformations located outside the constant moment region and they suggested that it could be designed by displacing the loads a distance equal to the length of the plastic hinge, $L_{p,}$ which was initially stated by Corley (1966), and later modified by Mattock (1967). In the end, Harajli and Hijazi suggested and modified the proposed expression of Mattock as follows:

$$L_p = L\,[1/(L/Lo) + 1/(L/d_{psu}) \qquad (2.1)$$

Where,

L = span length between supports;

Lo = length of flexural span;

d_{psu} = distance from extreme compression fibre to centroid of the unbonded tendons;

Tan and Ng (1997) conducted several tests on simply supported beam and each beam accompanied with straight external tendon of span-to-depth ratio 15 and finally from their tests, they reached in a conclusion that the change in eccentricity of tendons without deviators resulted in a lower load carrying capacity compared to beams with one or two deviators.

Tan (1998) further proceeded and conducted seven T-shaped beams, post tensioned with straight tendons to study the effect of concrete strength, shear reinforcement, and shear span on the failure mode of externally post-tensioned beams. Each beam was constructed with a deviator at the midspan and tested under simply supported conditions. The beams were each subjected to equal concentrated loads at third points, except for one, which was subjected to concentrated load at the midspan. Test results indicated that decreasing the concrete strength or the amount of shear reinforcement leads to shear type failure of the beam. When an appropriate concrete strength and amount of shear reinforcement are provided, flexural-type failure prevails even for shear span-to-depth ratio as low as 2.5.

Later Tan (2001) carried out an investigation of simple span reinforced concrete beams strengthened by external tendons that are anchored at midspan locations. Two series of simple-span T-beams, one strengthened with external cables and other with Carbon FRP tendons were examined. It was shown in the investigation that the tendons at locations less than a critical distance from the beam end would result in the strengthened beams performing satisfactorily in terms of ultimate load-carrying capacity. The test results indicated that it is possible to locally strengthen the beam by anchoring the tendons at interspan locations without compromising the deflection and cracking behavior. The process leads to shorter and hence more economical use of external tendons, as well as minimizing second order effects due to varying tendon eccentricities under load.

Pisani (1999) concluded into his strengthening by external post-tensioning that the load carrying capacity of RC and PC beams damaged by means of cyclic load history does not decrease if the maximum load generates stresses lower than yielding, when referring to

reinforcement, and lower than the concrete, when dealing with concrete. He assumed the crack is spread over a certain length and neglected shear deformation before and after cracking and tensile strength of the beam. If these conditions are fulfilled, the beams can be strengthened by means of external post-tensioning, and the load-carrying capacity of the improved structure will be greater and plus the load increment needed to cancel the negative bending moment added to the beam by external post-tensioning at ultimate. He suggested that, superimposing a small axial force in the old structure or, for instance, a force that satisfies inequality 1, and placing deviators when needed could achieve this goal. This usually means high eccentricity of the external cables. Together with the bending moment this external cables impose axial force.

This axial force also increases the shear strength of the old structure, which was previously stated by Harajli (1993). He tested several externally post-tensioned simply supported beams to examine the improving behavior of service load and flexural resistance of concrete beams. He had noticed different responses to flexural resistance with deviated tendon profiles and straight horizontal tendon profiles. He found that external post-tensioning with deviated profile have much more resistance on flexure compared to the straight horizontal profile when the area of steel was small. This is because of the progressive reduction of depth of the straight external post-tensioning tendons with increasing member deformation to failure and the draped tendon profile has deviators, which reduces the second-order effects, and contributing to a higher strength. He also stated that this could also be relevant in terms of shear resistance. It was also found that the ultimate deflections and load-deflections response of the specimens were similar for both types of profiles. He emphasized that shear cracks in the beam specimens were more apparent during preloading than at ultimate load resistance after external post-tensioning, which suggests that external post-tensioning has the ability to close shear cracks and as a result, improve serviceability to the point where deflections at ultimate after strengthening are still smaller than those experienced external post-tensioning seems to have the ability to improve both serviceability and strength condition.

All post-tensioning tendons suffer some loss of stress when held at constant strain over an extended period of time. Both during and after the post-tensioning operation, various factors come into play, which reduce the magnitude of the post-tensioning force in the concrete. This loss of post-tension can be very significant. The decrease in post-tensioning force in the tendon would exceed 20 percent in most situations (Faulkes et al., 1998). In case of unbonded tendons, which are used in post-tensioned structures the prestress loss also occurs. Burns, Helwig and Tsujimoto (1991) conducted a major research to find changes in force due to friction in unbonded tendons at different stages in the loading and stressing history. They found that the value of the peak tendon stress for determination of ultimate tendon stress should be calculated using friction losses at the point in question. It has been further discovered that the post-tension force used to calculate service load stresses, deflections, and cracking loads should be the tendon force effective at the point in question or the average force in that span considering the effect of friction losses.

It is necessary to predict changes in both the prestressing force and eccentricity of the external tendons for the purpose of the ultimate strength of members strengthened with external prestressing. Numerous investigations have been carried out to predict the stress in unbonded tendons at ultimate. The most common approach to predict the stress in the prestressing steel at ultimate for unbonded tendons is from the following equation:

$$f_{ps} = f_{pe} + \Delta f_{pe} \qquad (2.2)$$

Where,

f_{ps}= the ultimate tendon stress;

f_{pe} = the effective prestress (considered the reference state)

Δf_{ps} = stress increase due to any additional load leading to ultimate behavior.

Harajli (1990) conducted an analytical investigation in which he studied the effect of loading type and span-to-depth ratio on the stress at ultimate in unbonded tendons. He incorporated the span-to-depth ratio in the ACI 318-83 equation to allow for a continuous

transition for various span-to-depth ratios, and proposed the following prediction equation:

$$f_{ps} = f_{pe} + (10{,}000 + f'_c/100p_{ps})\,(0.4+8/(L/d_{ps})) \quad (2.3)$$

$$f_{ps} \leq f_{py} \quad (2.4)$$

$$f_{ps} \leq f_{pe} + 60{,}000 \quad (2.5)$$

Where,

f_{py} = yield strength of the prestressing steel
f'_c = concrete compressive strength
p_{ps} = ratio of prestressing steel
d_{ps} = depth of center of prestressing steel

He also mentioned that the proposed equation is excessively conservative for simply supported members loaded with third- point or uniform loading. He thus noted that a more accurate determination of fps could be based on strain compatibility analysis.

Burnns, Charnley, and Vines (1978) and Burns and Pierce (1967) undertook a large number of tests on the behavior of slabs post-tensioned with unbonded tendons. Their work led to modification of ACI Code recommendations related to the use of additional nonpost-tensioned reinforcement in these slab systems.

In a more recent experimental investigation of continuous slabs, Burns (1990) observed that increase in stress in unbonded tendons at ultimate depends on the number of spans being loaded and the tendon profile in each span. He thus warned that the increase in stress might not be as optimistic as predicted by the code if only one span is loaded to failure while the others are not loaded.

Pisani and Nicoli (1996) showed from their analysis of simply supported beams that the increase in stress, Δf_{ps}, in the external tendons due to loads close to ultimate was smaller than those experienced in internally unbonded tendons. They also noted that this behaviour was due to the reduction of external tendons with increase in load.

According to the Australian Standard for the prediction of the stress in unbonded tendons is given in Clause 8.1.6 of AS 3600. The equations are stated below:

For a span-to-depth ratio of 35 or less

$$f_{ps} = f_{pe} + 70 + f'_c bd_{ps}/100\ A_{ps} \leq f_{pe} + 400 \leq f_{py} \quad (2.6)$$

And For a span-to-depth ratio greater than 35

$$f_{ps} = f_{pe} + 70 + f'_c bd_{ps}/300\ A_{ps} \leq f_{pe} + 200 \leq f_{py}. \quad (2.7)$$

Where,

b = width of section

A_{ps} = area of prestressing steel

Previously in USQ projects have been done on shear strengthening of headstocks using external prestressing and some projects involving shear strengthening by external prestressing is currently ongoing.

The above discussion and investigation shows only the very small portions of researches, which have been done for last few years. For the strengthening of shear capacity I have adopted straight tendon profile rather than draped tendon profile as it can control both shear and flexural cracking.

2.3.2 Epoxy Repairing:

Dr Mehmet Celebi (1988) conducted a general study on epoxy repaired reinforced concrete beams for investigating the effectiveness of the epoxy injection process in restoring strength and the influence of the process on the energy absorption capacity and the stiffness of the test specimens. He used a series of four test beams, which were previously tested under combined moment and shear reversals according to preplanned scheme. The following results and conclusions are drawn from the testing of epoxy-repaired beams:

- The yielding of the longitudinal reinforcing bar spread continuously along the spans of the beams. An important result of this is the dissimilarity of the shape of the hysteresis loops of the original and repaired beams.

- The epoxy repaired beams developed strengths, which were considerably in excess of their original values. This was due to increase strength of the repaired regions. The increased strength in turn increased the overall stiffness of the specimen.

- The energy absorption capacities as measured from the area of the hysteresis loops of the repaired beams were very similar to those of the original beams. Normally, decrease in hysteresis loops would be expected. However, it seems that the increase in strength and development of new yielding region in the spans compensates the expected decrease.

- The aesthetics is effectively restored in the epoxy-repaired beams.

Catherine Wolfgram French, Gregory A.Thorp, and Wen-Jen Tsai (1990) carried out an investigation about epoxy repair techniques for moderate earthquake damage. They tended to compare the impact of two epoxy inject method and their efficiency on the damaged concrete structures. The conventional epoxy pressure injection method is not

effective in restoring on between the reinforcement and concrete, which indicated that the repaired specimens behave in a satisfactory manner except then restoring bond between the reinforcement and concrete. Another disadvantage of the pressure injection method is it has difficulty in repairing any offshoot cracks. To overcome such problem they proposed vacuum impregnation technique, which they expected, would be better solution than pressure injection method. For this purpose they constructed two reinforced concrete interior beam-column subassemblages with large diameter reinforcing bars. They made the following observations:

- Both repair techniques worked well. The repaired structures achieved over 85 percent of the initial stiffness of the originally undamaged structures.

- The repaired cracks did not reopen in the test of the repaired structures; new cracks tended to develop in the concrete adjacent to repaired crack.

- The strength and energy-dissipation capacities were restored in the repaired structures. The bond between the reinforcement and the concrete also appeared to be restored.

- Pressure injection had proven to be an effective method to repair moderate earthquake damage. These tests indicated that the vacuum impregnation procedure is equally effective for repairing such damage. They recommended that the vacuum impregnation procedure be used to repair large region of damage. The entire regions might be repaired at once with this procedure rather than repairing each crack individually.

In July 2002 NAHB Research Center, Inc. of United States of America finished testing and assessment of epoxy injection crack repair for residential concrete stem walls and slabs-on-grade for Consortium of Universities for Research in Earthquake Engineering of Richmond, California. They had used 18 stem walls and 18 slab test specimen to evaluate the performance of epoxy injection repair process. Two repetitions were performed for

each specimen type, loading condition, and crack condition. 12 flexural and 12 shear tests were performed on repaired specimens to determine the performance of the repaired specimens. Four uncracked slab specimens were also tested using the shear test setup intended to subject repaired cracks to a high transverse shear stress. Each crack was characterized as a <1/16-inch crack following initial testing with crack widths ranging from 0.03 inch to 0.06 inch. The 1/8 inch and 1/4 inch (cracks were created. The following list summarizes conclusions and recommendations supported by the test program:

- With appropriate selection and preparation of epoxy viscosity (Grade), proper mixing of components, and proper execution of the injection, crack repairs made from one side only of the concrete element were effective in creating a repair that was comparable to the uncracked strength of concrete specimens that were free of restrained shrinkage stress and that exceeded the unfactored code-nominal strength of concrete assumed in design. Therefore, access to all sides of an element is not required to achieve a fully effective crack repair.

- Crack repairs were completely effective for <1/16 inch and ¼ inch crack widths, in part because the epoxy viscosity selection appears straight forward.

- A variety of viscosities and methods were used for repair of the 1/8-inch wide cracks, several of which were successful. Unsuccessful repairs were the result of epoxy seeping out of the cracks in the sand bedding.

2.4 Shear Capacity Prediction Equation

2.4.1 Shear Capacity before Post Tensioning

According to AS3600 Clause 8.2.2 the design shear strength of a beam shall be taken as ϕV_u where

$$V_u = V_{uc} + V_{us} \quad (2.8)$$

Here, V_{uc} = Shear resisted by concrete at ultimate

V_{us} = Shear resisted by the stirrups

For the computation of the nominal shear resistence:

Shear resisted by concrete at ultimate,

$$V_{uc} = (\sqrt{f'_c} / 6)\, b_v\, d_o \quad (2.9)$$

And shear resisted by the stirrups

$$V_{us} = A_{sv}\, f_{sy.f}\, d_o / s \quad (2.10)$$

Where,

b_v = minimum effective web width;

d_o = beam depth from extreme compression fibre to centroid of outermost layer of tensile reinforcement;

A_{sv} = cross sectional area of one stirrup (both legs);

$f_{sy.f}$ = yield strength of stirrups;

s = centre-to-centre stirrup spacing, measured parallel to the longitudinal axis of the member;

According to AS 3600, the ultimate shear strength (V_{uc}) of a reinforced beam, excluding the contribution of shear reinforcement, can be calculated from the following equation:

$$V_{uc} = ß_1\, ß_2\, ß_3\, b_v\, d_o\, (A_{st}\, f'_c / b_v\, d_o)^{1/3} \quad (2.11)$$

Where,

$$ß_1 = 1.1\ (1.6 - d_o / 1000) \geq 1.1 \quad (2.12)$$

$$ß_2 = 1$$

Again an axial compressive force tends to delay inclined cracking; conversely, axial tension tends to precipitate such cracking. In AS 3600, the effect of axial force on V_{uc} is taken into account. Therefore, the value of factor $ß_2$ is different for members subjected to axial tension and for members subjected to axial compression.

$$ß_2 = 1 - (N^* / 3.5\ A_g) \geq 0 \quad (2.13)$$

For members subjected to axial tension

$$ß_2 = 1 + (N^* / 14\ A_g) \quad (2.14)$$

For members subjected to axial compression

And

$ß_3$ = 1 ; or may be taken as –

$= 2d_o / a_v$ but not greater than 2, provided that the applied loads and the support are orientated so as to create diagonal compression over the length a_v.

A_{st} = area of fully anchored tensile reinforcement;

N^* = absolute value of the design axial force;

A_g = gross area of the section;

a_v = the distance from the section at which shear is being considered to the face of the nearest support.

2.4.2 Shear strength of Post-tensioned beams

The effect of post-tensioned force on shear strength of beam has to be considered and according to AS3600 the ultimate shear strength (V_{uc}) of a prestressed beam is calculated

from the lesser value of flexure-shear cracking or web-shear cracking. The equations of shear strength for both cracking are given below:

Flexure-shear cracking

$$V_{uc} = ß_1\, ß_2\, ß_3\, b_v\, d_o\, ((A_{st} + A_{ps})\, f'_c / b_v\, d_o)^{1/3} + V_o + P_v \quad (2.15)$$

Web-shear cracking

$$V_{uc} = V_t + P_v \quad (2.16)$$

Where,

$ß_1$, $ß_2$, $ß3$ and A_{st} = as given in Eq 2.6 except that in determining $ß_2$, N^* is taken as the value of the axial force excluding prestress.

P_v = the vertical component of the prestressing force;

V_t = the shear force, which, in combination with the prestressing force and other action effects at the section, would produce a principal tensile stress of $0.33\sqrt{f'_c}$ at either the centroidal axis or the intersection of flange and web, whichever is more critical.

V_o = the shear force which would occur at the section when the bending moment at that section was equal to the decompression moment (M_o)

= M_o / (M^*/V^*) for simply supported conditions and M^*/N^* is the ratio of bending moment and shear force at the section under consideration, due to same design loading.

The decompression moment, M_o for a section is given as:

$$M_o = [\, P/A_g + Pey_b / I_g \,]\, I_g / y_b \quad (2.17)$$

Where,

P = prestressing force;

e = eccentricity of prestressing force from centroid of uncracked section;

y_b = distance from centroidal axis to bottom fibre;

I_g = second moment of area of the cross-section about the centroidal axis;

Vertical stirrups are most frequently used for shear reinforcement, because of their simplicity. Stirrups inclined at an angle α_v to be horizontal are also used, usually with α_v varying from about 40 to 60 degrees. For construction purposes, a longitudinal bar is placed in each corner near the compressive face for attachment of the vertical or inclined stirrup. Previously, it was common practice to bend up portion of the main tensile reinforcement at about 45 degrees and treat this also as shear reinforcement. However, AS3600 does not recommend bent up bars.

According to AS3600, the contribution to the ultimate shear strength by shear reinforcement in a beam (V_{us}) shall be determined from the following equations:

For perpendicular shear reinforcement:

$$V_{us} = (A_{sv}\, f_{sy.f}\, d_o/s)\, cot\theta_v \qquad (2.18)$$

For inclined shear reinforcement:

$$V_{us} = (A_{sv}\, f_{sy.f}\, d_o/s)\, (sin\alpha_v\ cot\theta_v + cos\alpha_v) \qquad (2.19)$$

Where,

s = centre-to-centre spacing of sear reinforcement, measured parallel to the longitudinal axis of the member.

θ_v = the angle between the axis of the concrete compression strut and the longitudinal axis of the member, taken conservatively as 45° or, more accurately, to vary linearly from 30° when $V^* = \phi V_{u.min}$ to 45° when $V^* = \phi V_{u.max}$.

α_v = angle between the inclined shear reinforcement and the longitudinal tensile reinforcement.

CHAPTER 3

DESIGN METHODOLOGY

3.1 Introduction

The following chapter presents the approaches, which are considered to determine the sectional size and longitudinal reinforcement of test specimen. The analytical and numerical calculations relating to the design of specimen have been discussed and described in this chapter. And furthermore the approaches that have been taken for the construction and the materials needed for the construction purposes are briefly mentioned in this chapter.

For the simplicity of construction purposes and maintenance rectangular section is selected. Although different section and span can be designed for this particular project effort but in this case the section and span have been selected according to the availability of formwork in the laboratory.

The test beams were designed so that beams will not fail in flexure rather it will fail in shear. To encourage shear failure, the ratio of flexural failure loading and shear failure loading is considered as 2. It was decided four point loading would be adopted to form shear failure in both end of the beam. In this regard the span to depth ratio is considered near 3 that would guarantee the beam would fail in shear rather than in flexure. Bending moment and shear force diagram for four point loading are shown in next page:

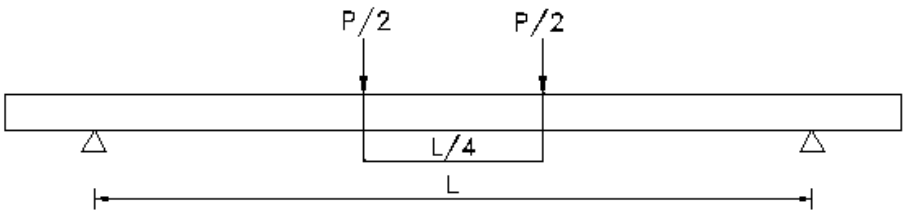

Figure 3.1 (a): Loading Pattern on the test beams

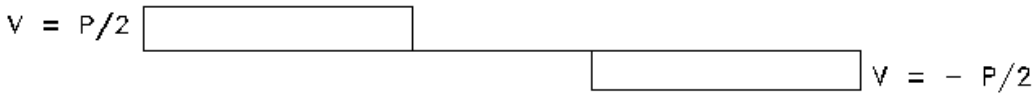

Figure 3.1 (b) : Shear Force Diagram

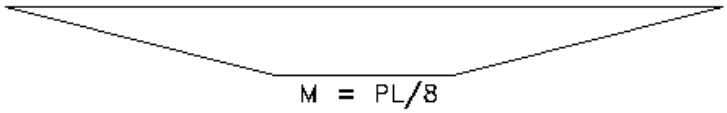

Figure 3.1 (c) : Bending Moment Diagram

From bending moment diagram it is apparent that the maximum shear occurs from the support to loading point region. So, the most critical section for shear is chosen two ends starting from support to loading point and thus the shear force *V* is ± P/2. Again from the bending moment diagram it is clear that maximum bending moment occur at midspan. The maximum design load is being chosen approximately half of the load, which will make flexure failure.

The four specimens with the purpose of testing were rectangular sections and post-tensioned beams with unbonded tendons. The beams were simply supported over 2000 mm (2m) of span having a total length of 2500 mm (2.5m). Basic specimen dimension can be seen in Figure 3.2.

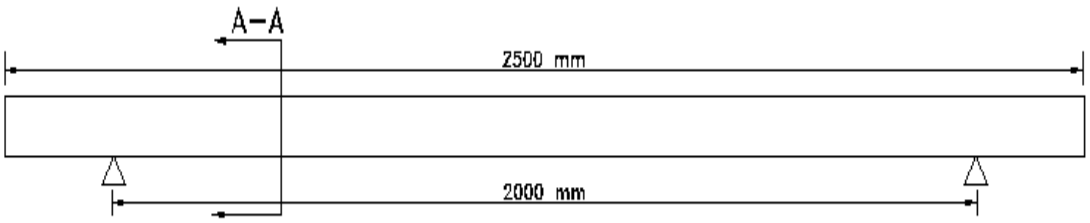

Figure 3.2: Basic specimen dimensions

The design process of the size and the spacing of the shear reinforcement can be considered as the critical and important step. The specimens had to be under reinforced in regards to the shear reinforcing to guarantee shear failure. To confirm shear failure, the adopted shear reinforcement spacing was much higher than minimum spacing according to AS 3600. A spreadsheet was set-up with varying stirrup sizes and spacings until an acceptable value was obtained. All the calculations regarding determination of stirrup sizes and spacing along with a summary table is given in Appendix D.

The ultimate moment capacity, M_u, the ultimate load,P_u, the shear capacity,V_u before and after strengthening and the stress in the external rod due to external prestressing will be calculated in this chapter. Sample calculations will be performed for specimens with effective prestress force, f_{pe} of 100 KN and 150KN.

3.2 Preliminary Design

The ultimate moment capacity, M_u, the ultimate load, *Pu*, the shear capacity, *Vu* of the design specimen before strengthening is described in this section.

The rectangular cross section is shown in Figure 3.2. The overall depth, *D* of the beam was 250 mm and the width of the beam; *b* was designed as 100 mm (Because the dimension of the available formwork in laboratory was 250 mm in depth and 100 mm in width).

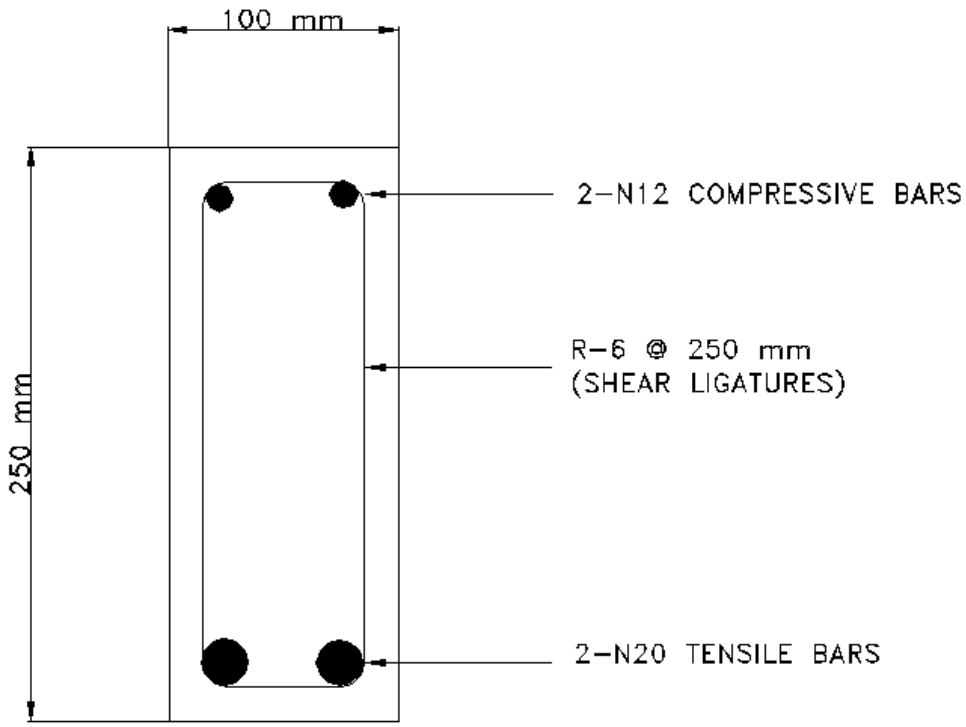

Figure 3.3: Section A-A of the design specimen

The section is doubly reinforced including 2 N-20 bars as tensile reinforcement and 2 N-12 bars as compressive reinforcement. R6 ligatures were used as shear reinforcement. The moment capacity of doubly reinforced section was calculated using the limiting strain criterion for a doubly reinforced section and the AS3600 rectangular stress block seen in Figure 3.4. It is assumed that M_u occurs at a value extreme fibre concrete strain, ε_{cu}, which is taken as 0.003. The shear capacity of the section also calculated according to AS3600 Clause 8.2.7.1 without strengthening. The estimation of the specimens shear capacity after prestressing had done according to AS3600 Clause 8.2.7.2. The exposure classification for Toowoomba is B1 (according to AS3600 Table 4.3) and thus the design concrete strength; f'_c is 32 MPa (according to AS3600 Clause 4.5). The cover was assumed 15 mm. Since the beam was designed to take prestress force, so it is expected that the beam would take quite a good amount of axial force because prestress force induced to the beam in longitudinal direction. So, smallest stirrup spacings were provided along a substantial length at the extreme end of the beam for preventing shear crack in at both ends. The spacing of R6 ligatures was adopted 250 mm throughout the beam but for

the extreme end the spacings was restricted at 50 mm. For N-type reinforcing bars the yield strength of the steel, f_{sy} was taken as 500 MPa and for R-bars; $f_{sy.f}$ was adopted as 250 MPa.

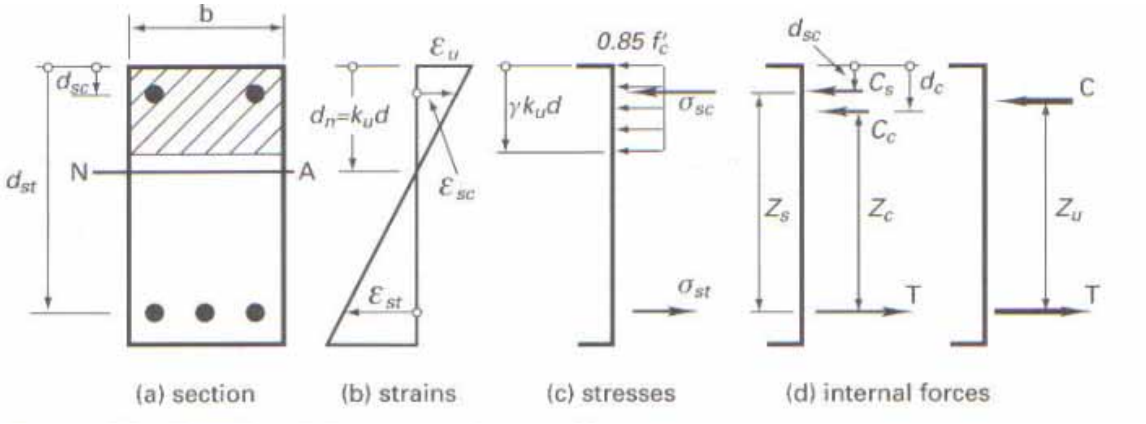

Figure 3.4: Doubly reinforced section at M_u

(Source: Faulkes et al., 1998)

In a doubly reinforced section at ultimate moment, the resultant compressive force, C consists of components C_c in the concrete and C_s in the compressive steel. The calculations regarding bending moment are set out below:

Distance from the extreme compressive fibre of the concrete to the centroid of compressive reinforcement, $d_{sc} = 15 + 6 + 12 / 2$

$\Rightarrow d_{sc} = 27$ mm

Depth to reinforcing steel, $d_{st} = 250 – 15 – 6 – 10$

$\Rightarrow d_{st} = 219$ mm

Area of compression steel, $A_{sc} =$ 2-N12

$\Rightarrow A_{sc} = 2 \times \pi \times 6^2$

$\Rightarrow A_{sc} = 226.195$ mm^2

Area of tensile steel, A_{st} = 2-N20

$\Rightarrow$ $A_{st} = 2 \times \pi \times 10^2$

$\Rightarrow$ $A_{st} = 628.32 \text{ mm}^2$

According to Clause 8.1.2.2 of AS 3600, the ratio of the depth of the assumed rectangular compressive stress block to d_n at M_u, γ is:

γ = 0.85 – 0.007 (f'_c – 28) within limits of 0.65 to 0.85;

$\Rightarrow$ γ = 0.85 – 0.007 (32 – 28) [as f'_c = 32 MPa]

$\Rightarrow$ γ = 0.822

The neutral axis depth, d_n can be calculated assuming compression steel yielding:

$$d_n = (f_{sy} A_{st} - f_{sy} A_{sc}) / (0.85 \times f'_c \times b \times \gamma) \quad (3.1)$$

$\Rightarrow$ $d_n = (500 \times 628.32 - 500 \times 226.195) / (0.85 \times 32 \times 100 \times 0.822)$

$\Rightarrow$ d_n = 73.65 mm

Checking k_u, neutral axis parameter, being the ratio, at ultimate strength and under any combination of bending and compression, of the depth to the neutral axis from the extreme compressive fibre to d (depth to resultant force in tensile steel at M_u). To ensure ductility according to AS 3600 Clause 8.1.3, k_u should not exceed 0.4.

$k_u = d_n / d_{st}$

$\Rightarrow$ k_u = 73.65 / 219

$\Rightarrow$ k_u = 0.33 < 0.4 (ok)

Checking the assumption that compression steel has yielded:
From the linear strain diagram:

$$\varepsilon_{sc} = \varepsilon_{sc} \times (d_n - d_{sc}) / d_n \quad (3.2)$$

$\Rightarrow \quad \varepsilon_{sc} = 0.003 \times (73.65 - 27) / 73.65$

$\Rightarrow \quad \varepsilon_{sc} = 0.002$

Since $\varepsilon_{sc} < \varepsilon_{sy}$ (0.0025), the assumption is incorrect. So neutral axis depth has to be recalculated. It can be assumed that the compressive steel is in the elastic range, i.e.:

$$C_s = (E_s \times \varepsilon_u \times A_{sc}) \times (k_u d_{st} - d_{sc}) / (k_u \times d_{st}) \qquad (3.3)$$

Trial positions of the neutral axis can be checked until the equilibrium requirement, that the sum of the horizontal forces must be zero, is satisfied. Alternatively, a quadratic equation for k_u can be obtained from this requirement:

$$k_u^2 + u_1 k_u - u_2 = 0 \qquad (3.4)$$

Where,

$$u_1 = (\varepsilon_u \times E_s \times A_{sc} - f_{sy} \times A_{st}) / (0.85 \times f'_c \times b \times \gamma \times d_{st}) \qquad (3.5)$$

$$u_2 = (\varepsilon_u \times E_s \times d_{sc} \times A_{sc}) / (0.85 \times f'_c \times b \times \gamma \times d^2_{st}) \qquad (3.6)$$

Therefore,

$u_1 = (0.003 \times 200 \times 10^3 \times 226.195 - 500 \times 628.32) / (0.85 \times 32 \times 100 \times 0.822 \times 219)$

$\Rightarrow \quad u_1 = - 0.307$

And $u_2 = (0.003 \times 200 \times 10^3 \times 27 \times 226.195) / (0.85 \times 32 \times 100 \times 0.822 \times 219^2)$

$\Rightarrow \quad u_2 = - 0.0322$

This gives the following quadratic equation:

$$k_u^2 - 0.307\, k_u - 0.0322 = 0$$

Solving with CASIO f_x-570W calculator,

$k_u = 0.39 < 0.4$ (ok)

Substituting this value in equation 3.4 give:

$$C_s = (200\times10^3 \times 0.003) \times (0.39 \times 219 - 27) \times 226.195 / (0.39 \times 219)$$

$$\Rightarrow \quad C_s = 92813.84 \text{ N}$$

Now calculating the compressive forces in the concrete:

$$C_c = 0.85 \times f'_c \times b \times \gamma \times k_u \times d_{st}$$

$$\Rightarrow \quad C_c = 0.85 \times 32 \times 100 \times 0.822 \times 0.39 \times 219$$

$$\Rightarrow \quad C_c = 190963.094 \text{ N}$$

Therefore, the ultimate moment capacity of the design specimen:

$$M_u = C_s (d_{st} - d_{sc}) + C_c (d_{st} - 0.5 \times \gamma \times k_u \times d_{st}) \qquad (3.7)$$

$$\Rightarrow \quad M_u = 92813.84 (219 - 27) + 190963.094 (219 - 0.5 \times 0.822 \times 0.39 \times 219)$$

$$\Rightarrow \quad M_u = 57.7 \text{ KN-m}$$

Checking whether tensile steel is at yield:

$$\varepsilon_{st} = \varepsilon_u \times (d_{st} - k_u \times d_{st}) / (k_u \times d_{st}) \qquad (3.8)$$

$$\Rightarrow \quad \varepsilon_{st} = 0.003 \times (219 - 0.39 \times 219) / (0.39 \times 219)$$

$$\Rightarrow \quad \varepsilon_{st} = 0.0047 > 0.0025$$

Since, $\varepsilon_{st} > \varepsilon_{sy}$ (0.0025), the assumption is correct. So the tensile steel has yielded.

The maximum load capacity of the beam can be calculated as below:

Moment capacity = Load capacity of the beam × distance between the loading point and the support

$M_u = P_1 \times L$

$\Rightarrow \quad P_1 = M_u / L$

$\Rightarrow \quad P_1 = 57.7 / 0.75$

$\Rightarrow \quad P_1 = 77$ KN

Therefore, the ultimate load that the beam can withstand is 2 x 77 KN = 154 KN. (As four point loading has adopted)

The shear strength, *Vu* must be less than the load causing ultimate moment capacity because the specimen must fail in shear rather than flexure.

According to AS 3600, the ultimate shear strength (V_{uc}) of a reinforced beam, excluding the contribution of shear reinforcement, can be calculated from the following equation:

$$V_{uc} = ß_1\, ß_2\, ß3\, b_v\, d_{st}\, (A_{st}\, f'_c / b_v\, d_{st})^{1/3}$$

Where,

$ß_1 = 1.1\,(1.6 - d_{st} / 1000) \geq 1.1$

$\Rightarrow \quad ß_1 = 1.1\,(1.6 - 219 / 1000) \geq 1.1$

$\Rightarrow \quad ß_1 = 1.52 > 1.1$ (ok)

Again, $ß_2 = 1$ (as there is no significant axial tension and compression)

And $ß_3 = 1$;

Therefore,

$V_{uc} = 1.52 \times 1 \times 1 \times 100 \times 219\,(628.32 \times 32 / 100 \times 219)^{1/3}$

$\Rightarrow \quad V_{uc} = 32.21$ KN

According to AS3600 Clause 8.2.2 the design shear strength of a beam shall be taken as ϕV_u where

$V_u = V_{uc} + V_{us}$

Where,

V_{us} = Shear resisted by the stirrups

Now calculating the maximum shear strength resisted by the shear reinforcement in accordance to AS 3600 Clause 8.2.10:

$V_{us} = (A_{sv}\, f_{sy.f}\, d_{st}/s)\, \cot\theta_v$

Where,

$\theta_v = 30° + 15° [(A_{sv} - A_{sv,min})/(A_{sv,max} - A_{sv,min})] \geq 30° \leq 45°$ (3.9)

Where,

A_{sv} = cross sectional area of shear reinforcement

$A_{sv,\,min}$ = cross sectional area of minimum shear reinforcement

$A_{sv,max}$ = cross sectional area of maximum shear reinforcement

$A_{sv} = 2(\pi \times 3^2)$

$\Rightarrow A_{sv} = 56.55\ mm^2$

And, $A_{sv,\,min} = 0.35 \times b \times s / f_{sy,f}$ (3.10)

$\Rightarrow A_{sv,\,min} = 0.35 \times 100 \times 250 / 250$

$\Rightarrow A_{sv,\,min} = 35\ mm^2$

Again, $A_{sv,\,max} = b \times s\, (0.2\, f'_c - (V_{uc}/bd_{st})) / (f_{sy,f})$ (3.11)

$\Rightarrow A_{sv,\,max} = 100 \times 250\, (0.2 \times 32 - (32.21/(100 \times 219))) / (250)$

$\Rightarrow A_{sv,\,max} = 639.853\ mm^2$

Therefore,

$\theta_v = 30° + 15° [(56.55 - 35)/ (639.853 - 35)]$

$\Rightarrow \quad \theta_v = 30.534° \geq 30°$ (ok)

So, the ultimate shear strength by shear reinforcement in the beam, V_{us}

$V_{us} = (56.55 \times 250 \times 219/250)\ cot 30.534°$

$\Rightarrow \quad V_{us} = 21$ KN

So the ultimate shear strength of the rectangular beam is the shear resisted by the concrete at maximum plus the shear resisted by the stirrups:

$V_u = V_{uc} + V_{us}$

$\Rightarrow \quad V_u = 32.21 + 21$

$\Rightarrow \quad V_u = 53.21$ KN

Therefore, the shear capacity of the beam is 2 x 53.21 or 106.42 KN. (As four point loading is adopted)

The shear capacity, *Vu* (106.42KN) of the beam is less than the ultimate load (154 KN) capacity. So it is obvious that, the beam will fail in shear.

3.3 Design of Externally Post-tensioned Rectangular Beam

The effect of post-tensioning force on shear strength of beam has to be considered and according to AS3600 the ultimate shear strength (V_{uc}) of a post-tensioning beam is calculated from the lesser value of flexure-shear cracking or web-shear cracking. The equations of shear strength for flexure-shear cracking is given below:

$$V_{uc} = ß_1\, ß_2\, ß3\, b_v\, d_{st}\, ((A_{st} + A_{ps})\, f'_c / b_v\, d_o)^{1/3} + V_o + P_v \qquad (3.12)$$

Here, as the external post-tensioning follows a straight tendon profile, the vertical component of the post-tensioning force, $P_v = 0$. The arrangement of the post-tensioning bars is shown below in figure 3.5. The post-tensioning bars are each 16mm in diameter with a distance of 30 mm from the side of the beam. The section properties are same from previous calculations with an eccentricity, e of 40mm. The total shear strength of the beam after applying 100 KN and 150 KN respectively can be calculated. The maximum post-tensioning force can be applied on the beam is 166 KN.

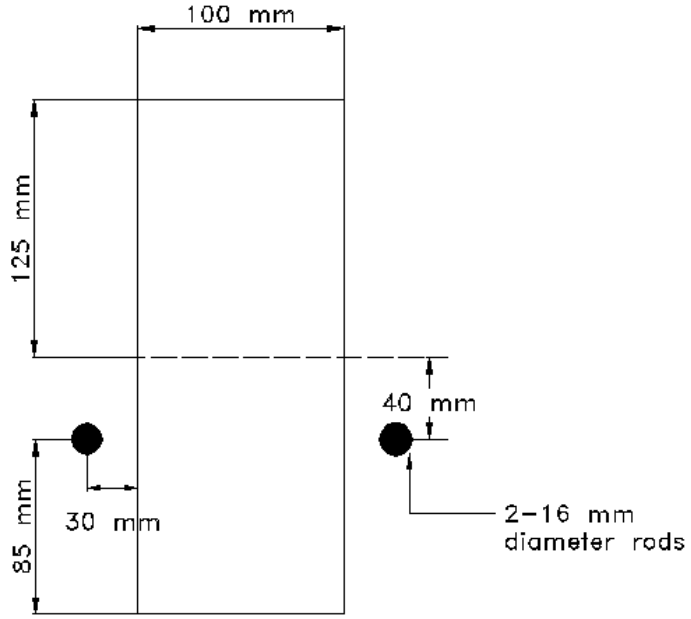

Figure 3.5: Post-tensioning bar arrangement

3.3.1 Determination of maximum external post-tensioning load

Area of the section,

A_g = 250 x 100 = 25000 mm^2

I_g = second moment of area of the cross-section about the centroidal axis

$= bd^3/12$

$$\Rightarrow \quad I_g = (100 \times 250^3)/12$$

$$\Rightarrow \quad I_g = 130.21 \times 10^6 \text{ mm}^4$$

Z_g = the section modulus of an uncracked cross section

$Z_g = I_g / (D/2) = 130.21 \times 10^6 / 125$

$$\Rightarrow \quad Z_g = 1.042 \times 10^6$$

Beam self weight, w = area of the section x density of the concrete

$\Rightarrow$ w = 0.25 x 0.1 x 24 = 0.6 KN /m

(Assuming density of the concrete is 2400 kg/m3)

Eccentricity, e = 40 mm

When the tendons are stressed the resulting internal bending moment will normally exceed the moment caused by the self-weight of the beam causing tensile stresses in the top of the beam and compressive stresses in the bottom. If compressive stresses are positive then, to ensure that stresses are not excessive, we have, at midspan.

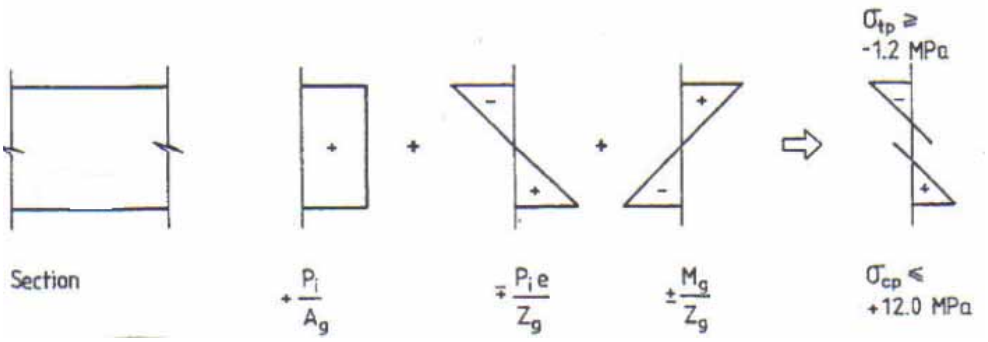

Figure 3.6: Effect of post-tension and applied loads

(Source: Figure 6.3 Faulkes et al., 1998)

Now, bending moment at midspan to the self weight of the slab, $M_g = wL^2/8$

$$\Rightarrow \quad M_g = 0.6 \times 2^2/8$$

Therefore,

M_g = 0.3 KN-m

For the top fibres,

$$P_i/A_g - (P_i \times e / Z_g) + M_g/Z_g \geq -1.2 \text{ MPa}$$

$$\Rightarrow \quad P_i/25000 - (P_i \times 40)/(1.042 \times 106) + (0.3 \times 106)/(1.042 \times 106) \geq -1.2$$

$$\Rightarrow \quad P_i \leq 923 \text{ KN}$$

For the bottom fibres,

$$P_i/A_g + (P_i \times e / Z_g) - M_g/Z_g \leq 12 \text{ MPa}$$

$$\Rightarrow \quad P_i/25000 + (P_i \times 40)/(1.042 \times 106) - (0.3 \times 106)/(1.042 \times 106) \leq 12$$

$$\Rightarrow \quad P_i \leq 157 \text{ KN}$$

Thus, to ensure the compressive stresses at midspan do not exceed 12.0 MPa the initial prestress force cannot exceed 157 KN. Selection of the smaller of the two calculated values of P_i will ensure that both stresses are not exceeded. Hence, $P_i \leq 157$ KN.

Under full load after all losses have occurred:

At this stage the applied loads will cause compressive stresses to develop in the top fibres and tensile stresses to (perhaps) develop in the bottom fibres. To ensure that these stresses are not excessive, at midspan stresses are shown in below:

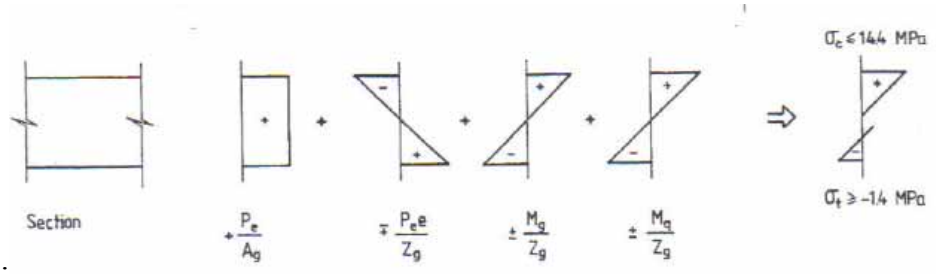

:

Figure 3.7: Stress distribution with increasing M

(Source: Figure 6.4 Faulkes et al., 1998)

Where, M_q = bending moment at midspan due to the superimposed live load = $q \times L^2 / 8$

Here,

Live load, q = 0,

Therefore, $M_q = 0$

For the top fibres,

$$P_e/A_g - (P_e \times e / Z_g) + M_g/Z_g + M_q/Z_g \geq 14.4 \text{ MPa}$$

$$\Rightarrow P_e/ 25000 - (P_e \times 40)/ (1.042 \times 106) + (0.3 \times 106) / (1.042 \times 106) + 0 \geq 14.4$$

$$\Rightarrow P_e \leq 8753 \text{ KN}$$

For the bottom fibres,

$$P_e/A_g + (P_e \times e / Z_g) - M_g/Z_g - M_q/Z_g \geq -1.4 \text{ MPa}$$

$$\Rightarrow P_e/ 25000 + (P_e \times 40)/ (1.042 \times 106) - (0.3 \times 106) / (1.042 \times 106) + 0 \geq -1.4$$

$$\Rightarrow P_e \leq 12.63 \text{ KN}$$

Selection of the greater of the two calculated values of Pe will ensure that both stresses are not exceeded.

Hence, $P_e \leq 8753$ KN

To ensure that the stresses at both critical stages of the loading history are not excessive, then

$8753 \text{ KN} \geq P_i \geq 157 \text{ KN}$

Choosing the lower bound in order to minimize both the amount of prestressing steel and average effective prestress, adopting

$P_i = 157$ KN

Assuming there is no time-dependent prestress loss and friction loss.

Now checking shear strength and the stresses on the external load after applying 100 KN and 150 KN prestress forces and checking whether the external tendon can withstand both prestress force. Based on the above criteria the amount of prestress force will be selected for this particular investigation.

3.3.1.1 Application of 100 KN Post-tension Force

The area of the post-tensioning steel is:

$$A_{pt} = 2(\pi \times 8^2)$$

$$\Rightarrow \quad A_{pt} = 402.12 \text{ mm}^2$$

Using equation 2.13 the decompression moment, M_{dec} can be calculated for the section. So,

$$M_{dec} = [\, P/A_g + Pey_b / I_g \,]\, I_g / y_b$$

Where,

P = External prestress force = 100 KN

A_g = area of the rectangular beam = 250 x 100

= 25000 mm2

e = eccentricity = 40 mm

y_b = distance from centroidal axis to bottom fibre

= 125 mm

I_g = second moment of area of the cross-section about the centroidal axis

$= bd^3/12$

$\Rightarrow \quad I_g = (100 \text{ x } 250^3) /12$

$\Rightarrow \quad I_g = 130.21 \text{ x } 10^6 \text{ mm}^4$

Therefore,

$M_{dec} = [(100 \text{ x}10^3/ 25000) + (100 \text{ x } 10^3 \text{ x } 40 \text{ x}125)/ (130.21 \text{ x } 10^6)] (130.21 \text{ x } 10^6)/ 125$

$= 8.1667$ KN-m

Now the shear force (V_{dec}) which would occur at the section when the bending moment at that section was equal to the decompression moment (M_{dec}) can be evaluated using equation:

$$V_{dec} = Mdec / (M^*/V^*) \quad (3.13)$$

[For simply supported conditions and M^*/N^* is the ratio of bending moment and shear force at the section under consideration, due to same design loading.]

Here,

M_{dec} = 8.1667 KN-m

M^* = 115.4 KN-m

V^* = 106.42 KN

$\Rightarrow$ V_{dec} = 8.1667 / (115.4/106.42)

$\Rightarrow$ V_{dec} = 7.52 KN

And the ultimate contribution of the shear strength by the concrete at ultimate and the external post-tensioning is:

$$V_{uc} = 1.52 \times 1 \times 1 \times 100 \times 219 ((628.32 + 402.12)\ 32 / (100 \times 219))^{1/3} + 7.52 + 0$$

$\Rightarrow$ V_{uc} = 45.67 KN

The total shear capacity of this externally post-tensioned headstock from equation 2.8 is:

$$V_u = V_{uc} + V_{us}$$

$\Rightarrow$ V_u =45.67 + 21

$\Rightarrow$ V_u =66.67 KN

After applying post-tensioning force of 100 KN the shear capacity of the beam increased from 106.42 KN to 133.34 KN, which means the specimen gain about 25.3% more shear strength after strengthening. It is further noticeable that the ultimate shear capacity of the

beam do not exceeded the ultimate load capacity for flexure failure, which gives assurance of shear failure.

3.3.1.2 Application of 150 KN Post-tension Force

The area of the post-tensioning steel is:

$$A_{pt} = 2(\pi \times 8^2)$$

$$\Rightarrow \quad A_{pt} = 402.12 \text{ mm}^2$$

Using equation 2.13 the decompression moment, M_{dec} can be calculated for the section. So,

$$M_{dec} = [P/A_g + Pey_b / I_g] I_g / y_b$$

Where,

P = External prestress force = 150 KN

A_g = area of the rectangular beam = 250 x 100

= 25000 mm2

e = eccentricity = 40 mm

y_b = distance from centroidal axis to bottom fibre

= 125 mm

I_g = second moment of area of the cross-section about the centroidal axis

$= bd^3/12$

$\Rightarrow \quad I_g = (100 \text{ x } 250^3) /12$

$\Rightarrow \quad I_g = 130.21 \text{ x } 10^6 \text{ mm}^4$

Therefore,

$M_{dec} = [(150 \text{ x} 10^3 / 25000) + (150 \text{ x } 10^3 \text{ x } 40 \text{ x} 125) / (130.21 \text{ x } 10^6)] (130.21 \text{ x } 10^6) / 125$

$= 12.25$ KN-m

Now the shear force (V_{dec}) which would occur at the section when the bending moment at that section was equal to the decompression moment (M_{dec}) can be evaluated using equation:

$$V_{dec} = Mdec / (M^*/V^*) \quad (3.12)$$

[For simply supported conditions and M^*/N^* is the ratio of bending moment and shear force at the section under consideration, due to same design loading.]

Here,

M_{dec} = 12.25 KN-m

M^* = 115.4 KN-m

V^* = 106.42 KN

$\Rightarrow$ $V_{dec} = 12.25 / (115.4/106.42)$

$\Rightarrow$ $V_{dec} = 11.3$ KN

And the ultimate contribution of the shear strength by the concrete at ultimate and the external post-tensioning is:

$$V_{uc} = 1.52 \times 1 \times 1 \times 100 \times 219 ((628.32 + 402.12)\ 32 / (100 \times 219))^{1/3} + 11.3 + 0$$

$\Rightarrow$ $V_{uc} = 49.45$ KN

The total shear capacity of this externally post-tensioned girder from equation 2.8 is:

$$V_u = V_{uc} + V_{us}$$

$\Rightarrow$ $V_u = 49.45 + 21$

$\Rightarrow$ $V_u = 70.45$ KN

After applying post-tension force of 150 KN the shear capacity of the beam increased from 106.42 KN to 140.9 KN, which means the specimen gain about 39.4% more shear strength after strengthening. It is further noticeable that the ultimate shear capacity of the

beam do not exceeded the ultimate load capacity for flexure failure, which gives assurance of shear failure.

3.3.2 Prediction of Stresses in the External Rods Due to Post-tensioning:

In an unbonded tendon, slip occurs between steel and concrete, and the strains in the prestressing strand tend to balance over considerable lengths of the beam, hence reducing the peak stress levels which would otherwise take place at cracks. In the extreme case if zero bonds and zero friction, the steel stress is constant over the full length of the beam. This extreme situation might be reasonably assumed for some cases of external prestressing. In the case of internal unbonded post-tensioning, considerable friction usually develops between the steel and the duct, so that some concentration of stress occurs in the peak moment regions.

This section will present calculations to the projected stress increase for specimens with an effective prestress force of 100 KN and 150 KN (each rod carries 50 KN and 75 KN respectively), based on equations suggested from AS3600.

According to the Australian Standard for the prediction of the stress in unbonded tendons is given in Clause 8.1.6 of AS3600. The equation is stated below:

For a span-to-depth ratio of 35 or less

$$f_{ps} = f_{pe} + 70 + f'_c b d_{ps}/100\, A_{ps} \leq f_{pe} + 400 \leq f_{py}$$

3.3.2.1 Stress in the external rods during 100 KN (50 KN load on each rod)

Here,

f_{ps} = stress in prestressing steel at M_u

f_{pe} = the effective stress in the tendon = 50 KN / area of prestressing steel

$= 50 \times 10^3 / 201.06$

$= 248.68$ MPa

b = width of the beam = 100mm

d_{ps} = depth of the prestressing steel = 85 mm

A_{ps} = area of prestressing steel = 201.06 mm^2

f_{ps} = yield stress of each road = 930 MPa

Therefore,

$f_{ps} = 248.68 + 70 + (32 \times 100 \times 85)/(100 \times 201.06) \leq 248.68 + 400 \leq f_{py}$

$\Rightarrow \quad f_{ps} = 332.21 \leq 648.68 \leq 930$ MPa

Which satisfies the design requirement as the ultimate tendon stress is well lower than the yield stress of each rod.

3.3.2.2 Stress in the external rods during 150 KN (75 KN load on each rod)

Here,

f_{ps} = stress in prestressing steel at M_u

f_{pe} = the effective stress in the tendon = 75 KN / area of prestressing steel

$=75 \times 10^3 / 201.06$

$= 373.02$ MPa

b = width of the beam = 100mm

d_{ps} = depth of the prestressing steel = 85 mm

A_{ps} = area of prestressing steel = 201.06 mm^2

f_{ps} = yield stress of each road = 930 MPa

Therefore,

$f_{ps} = 373.02 + 70 + (32 \times 100 \times 85)/(100 \times 201.06) \leq 373.02 + 400 \leq f_{py}$

$\Rightarrow \quad f_{ps} = 456.55 \leq 773.02 \leq 930$ MPa

Which satisfies the design requirement as the ultimate tendon stress is well lower than the yield stress of each rod.

3.4 Selection of post-tension force

Below table 3.1 presents shear strength before and after applying post-tensioning. It also represents the total stresses and total load carried by the external rod during post-tensioning.

Table 3.1: Summarized result of shear capacity and stresses in the external rod.

Post-tension Force (KN)	Shear capacity before strengthening Vu (KN)	Shear capacity after strengthening Vu (KN)	Stresses in the External Rod (MPa)	Load Carried by External Rod (KN)
100	106.42	133.34	332.21	66.8
150	106.42	140.9	456.55	91.8

Although application of 150 KN post-tension force can be adopted without damaging the prestressing rod but to be in the conservative side and for the purpose of reducing stresses and loads in the tendons 100 KN prestress force have been selected. It can be noticed from the table that increases of 50 KN prestress forces only give additional (140.9 – 133.34) or 7.56 KN shear strength.

3.5 Design Summary

The final design of the reinforcement and the spacing is given in Figure 3.8. As it was mentioned before that the extreme end of the beam had to encounter numerous longitudinal loads during post-tensioning so small spacing had been adopted to prevent shear cracking.

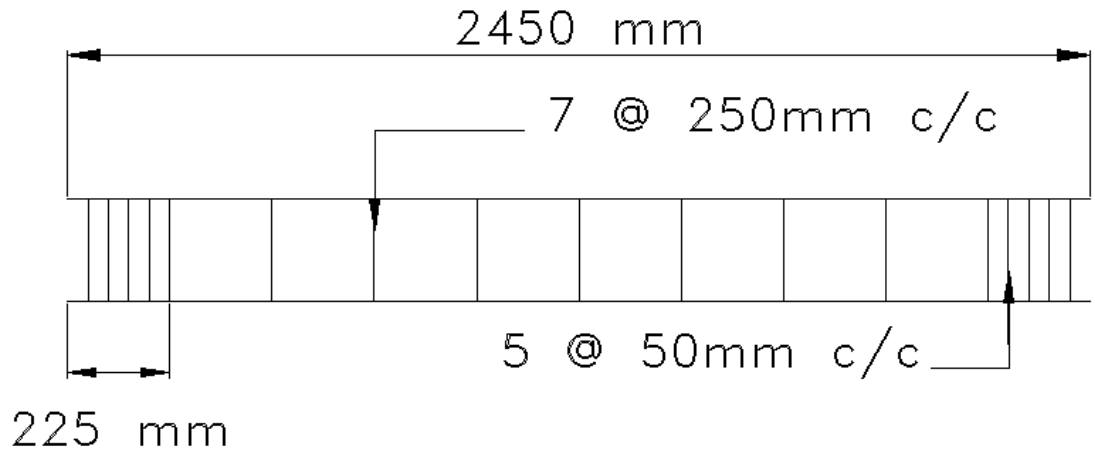

Figure 3.8: Final detail reinforcement design of the rectangular beam

The final design of the specimen has met the following requirements:

- The shear capacity, V_u of the design section has not exceeded the ultimate load capacity of the beam. As a result the design section will fail in shear rather than flexure.
- The ultimate tendon stress, f_{ps} is not greater than the tendon yield stress, f_{py}, which means the tendon, will not fail during loading.

CHAPTER 4

EXPERIMENTAL METHODOLOGY

4.1. Introduction

This chapter gives a detail idea about the adopted procedures that was taken during construction of the four specimens and the different load cases for each girder. The arrangement of materials prior to construction of the specimen and instrumentation of girders before testing phase is explained in detail. This project involved heavy loading machineries and particularly during post-tensioning. As a result, health and safety issues during construction and testing will also be covered.

4.2 Experimental Methodologies

As previously mentioned, total four specimens would be constructed to conduct testing for this project and later test results of the four beams would be compared to find the effectiveness of the external post-tensioning for shear strengthening of girders with epoxy repairing. Load cases were different for four beams with different preloading depending on the width of shear crack and same post-tension load were adopted for all beams except the control beam.

The first specimen, B1 considered as a control specimen. Therefore, no external post-tension force was applied on this beam to increase the shear capacity. It was designed to measure the ultimate shear capacity of the beam.

For specimen B2 shear crack was initiated after preloading. The scale of preloading largely dependent on observation of the crack width developed at the time of loading. The beam was preloaded until 1 mm shear crack was developed. After initiating crack, 100 KN external post tension force applied to reduce the shear cracking width and

strengthening the beam. The reason for selecting 100 KN external post-tensioning force was mentioned on Chapter 3. No epoxy repairing was adopted for beam B2.

Beam B3 was strengthened by external post-tension force without initiating crack by preloading. The external post-tension force was same as adopted for beam B2. The reason for adopting same scale of post-tension force was to compare the ultimate shear capacity of the three post-tensioned beams.

B4 beam was loaded in two stages. First shear crack was initiated by preloading and based on the observation of the shear crack width formation the scale of loading was determined. After the formation of 1 mm shear crack the loading was stopped. Later shear crack was repaired by epoxy and strengthened with 100 KN external post-tensioning force. Below table 4.1 summarizes the adopted load cases for this project. Whereas, table 4.2 describes the test variables adopted during testing of four girders.

Table 4.1: Adopted different load cases for testing

Specimen	Preloading	Epoxy	Post-tensioning
1	X	X	X
2	√	X	√
3	X	X	√
4	√	√	√

.

Table 4.2: Experimental test variables

Specimen	Post-tension force (KN)	Design f'c (MPa)	Design, $f_{sy.f}$ (MPa)	Remarks
1	0	32	250	Control beam
2	100	32	250	Same post-tension force
3	100	32	250	Same post-tension force
4	100	32	250	Same post-tension force

4.3 Construction of the Specimens

The process involved for the construction of the four specimens was almost similar. The different stages adopted during the formation of four specimens are summarized below:

1. Selection of Formwork
2. Ordering the reinforcement
3. Measuring, cutting and bending of shear ligatures.
4. Preparing the reinforcement cage.
5. Placing of steel strain gauges.
6. Preparing the formwork and placing the reinforcement cage in the formwork.
7. Pouring the concrete.
8. Curing the specimen.
9. Removing the specimen from the formwork.
10. Placing the concrete strain gauges.
11. Preparing the specimen for testing.

Every step will be described below to give a detail idea about the consideration and procedures involved during construction phase of the specimens.

4.3.1 Selection of Formwork

In this project, the existing formwork that was used previously by research students and practice course students had been used. It was mentioned on previous chapter that, the design of the specimen was conducted considering the cross section of the existing available formwork in the USQ Z1 laboratory. The available length of the total formwork was 3000 mm. as the span length of the testing beam was selected 2500 mm with effective length of 2000 mm; two wooden blocks was attached with clamp was used to shorten the length during pouring of concrete.

4.3.2 Ordering the Reinforcement

Due to the unavailability of sufficient R6 ligatures, N-12 and N-20 bars for specimens in USQ, reinforcement was ordered and it was obtained by local supplier. Smooth R6 bars used as shear ligatures while deformed N-12 and N-20 bars were used for compressive and tensile reinforcement of the beams. It is also mentionable that, for the strengthening of the beam by external post-tensioning, 16 mm diameter threaded rods were obtained later by local supplier. The capacity of the 16 mm rods was 930 MPa.

4.3.3 Measuring, cutting and bending of shear reinforcement

The total length of the bottom tension and top compression bar was 2450 mm. Electric Grinder was used to cut the bottom and top reinforcement bars. Due to small sizes of the shear ligatures, cutting was done using standard bolt cutters. Figure 4.1 shows the bending jig, which was used to bend the shear stirrup. Once the bending positions along the length of the bars were marked, a vice was used to bend the stirrups into shape. Figure 4.2 demonstrate the completed stirrup using bending jig.

Figure 4.1: Bending Jig

Figure 4.2: Shear Stirrup

Total 62 stirrups had been used for four specimens. 11 stirrups were made for control specimen and 51 stirrups for remaining three specimens with 17 stirrups each. The spacing and the detailing of the shear stirrups had been described on Chapter 3.

4.3.4 Preparation of Reinforcement cage

The assembling of the reinforcement cage was done after the bending of shear stirrups. Wire ties were used to assemble the reinforcing cage seen in figure 4.3.

Figure 4.3: Steel Reinforcement Cage

Two reo cage assembly trestles had been used for assembling reinforcement cage. Two N-12 compression bars were cut to length and a bundle of prebent ligatures were placed over the trestles. The stirrups were then spaced out according to the position of each stirrup and tied into position with light tie wires. After that the additional N-20 tensile bars were placed and tied with light tie wires.

4.3.5 Placing the Steel Strain Gauges

Four TML strain gauges were used for each beam. Two steel strain gauges were placed on each side of the girder, as from shear force diagram it was expected that the maximum shear failure load would develop in these particular areas. The rest of the steel strain gauges were installed in the middle bottom tensile reinforcement of the beam. The arrangement of these four 2 mm length gauges can be seen in Appendix C.

Before the placement of the gauges in the specified position extreme care was taken to prevent any damage. Abrasive papers were used to smooth the shear ligatures and electrical grinders were used for smoothing the tensile bars. Later acetone was used to clean the surface from dust and debris. Figure 4.5 shows the placement of steel strain gauges in the tensile bars of the beam before concreting.

Figure 4.4: Placing of Steel Strain gauges

Individual wire was separated and later CN adhesive glue was used to attach the gauges with the steel bars. Wax was then put on the gauges to ensure a watertight seal. To ensure no moisture and water would get into the gauges during pouring of concrete an extra waterproof tape was used to wrap around the gauges. All the strain gauges were tested by multimeter to ensure that they were working properly.

4.3.6 Preparing the Formwork and Placing the Reinforcement Cage

Form oil was applied before placing the reinforcement cage in the formwork to prevent sticking between the concrete and the formwork during the removal of the formwork. Eight squares wooden blocks of 15 mm depth were used as reo chairs and placed below

the reinforcement cage to provide cover for the under-side of the specimen. As only one formwork was available, only one specimen could be cast one at a time. Figure 4.6 show the placement of the reinforcement cage in the formwork after applying form oils.

Figure 4.5: Placement of reinforcement cage in the formwork.

Special care had been taken to prevent damage of the steel strain gauges during the placement of the reinforcement cages in the formwork. For the lifting of the beam two additional V-shaped bent bars were tied 500 mm far from each extreme side of reinforcement cage. Special configuration was considered in each extreme side of the beam for the attachment of the external post-tension rods. Four M10 ferrules were placed to each end of B2, B3 and B4 specimens. For providing M10 ferrules, wooden blocks were prepared by an experienced carpenter at USQ Z4 workshop. The detail design of the wooden block is shown in Appendix E. Finally the wires from the strain gauges were taped together and were placed in plastic bags to make sure that it would not damage during the pouring of concrete.

4.3.7 Pouring the Concrete

Ready mix concrete was used for the concreting purpose in this project and local supplier supplied it. Although design strength of 32 MPa and a slump of 80 mm with an average particle size of 20 mm concrete was ordered but variation of concrete slumps were measured during slump tests. Table 4.3 shows the slump test results of the four batches concrete which was used during concreting.

Table 4.3: Slump test result of ready mix concretes.

Concrete Batch no	Beam No	Slump test result (mm)
1	1	110
2	4	Unable to measure because of high water content in concrete
3	3	60
4	2	120

A wheelbarrow was used to pour the concrete in the formwork and concrete was compacted by vibrator. Care was taken during concrete work for preventing any damage of steel strain gauges. During the pouring of concrete in the formwork seven 100 mm diameter and two 150 mm diameter cylinder was also cast to measure the compressive test of the concrete of each specimen. Finally after concreting, formwork was covered by clean rags to prevent water loss from specimen. Figure 4.6 shows the concrete cylinder moulds after pouring the concrete.

Figure 4.6: Concrete cylinders cast in moulds

Concreting was done before settings occurred and figure 4.7 shows the specimen after concreting.

Figure 4.7: Recently cast specimen

4.3.8 Curing and Removal of Specimens from the Formwork

To prevent shrinkage cracks and reduce water loss each specimen was cured at least once in a day. Formwork was loosened and slid backwards of the beam four days after pouring. Figure 4.8 shows the beam after removal of formwork.

Figure 4.8: Beam after stripping

4.3.9 Placing the Concrete Strain Gauges

Seven 30 mm TML strain gauges were installed on each specimen for acquiring data of concrete strain during testing. A set of three concrete strain gauges was placed on each predicted concrete crushing side of the beam. One concrete strain gauge was placed on the top middle section of the beam. The arrangement of the concrete strain gauges in the beam is shown in Appendix C.

Before placing the strain gauges the surface was cleaned by a wire brush and later the surface was smoothened by sandpaper. Finally acetone was used to clean the surface and CN adhesive glue was applied to attach the concrete strain with the concrete beam. Figure 4.9 shows the final strain gauge attached to the surface.

Figure 4.9: Concrete dial gauges

4.3.10 Preparing the specimen for Testing

Strain gauges were soldered to connections and plug into the system 5000 data acquisition system to record data during testing. Total 10 connections were used for each beam. A complete soldered strain gauge connection is shown in figure 4.10.

Figure 4.10: Strain gauge wires soldered with connection

Before testing, grid was drawn on both end of the beam as predicted shear cracks would develop in these regions. Using these grids the slope of the shear cracks development of four beams would be compared after testing.

4.4 Testing the Specimens

4.4.1 Test Setup

The test setup of three post-tensioned beams was same and for control beam different test setup was adopted. The number of components involved during testing is outlined below:

1. Specimen supporting system
2. Spreader Beam
3. Instron Loading machine
4. Load Cells
5. Load Variable Displacement Transducer (LVDT)
6. System 5000

7. Anchoring System

Each of these materials has been described in detail below:

Specimens Support: 2C100-10 steel plates were placed at desired location before organizing the test set-up. Supports were placed on the top of the steel plates after measuring the exact location. Two triangle shaped steel blocks were used as support and 20 mm thick of metal plate was placed between the concrete girder and support to prevent local cracks. Figure 4.11 shows the supporting system arrangement of the girders.

Figure 4.11: Main support arrangement for girders.

Spreader Beam: Spreader beam was used for the application of four point loading on the beam. The load bearing capacity of the spreader beam is 100 KN with a total length of 1000 mm. The adopted loading span was 500 mm and care was taken as it had a limited load bearing capacity. Deflections were not considered, as not major deflections occurred during loading on spreader beam. Figure 4.12 shows the placement of the spreader beam on the top of the beam.

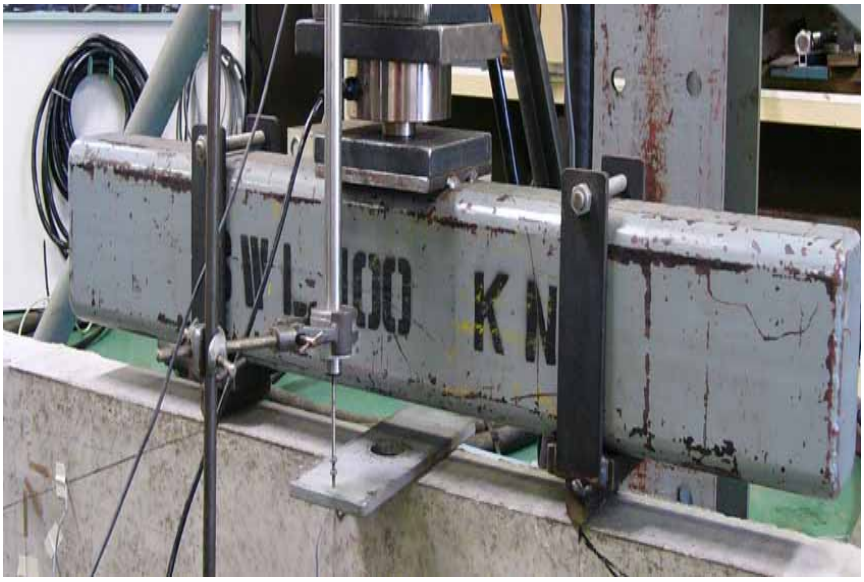

Figure 4.12: Placement of Spreader beam on concrete girders.

Instron Loading machine: The load limit of the hydraulic loading ram is 250 KN with a maximum travel of 150 mm. Due to maximum travel limitation; the test setup was designed so that the beam could fail within the travel limit of the loading ram considering maximum deflection could occur during loading. The appropriate height of the loading ram was installed after adjusting the height of the loading point by placing steel plates. Figure 4.13 shows the load application on girders by loading ram.

Figure 4.13: Loading ram of Instron machine

Load Cells: Three thru-hole types of load cells (one 222 KN load cell and two 440 KN load cells) were used to measure the applied load and the post-tensioning forces in the external bars. Two load cells were placed on the dead anchorage end of the external cables to measure the cable force and one load cell was positioned under the loading ram to measure the load applied by Instron machine. Figure 4.14(a) and 4.14(b) demonstrates the placement of the load cells on the dead anchorage end and under the loading ram:

Figure 4.14(a) Load Cells on dead anchorage end

Figure 4.14(b): Load Cells under the loading ram of Instron Machine

Load Variable Displacement Transducer (LVDT): LVDT was used to measure the deflection of the beam during the application of loading. The maximum travel limit of LVDT was ±50 mm. Figure 4.17 gives a detail view of LVDT measuring deflection data during loading.

Figure 4.15: Installation of LVDT during testing of beam

System 5000 Data Acquisition System: System 5000 system was used to collect data during loading. It can accommodate up to 20 channels. Total 14 channels were used to supply data to this system during loading and data were recorded through Strain Smart Program. 10 channels were used for strain gauges, 3 channels for load cells and 1 channel used to record data of LVDT.

Anchoring System: the anchorage system was made of one C150-10 steel section and this steel section incorporated with 18 mm hole through which 16 mm diameter post-tensioned threaded bars passed (Figure 4.16). The end of the threaded bars was attached with nuts on bearing plates, which had a hole to receive the bars. These bearing plates were made of high strength steel. Short length of the bar was provided at the dead end, sufficient to attach the load cell, bearing plates and nuts. As the live end length also

insufficient an extra threaded rod of 1000 mm was used for providing enough length for the process of jacking. Two extra concrete blocks were placed to support the hydraulic jack during post-tensioning.

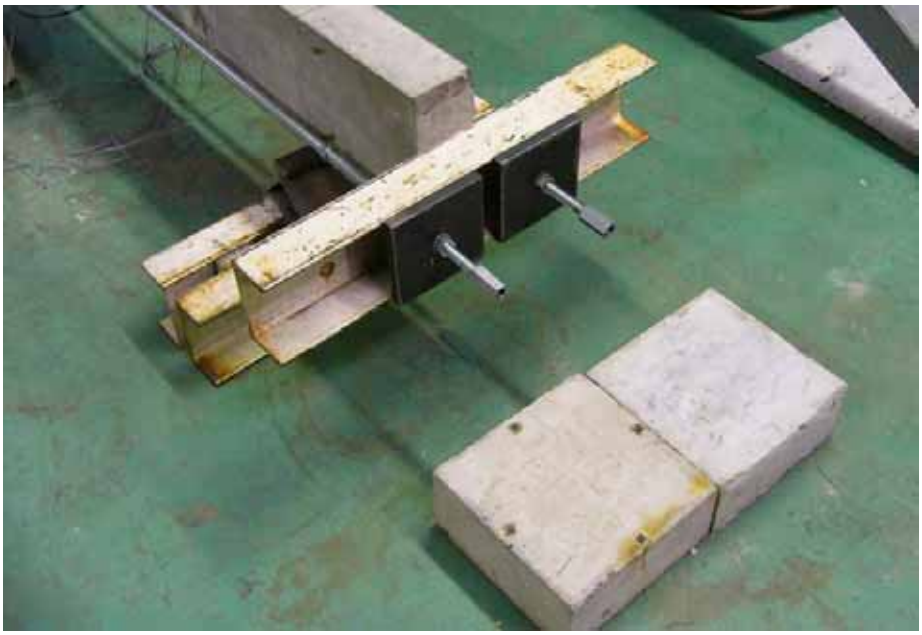

Figure 4.16: Anchoring system for post-tensioned beam.

4.4.2 Testing Procedure

The four specimens were loaded in 1 mm/hour increment by loading ram. The testing procedure of four specimens will be described in detail in this section.

4.4.2.1 B1 Beam

B1 beam was the control beam and it was tested to find the ultimate load bearing capacity of the beam without post-tensioning. The loading by Instron machine was continued until the beam was failed in shear. Loading was temporarily held constant after increment of around 20-30 KN to check the shear crack development and crack width was measured using crack-width identification card. Load, deflections of the beam during loading,

concrete strain and steel reinforcement strain were recorded by System 5000 data acquisition system. Figure 4.17 shows the beam B1 during loading.

Figure 4.17: Beam B1 during testing.

4.4.2.2 B2 Beam

B2 beam was preloaded to initiate the shear crack. Preloading was stopped at 75 KN. The load was released and the external post-tensioning rod was attached. Each threaded rod was stressed using a manually operated hydraulic jack and each rod was post-tensioned in small increment of around 20-30 KN and shifted to another rod after each increment. Figure 4.18 shows the hydraulic jack stressing the external rod. Stressing of the rods stopped when the combined post-tension force reached to 100 KN. After strengthening of the beam by external post-tensioning the load was applied continually until shear failure occurred. Load, deflections of the beam during loading, concrete strain and steel reinforcement strain readings were monitored automatically by System 5000 data acquisition system. During loading the propagation of the shear crack was also recorded manually. Figure 4.19 shows the beam B2 during loading.

Figure 4.18: Post-tensioning jack stressing threaded rods.

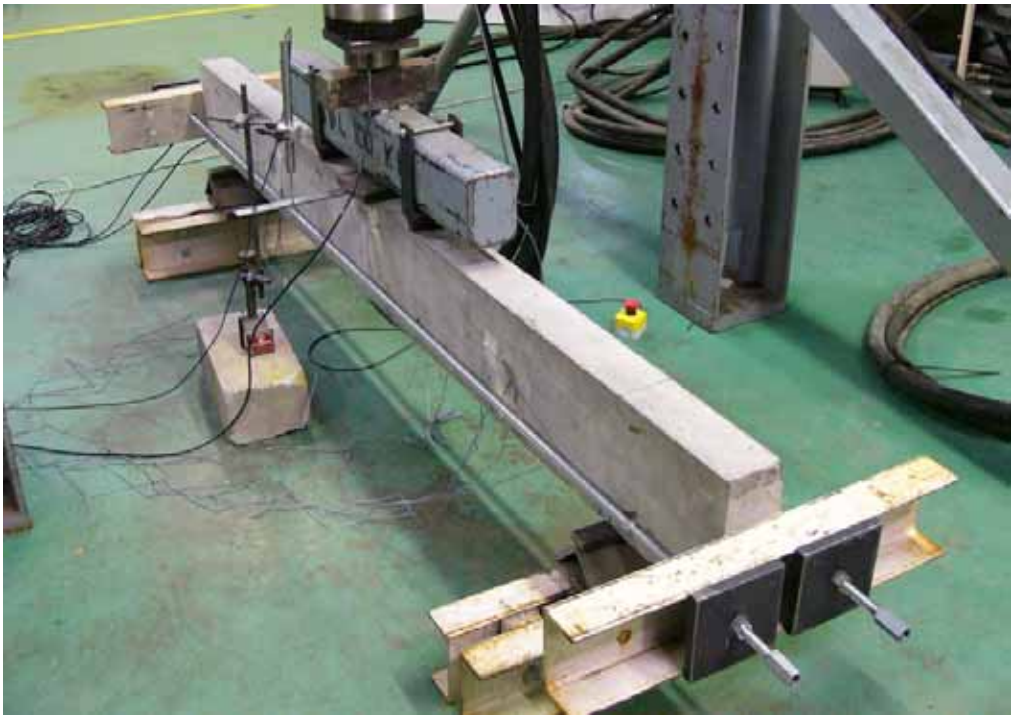

Figure 4.19: Beam B2 during testing

4.4.2.3 B3 Beam

B3 beam was strengthened with out initiating any shear crack by preloading. Each threaded rod was stressed by post-tension force in small increment of around 20-30 KN and shifted after each increment of loading. Stressing of the rods stopped when the combined post-tension force reached to 100 KN. The load was applied continually until the beam failed in shear. Load, deflections of the beam during loading, concrete strain and steel reinforcement strain readings were monitored automatically by System 5000 data acquisition system. During loading the initiation and propagation of the shear crack was also recorded manually. Figure 4.20 shows the beam B3 during loading.

Figure 4.20: Beam B3 during testing

4.4.2.4 B4 Beam

B4 beam was preloaded up to 72.3 KN to initiate certain width (1 mm as beam B2) of the shear crack. The load was released and the crack was repaired by epoxy. The application of the epoxy was conducted in two part processes.

1. The crack was sealed by using Fosroc Lockset E hardener. Four plastic needles were installed to inject epoxy into the crack. Required hole was constructed on the crack to attach needles. Figure 4.21(a) shows the construction of hole on the crack, whereas figure 4.21(b) describes the installation of plastic needles and application of Fosroc Lockset E hardener on the crack.

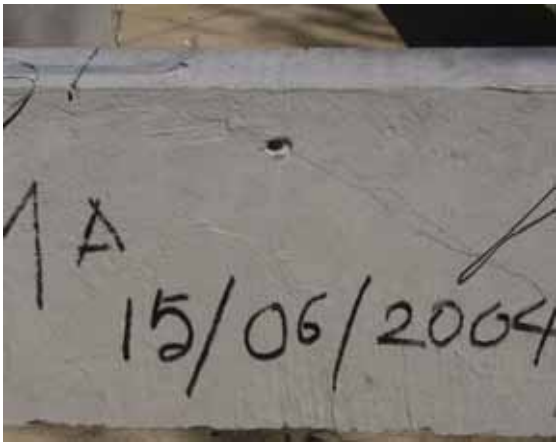

Figure 4.21(a) Construction of hole for installing plastic needle

Figure 4.21(b) Installation of plastic needle and application of Fosroc Lockset E hardener

2. After couple of days the cracks were examined by inserting water to check whether any crack remained unsealed. No cracks were found unsealed during injecting water. Later Nitofill LV epoxy was inserted through the injection. Care

was taken during the operation of injecting epoxy in the crack. Figure 4.22 shows the application of epoxy in the shear crack through the injection.

Figure 4.22: Application of epoxy in shear crack.

After the application of epoxy it was left for 3 days to set. Later the repaired beam was shear strengthened by external post-tensioning according to same procedure followed for B2 and B3 beams. Finally load was continuously applied on the beam until B4 beam was fully failed in shear. After increment of around 20-30 KN loading held constant to check the initiation and propagation of crack.

4.5 Safety Issues

The operation of external post-tensioning involved the use of considerable amount of forces. Appropriate precautions were taken to prevent accidents as these could have very serious consequences. During stressing personals were kept outside of the stressing area

as in the event of failure of the external bar or parts of the equipment and jack could be slipped out from the end of the equipment.

The mixture of Fosroc Lockset E hardener is injurious for skin and it has a hazardous effect in inhalation. For that reason, Disposable gloves and mask were worn during the application of Fosroc Lockset E hardener. The only way to remove this mixture from the skin is to use paint thinner, which causes severe irritation. The same precaution was also adopted during the operation of injecting epoxy.

A risk assessment was prepared before the test specimens started. The detail of risk assessment is given in Appendix D.

4.6 Conclusion

The preparation of specimens and processes adopted to set up the testing of girders with or without external post-tensioning and epoxy repairing has been discussed in this chapter. The results obtained from these testing have been analyzed and discussed on chapter five.

CHAPTER 5
TEST RESULTS AND DISCUSSIONS

5.1 Introduction

This chapter presents an analysis of experimental results, which was gathered during the testing stage and it tends to investigate some unexpected results. These results will be compared with the predicted design equations recommended by AS3600 and the results formulated from general shear capacity formula considering web-shear crack. Observations of four beams cracks during loading and post-tensioning have been described. Furthermore, the behaviors relating loads, deflections, strains, cracks and post-tension force in external rods are mentioned in this particular chapter.

5.2 Concrete strength

The strength and failure of the specimen is dependent on the concrete strength. Concrete is strong in compression and before cracking majority of the load is carried by concrete rather than steel reinforcement. Compression strengths of the specimen were found by conducting compression test on concrete cylinders. Figure 5.1 shows the cylinder compression test using Avery testing machine.

Figure 5.1: Cylinder Compression Test (Avery Testing Machine)

These cylinders were cast on the same day as their respective specimens, using the same batch of the batch concrete. For obtaining the accurate concrete strength of the each beam they were tested on the same day as their respective specimen. Table 5.1 shows a summary table of the concrete strengths values for each specimen.

Table 5.1: Cylinder compression test results

Beam No	Average Maximum Load (KN)	Compressive Strength (MPa)
1	189	24
2	187	24
3	283	36
4	140	18

5.3 Load and Deflections

The change of deflections with applied load has been discussed in this particular part. As the load case was different, the load-deflection curve of the tested four beams shows different shapes of graphs. The reason for obtaining different shapes of curves are described and investigated in this section. It is mentionable that only mid span deflection has been considered as maximum deflection occurs in the mid span. This section separately explains about load-deflection curve for every beam and in the end the results have been compared and been showed in a combined graph.

B1 Beam

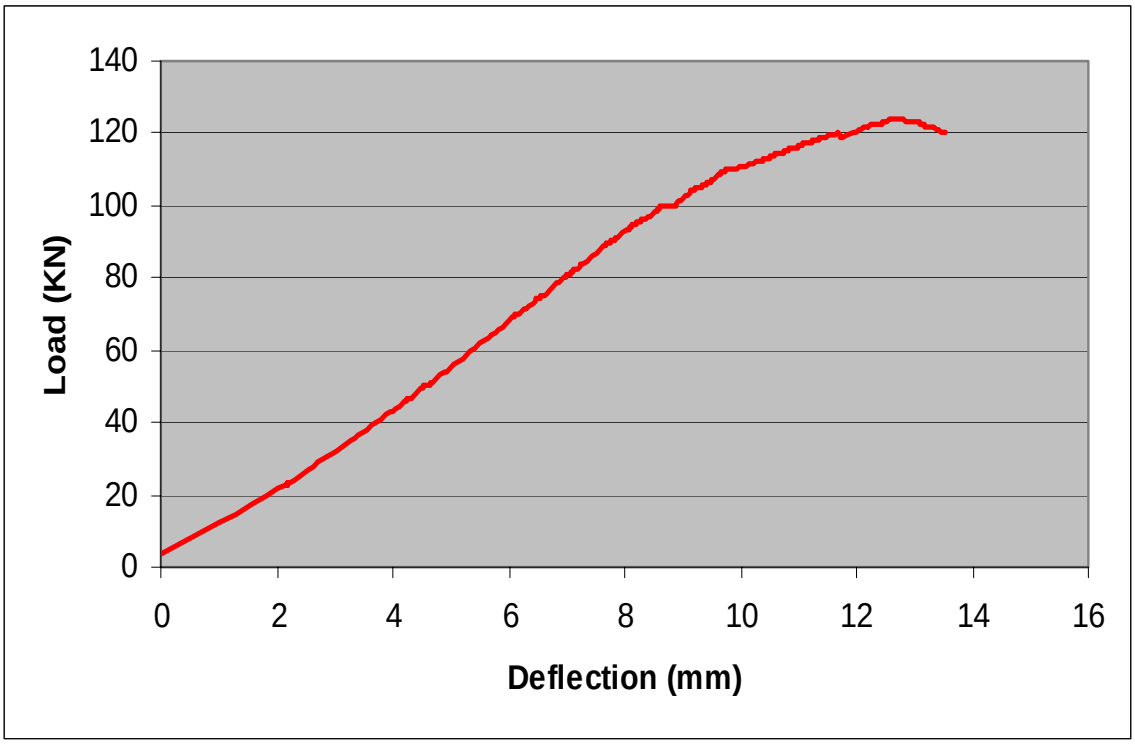

Figure 5.2: Load Vs Deflection Curve for Beam 1

Figure 5.2 shows the load-deflection curve for beam 1, which was considered as a control beam. The slope of the graph is fairly constant until 50 KN. At this point, the first shear cracking was observed. After the appearance of first crack beam stiffness was reduced.

From this point onwards, the load is increasingly transferred from the concrete to the stirrups with the increasing of the load. The beam showed not much increase of deflection up to the loading of 100 KN due to initial error in loading on B1 beam which will be discussed later on crack pattern section. From this point onward the slope becomes shallower up to the maximum load of 122 KN. The crack was started to open up from 100 KN. The corresponding deflection at this point is 13 mm. At 122 KN the beam was failed and the shear stirrups had reached yield. As a result as the loading was continued to increase, the deflection of the beam also continued to increase.

B2 Beam

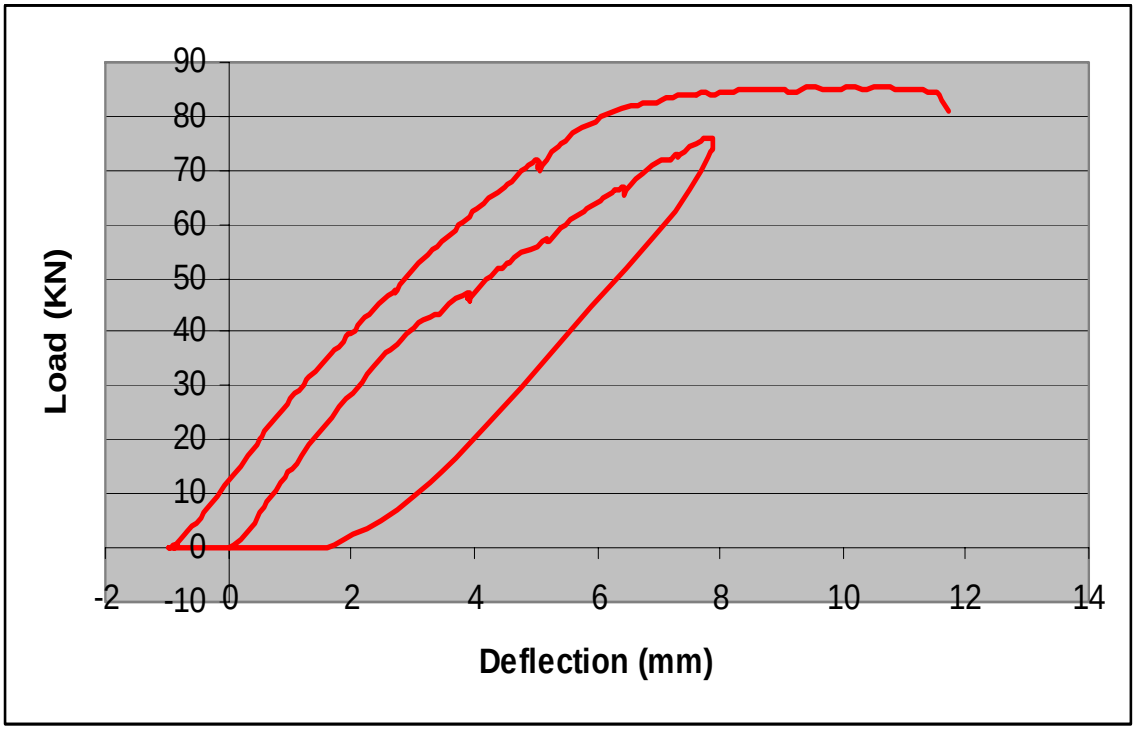

Figure 5.3: Load Vs Deflection Curve for Beam B2

The response of applied load versus mid span deflection of beam B2 is shown in figure 5.3. Initially the beam was preloaded without applying post-tensioned force and epoxy to form crack in the beam. During preloading beam 2 showed very much similar behaviour as beam 1. The slope of the graph is constant until the shear crack develops 45 KN. After

the initiation of first crack, the slope of the graph becomes shallower. The crack was opened up with the increasing of loading and loading was continued up to 75 KN. The maximum crack width of the beam at 75 KN was 1 mm and the deflection at this point comes around 8 mm.

And then the beam was unloaded and the residual deflection found was 1.85 mm. Later the beam was strengthened with 100 KN external post-tensioning force and the beam deflection reduced to -1 mm (upward). This is due to the axial compressive force exerted over the length of the specimen, which causes upward deflection of the beam. The crack widths were also reduced and it came up to 0.3 mm. Again the beam was loaded and loading was continued until the beam reached its ultimate capacity and failure occurred eventually.

It can be noticed from the graph that the beam deflection is reduced due to post-tensioned force. The curve shows linear development up to 71 KN loading and after that the beam shows rapid increase of deflection with the increase of loading. This is because the crack width is opened up rapidly from this point onwards. The applied maximum load was 86.3 KN. The corresponding deflection at maximum loading was around 11.019 mm. Compared with the first beam B1 the maximum loading reduced to 35.7 KN. That means the load carrying capacity of the beam reduced to 29%.

B3 Beam

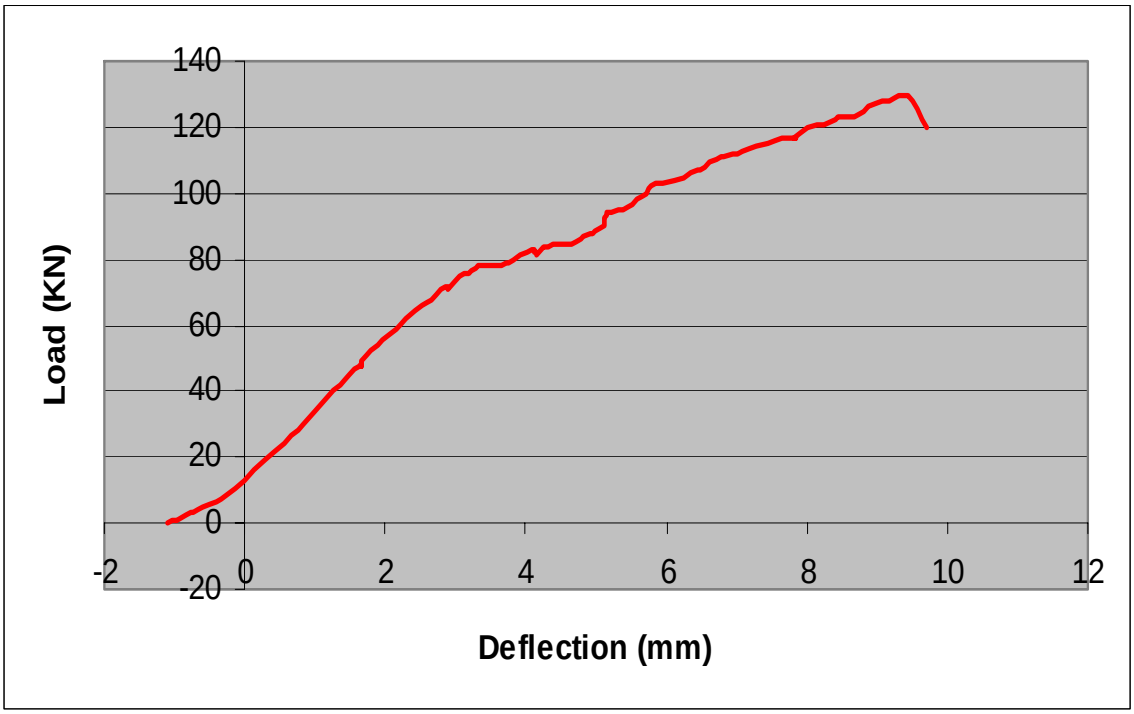

Figure 5.4: Load Vs Deflection Curve for Beam 3

Figure 5.4 shows the load-deflection characteristics of beam B3. Before applying load the beam was strengthened with external post-tensioned force of 100 KN. As post-tensioned force produce upward deflection the beam encountered negative deflection and the initial deflection of the beam before applying load was 1 mm upward. First crack appear at around 78 KN. From this point on the graph, the curve becomes shallower as the load transfer from the concrete to shear stirrup. The deflection increases constantly with the increase of the loading after initial crack and the maximum load was obtained 130.3 KN. The corresponding deflection comes around 9.425 mm and the maximum crack width was 2 mm.

B4 Beam

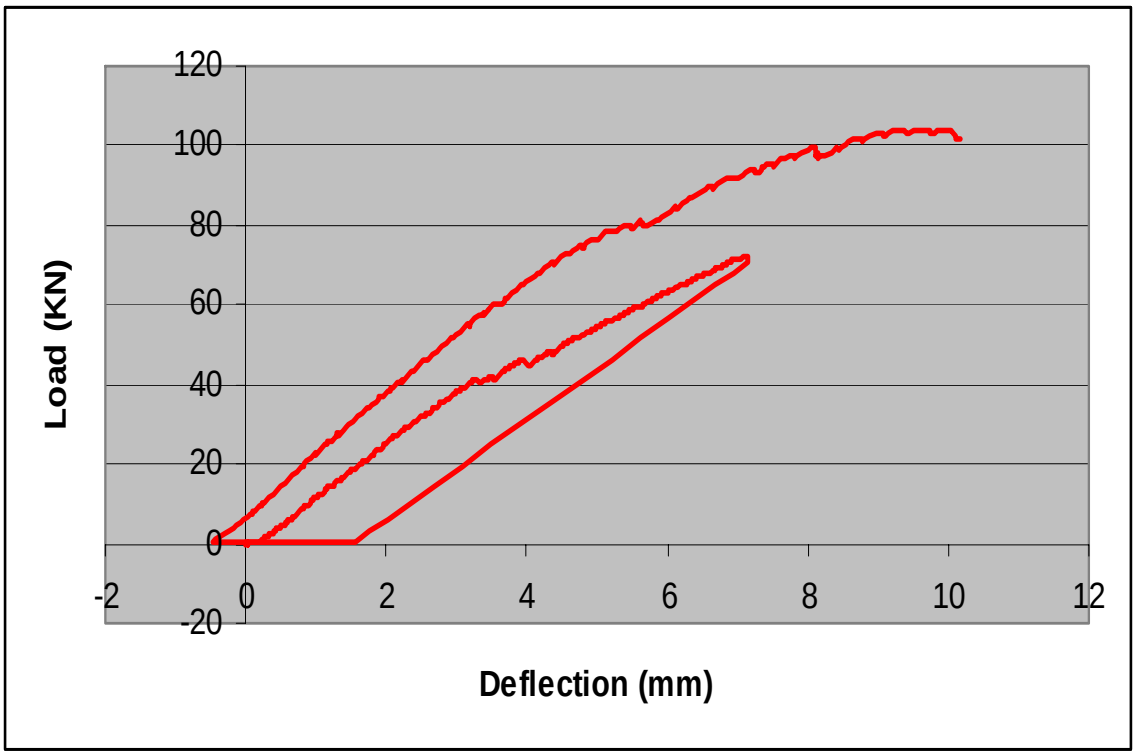

Figure 5.5: Load Vs Deflection Curve for Beam 4

Load versus deflection response for beam B4 is shown in figure 5.5. Initially the beam was cracked by preloading. The first crack was observed at around 42 KN. After that the loading was continued up to 72.3 KN. From 42 KN the curve becomes shallower as the transformation of the force from concrete to sheer stirrup. The loading was stopped at 72.3 KN. The deflection come around 7.14 mm and the maximum crack width at this point was 1 mm.

And then the beam was unloaded and the residual deflection found was 1.8 mm. Later the crack was repaired by epoxy and strengthened with 100 KN external post-tensioning force. As external post-tensioned force produces upward deflection of the beam deflection reduced to -0.47 mm (upward). Again the beam was loaded and loading was continued until the beam reached its ultimate capacity in shear and failure occurred eventually.

From the figure it can be noticed that the curve gradient is constant up to 77 KN. The first cracking was observed at around 77 KN. The curve becomes shallower as a result of maximum load carried by shear stirrup. And from this point onward, the beam shows rapid increase in deflection with the increasing of loading on the beam. The maximum load found was 103.95 KN. The corresponding deflection was 9.56 mm. Comparing with the B3 beam the beam shows a reduction of 26.35 KN loads. This is due to the higher concrete strength of B3 at 36 MPa comparing to the 18 MPa concrete strength of B4.

5.3.1 Comparison of Load-Deflection responses of 4 beams

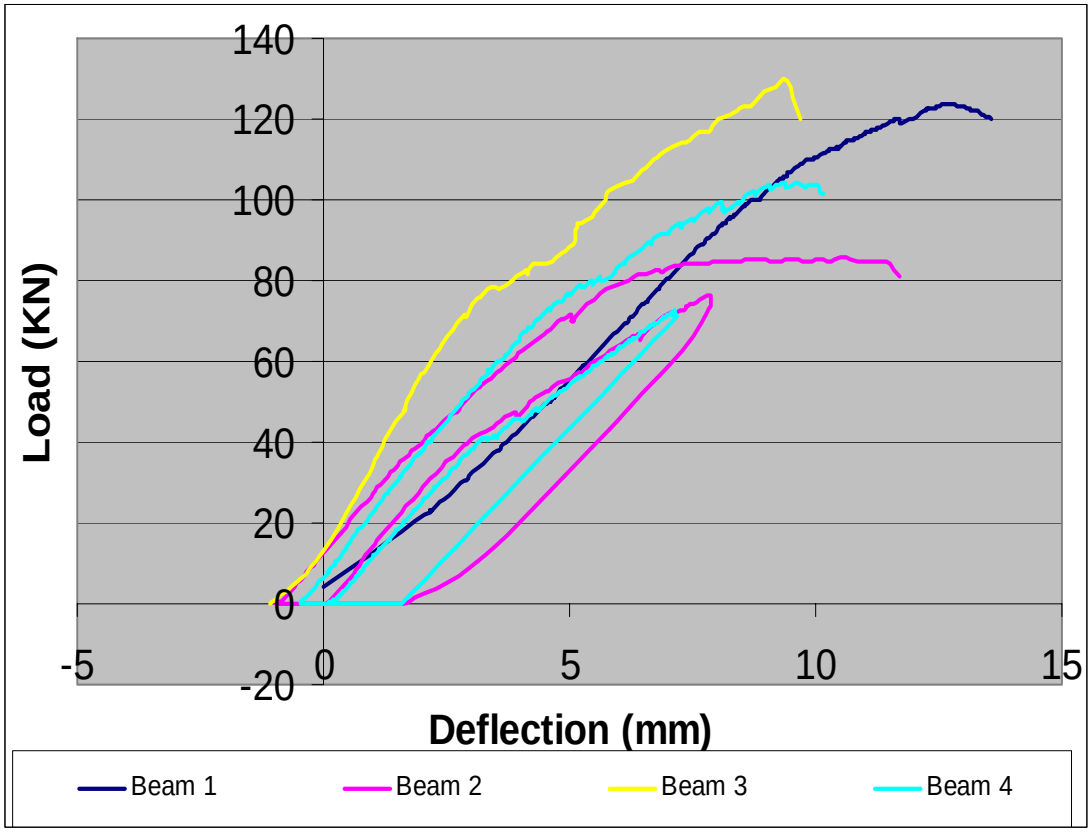

Figure 5.6: Load Vs Deflection Curve for 4 Beams

The overall load-deflection characteristic of the beams is shown in figure 5.6. Before post-tensioning it can be seen from the initial linear slopes of B1, B2 and B3 that the gradient is different. This load-deflection response is due to the strength of the concrete.

The stronger the concrete the steeper will be the gradient of the load-deflection response. Although the concrete strengths of the B1 and B2 are same but it shows different gradient due to some error which occurs during the loading on B1.

It can be seen also from the graph that, incase of B2 and B4 after the initiation of first crack during preloading around 45-50 KN the slopes become shallower at the same rate. And in case of initial crack development of B3 and B4 beams after post tensioning the slopes become shallower after around 78-80 KN as the load is transferred from the concrete to shear stirrups.

Apart from control beam, the maximum applied load noticed for three specimens after shear strengthened with external post-tension is 130.3 KN. The control specimens have load capacity of 122 KN. The ultimate load capacity of B1 was 86.3 KN, 34% less than B3 and 27.4% less than B1. So, specimen B2 could not be strengthened with the use of external post-tensioning alone. Whereas, the ultimate load carrying capacity of B4 was found 103.95 KN, 20.22% less strength than B3 and 17% increase strength than B2. One reason behind the high difference between the ultimate load carrying capacity between B3 and B4 is the variation of concrete strength. Therefore, it can be concluded that the epoxy repairing of B4 and strengthening by external post-tensioning gives better shear load carrying capacity than without repairing the crack with epoxy.

The ultimate deflections of the four beams were 13 mm, 11.019 mm, 9.425 mm and 9.56 mm respectively. Beam B2 although shows a small reduction of deflection from 13 mm to 11.019 mm comparing the control beam but shows the higher deflection comparing to B3 and B4, which means B2 beam could not be strengthened with the use of external post-tensioning on its own. The B4 beam which was strengthened by external post-tensioning after epoxy repairing gives 27.5% improvement in deflection comparing to B1, and 13.2% improvement in deflection comparing to B2 and gives almost the same deflection as B3. Due to the less concrete strength B4 beam shows a bit higher deflection than B3. As a result, it can be deduce the point that, the shear strengthening of B4 beam

by external post-tensioning with epoxy repairing gives less deflection and better serviceability.

A summary of these four beam test results is given below in Table 5.2:

Table 5.2: Deflection Vs Shear capacity of four beams

Beam No	Preloading (KN)	Post-Tensioned (KN)	Epoxy	Ultimate Deflection (mm)	Shear Capacity (KN)
1	X	X	X	13	122
2	75	100	X	11.019	86.3
3	X	100	X	9.425	130.3
4	72.3	100	√	9.56	103.95

From these results, it can be said that, the external post-tensioning with epoxy repairing does have the ability to increase the shear load capacity and decrease the deflection of the girder, as the external post-tensioning increase the stiffness of the girder. As a result it gives better serviceability.

5.4 Crack Observation

The final failure crack pattern developed after the loading for each beam was almost the same. Every beam failed in shear as expected rather than flexure. In this particular investigation all 4 beams have failed in shear-compression as failure occurs by crushing of the compressive concrete and it occurs before the full flexural moment capacity. And it was observed that web-shear type of cracking occurs for each and every beam, which reflects that the beam fails in shear compression.

The crack widths were differed after the application of external post-tensioning and the visual inspection of the development of the cracks was made after 20-30 KN intervals. Below the crack investigation of 4 beams had been described and at the end of this section the comparison of crack width with the development of load has been shown.

B1 Beam

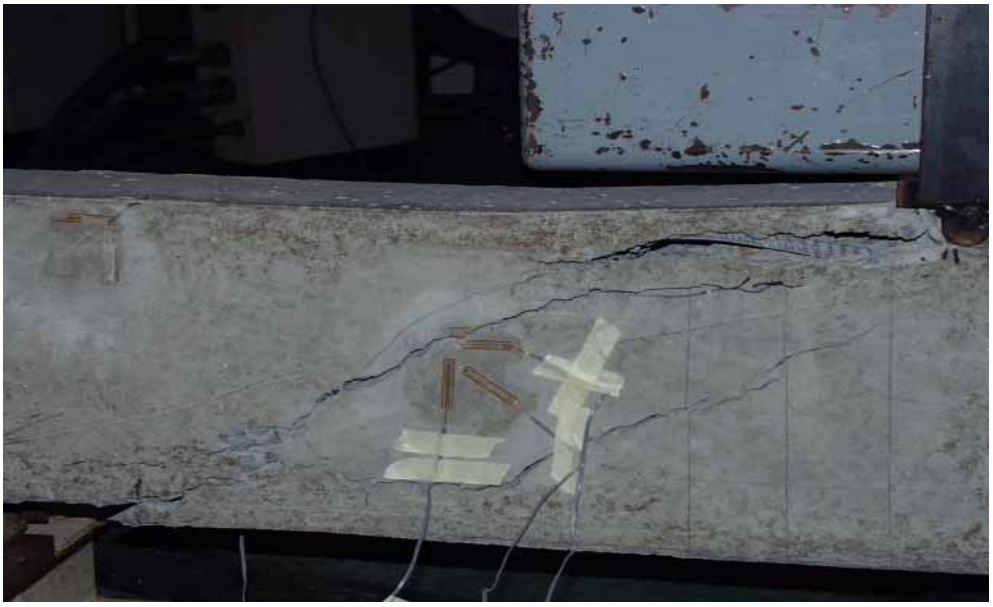

Figure 5.7: Failure Crack Pattern of Beam B1

Due to error of loading, the initiation of first shear crack of B1 beam was hard to figure out. Initially when loading was applied on the beam B1, the rate of loading was too high that in less than 5 seconds around 80 KN load was applied on the beam. As the data acquisition duration record was 5 seconds no data recorded in system five thousand machine. For the safety and precise results, the loading was stopped and a small shear crack was found starting from the support along the loading point of the beam during unloading. The precise load for the initiation of loading was not measured because of the frequent rate of loading. The width of the crack was measured 0.5 mm. Later the loading was started again, and small shear crack appeared along the loading point of the beam at a 50 KN load. It started at the point of the loading and moved down an approximately 45° angle towards the beam support. The crack was started to open up after 70 KN at this load the crack was measured 1 mm. At maximum load the crack width was 2 mm, decreasing to 1.5 mm when the specimen was un-loaded. The final crack pattern at maximum load can be seen in Figure 5.7.

B2 Beam

Figure 5.8: Preloading Crack Pattern of Beam B2

Figure 5.8 shows the crack pattern of beam B2 after preloading. Initial crack was appeared at 45 KN. The crack width measured was 0.3 mm and started to propagate at a 45° degree starting from support along the loading point of the beam. The maximum load applied during preloading was dependent on the crack development and the loading was stopped at 75 KN and the crack width was measured 1 mm. after the application of 100 KN external post-tensioning force, this crack closed up to 0.3 mm due to axial compressive force over the beam. The maximum crack width at failure load was 86.3 KN and the corresponding crack width was 2 mm. The final crack pattern after external post-tensioning is shown below in figure 5.9. Comparing crack pattern between B1 and B2 beam it is apparent that the final crack pattern is the same for each beam started from the support and finished at the loading point of the beam.

Figure 5.9: Failure Crack Pattern of Beam B2

B3 Beam

Figure 5.10: Failure Crack Pattern of Beam B3

Figure 5.10 shows the final crack pattern of B3 beam after post-tensioning. After the application of 100 KN external post-tensioned force the load was applied on the beam B3. The first shear crack appeared at 78 KN. The crack started to propagate from the support along the loading point of the beam. The maximum load achieved after the application of the external post-tensioning was 130.3 KN and the width of the crack comes around 2 mm.

B4 Beam

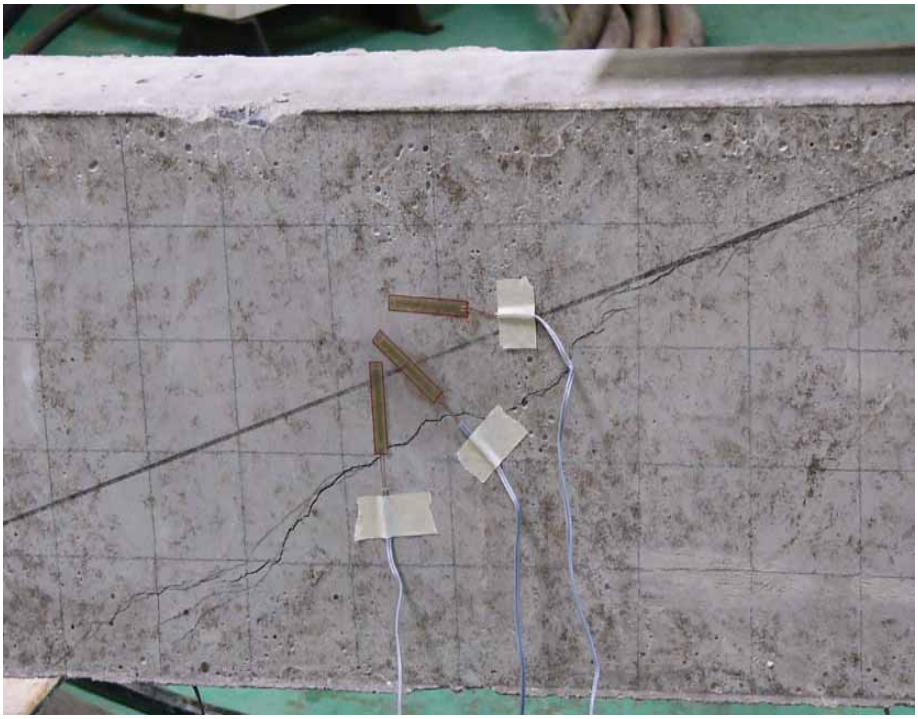

Figure 5.11: Preloading Crack Pattern of Beam 4

The loading pattern for the beam B4 was carried out in two stages. At first the beam was cracked by preloading. The first crack was observed at around 42 KN and width was measured 0.3 mm. the crack propagation shows the same pattern as before and the loading was carried out up to 72.3 KN. Figure 5.11 shows the preloading crack pattern of B4 beam. At this point the crack width was measured 1 mm. Later the crack was repaired by the epoxy and strengthened with 100 KN external post-tensioning force. The first

crack was appeared at 77 KN and the crack width measured was 0.3 mm. after the initiations of the first crack it shows rapid propagation of crack with the increase of loading. The maximum loading achieved after epoxy repairing and external post-tensioning was 103.95 KN. The maximum crack measured was 2 mm. Below the failure crack pattern after the application of epoxy and external post-tensioning is given. Figure 5.12 shows the final crack pattern after the application of epoxy and post-tensioning forces. Green line indicates the crack pattern, which was formed during preloading and was repaired by epoxy.

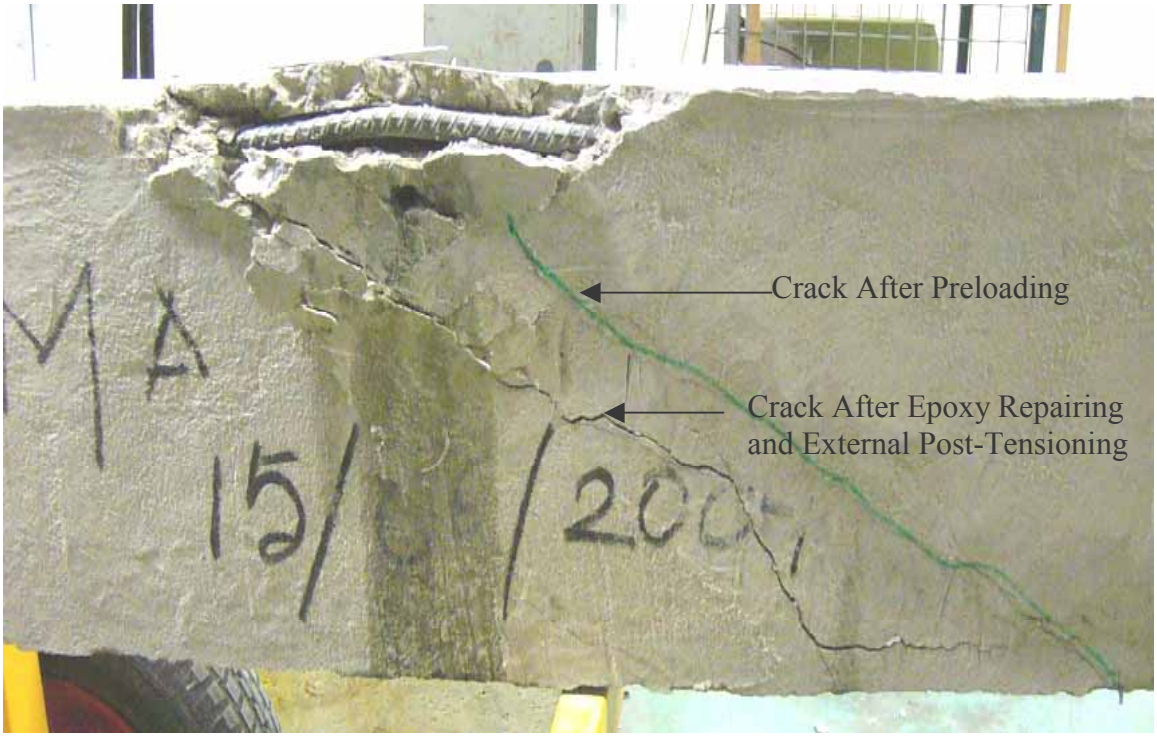

Figure 5.12: Failure Crack Pattern of Beam 4 after applying Epoxy and Prestressing

From figure 5.12 it is apparent that, the new crack is shifted from the previous crack. The compressive strength of the epoxy is much higher than the concrete strength of the beam (approximately 66-70 MPa for epoxy), which gives higher compressive strength of the preloading crack section. As a result, the new crack was developed and shifted from the previous crack, which occurred during preloading.

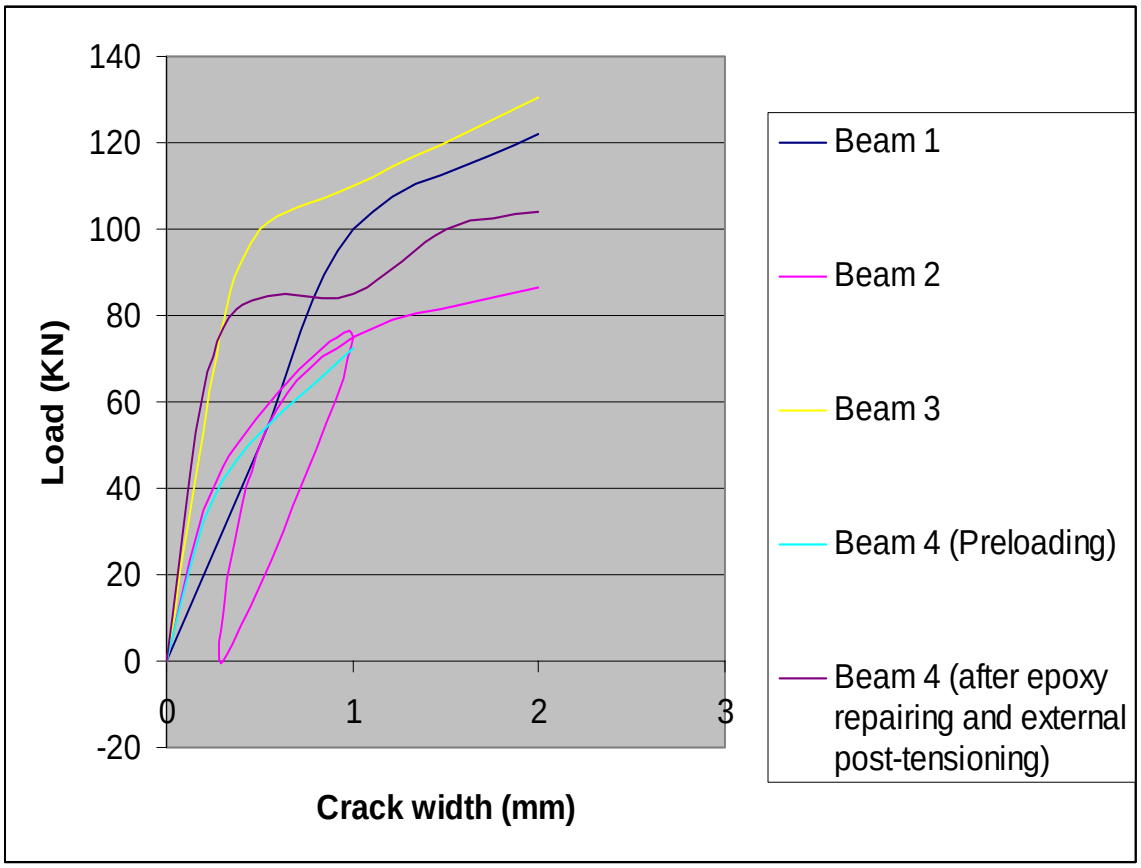

Figure 5.13: Applied Load Vs Crack Width Curve

Figure 5.13 shows the comparison of the crack width development during loading of four beams. From the graph it is obvious that, due to external post-tension force the crack formation delayed. It can be seen from the graph that, the beam shows rapid increase in crack formation after crack width reached 1 mm. This is because of the low cover adopted for each beam and as a result every beam shows premature failure. After the application of epoxy and 100 KN post-tensioned force the crack formation delayed comparing the initial crack formation during preloading. Which means epoxy repairing and external post-tensioning makes positive impact on beams serviceability.

5.5 Concrete Strain Distribution of Beams

A series of three concrete strain gauges was used on both ends of the beams to determine the principle strains and maximum shearing strains during loading. The angle of shear cracks during loading can also me calculated using the data of the shear strains. A sample calculation is included below, describing the steps involved in calculating these strains from the raw data gathered during loading. The sample calculation was done based on the raw data found when the loading (72.3 KN) occurs on the B4 beam.

The strain along a line at an angle θ to the x-axis direction is given by:

$$\varepsilon(\theta) = \varepsilon_x \cos^2\theta + \varepsilon_y \sin^2\theta + \gamma_{xy} \sin\theta \cos\theta \qquad (5.1)$$

Assuming,

ε_0	=	horizontal strain gauge data
ε_{90}	=	vertical strain gauge data
ε_{45}	=	diagonal strain gauge data

Therefore, the following equation can be developed from equation (5.1):

$$\varepsilon_0(\theta) = \varepsilon_x \cos^2\theta_0 + \varepsilon_y \sin^2\theta_0 + \gamma_{xy} \sin\theta_0 \cos\theta_0 \qquad (5.2)$$

$$\varepsilon_{90}(\theta) = \varepsilon_x \cos^2\theta_{90} + \varepsilon_y \sin^2\theta_{90} + \gamma_{xy} \sin\theta_0 \cos\theta_{90} \qquad (5.3)$$

$$\varepsilon_{45}(\theta) = \varepsilon_x \cos^2\theta_{45} + \varepsilon_y \sin^2\theta_{45} + \gamma_{xy} \sin\theta_0 \cos\theta_{45} \qquad (5.4)$$

When load was 122 KN the associated strain of concrete on B1 beam was:

$\varepsilon_x = \varepsilon_0 =$ - 403 x 10^{-6}

$\varepsilon_y = \varepsilon_{90} =$ --13x 10^{-6}

$\varepsilon_{45} = -11 \times 10^{-6}$

Substituting these values into Equation (5.4) to calculate the searing strain, γ_{xy} gives:

$$-11 \times 10^{-6} = -403 \times 10^{-6}\,(0.5) - 13 \times 10^{-6}\,(0.5) + \gamma_{xy}\,(0.5)$$

$$405 \times 10^{-6} = \gamma_{xy}\,(0.5)$$

$$\gamma_{xy} = 810 \times 10^{-6}$$

Having determined the strains ε_x, ε_y and γ_{xy}, the principal strains and maximum shearing strains can be found using Mohr's circle of strain, shown in Figure 5.14:

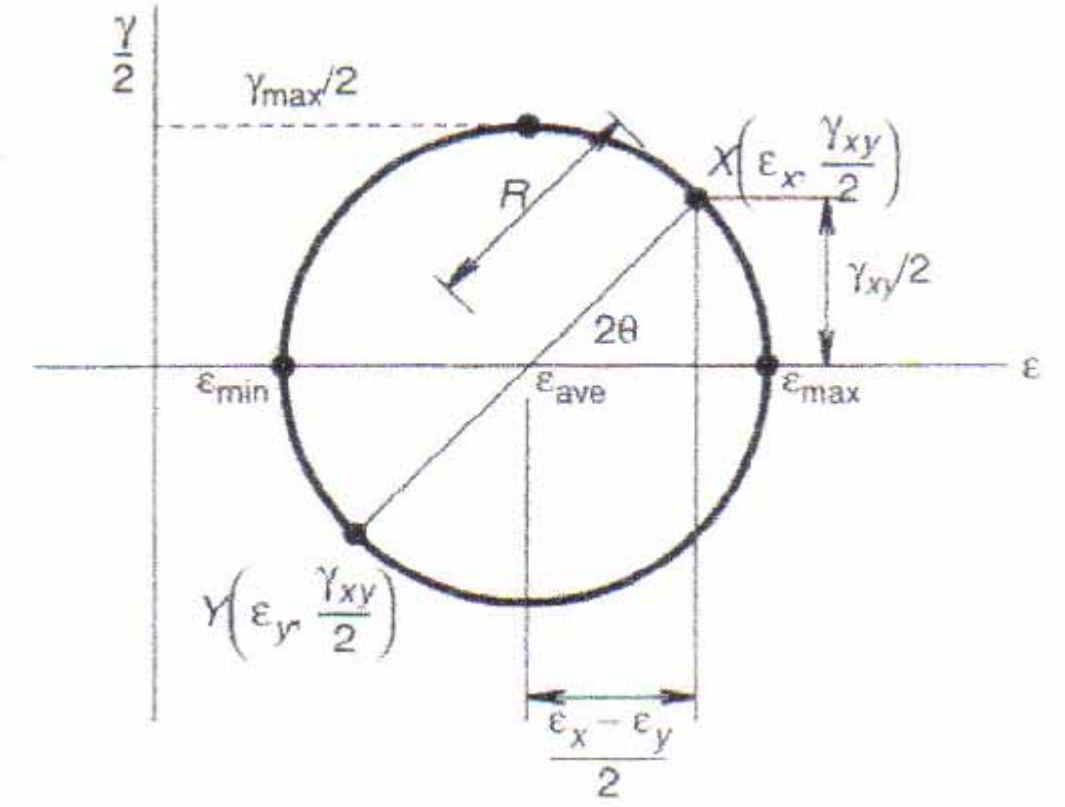

Figure 5.14: Mohr's circle of strain
(Source: Stress Analysis Study Book, 2001)

Where,

$\varepsilon_{ave} = (\varepsilon_x + \varepsilon_y)/2$ (5.5)

$= \{(-403 - 13) \times 10^{-6}\}/2$

$= -208 \times 10^{-6}$

$R = \sqrt{[\{(\varepsilon_x - \varepsilon_y)/2\}^2 + (\gamma_{xy}/2)^2]}$ (5.6)

$= \sqrt{[\{(-403 \times 10^{-6} + 13 \times 10^{-6})/2\}^2 + (810 \times 10^{-6}/2)^2]}$

$= 449.5 \times 10^{-6}$

$\varepsilon_{max} = \varepsilon_{ave} + R$ (5.7)

$= (-208 + 449.5) \times 10^{-6}$

$= 241.5 \times 10^{-6}$

$\varepsilon_{min} = \varepsilon_{ave} - R$ (5.8)

$= (-208 - 449.5) \times 10^{-6}$

$= -691 \times 10^{-6}$

$\gamma_{max} = 2R$ (5.9)

$\gamma_{max} = 2 \times 449.5 \times 10^{-6}$

$= 899 \times 10^{-6}$

$$\tan 2\theta = \gamma_{xy} / (\varepsilon_x - \varepsilon_y) \quad (5.10)$$

$= 810 \times 10^{-6} / (-403 \times 10^{-6} + 13 \times 10^{-6})$

$= -2.077$

Therefore,

$\theta = 32.14^{\circ}$

Which gives almost the same angle that was found during the loading on specimen B4. The plotting of the maximum principal strain and compression face strain against the load of the four beams have been discussed in this section:

B1 Beam

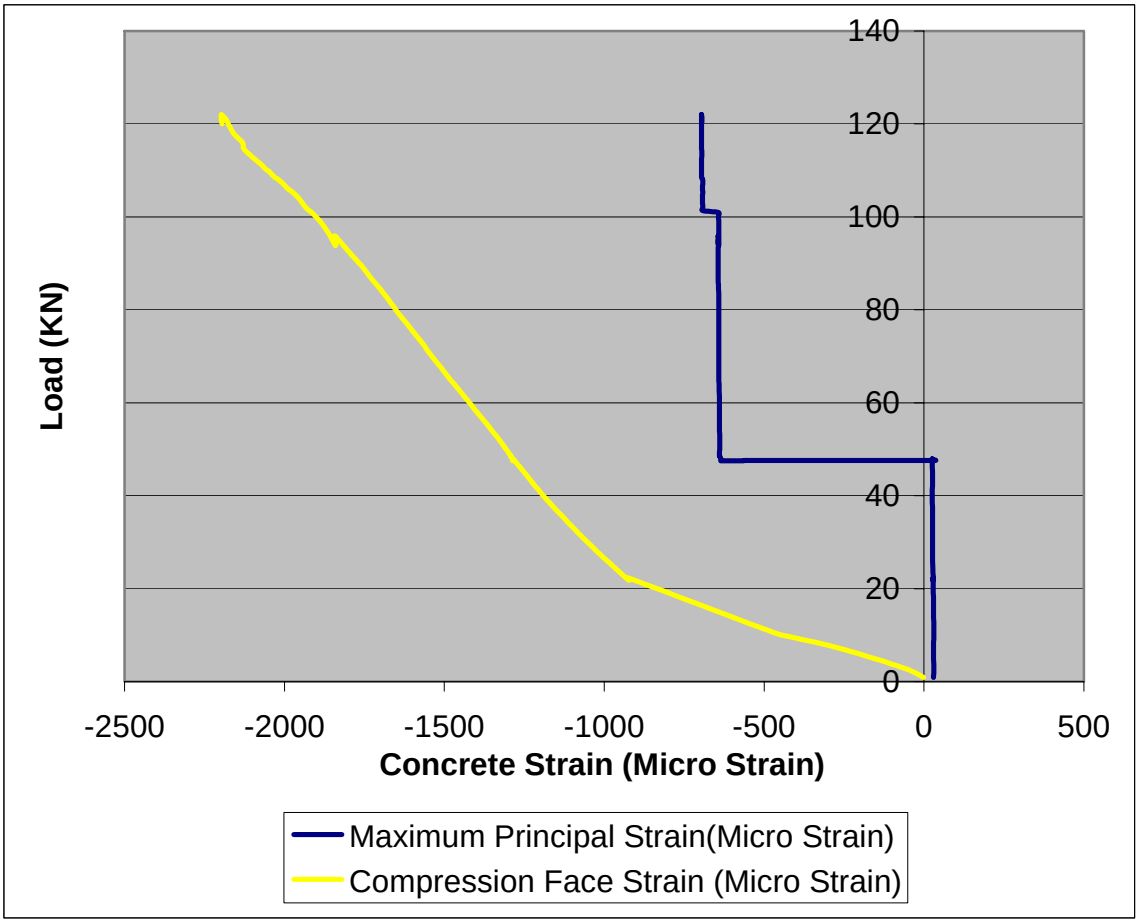

Figure 5.15: Load Vs Concrete Strain Curve for beam B1

Figure 5.15 shows the concrete strain development in B1 beam during increasing of loading. For beam B1, maximum principal strain observed on channel 6. From the graph it is obvious that maximum concrete strain occurs at top middle section (i.e. compression face section) of the beam. The maximum concrete strain measured was 2198 micro strain at compression face of the beam and the maximum principal strain was 655 micro strain. The negative sign indicates that concrete encountered compression during loading. In case of B1 beam, the initial concrete strain had been deducted from every recorded data to find the ultimate concrete strain because B1 encountered error in concrete strain value before applying the final loading.

B2 Beam

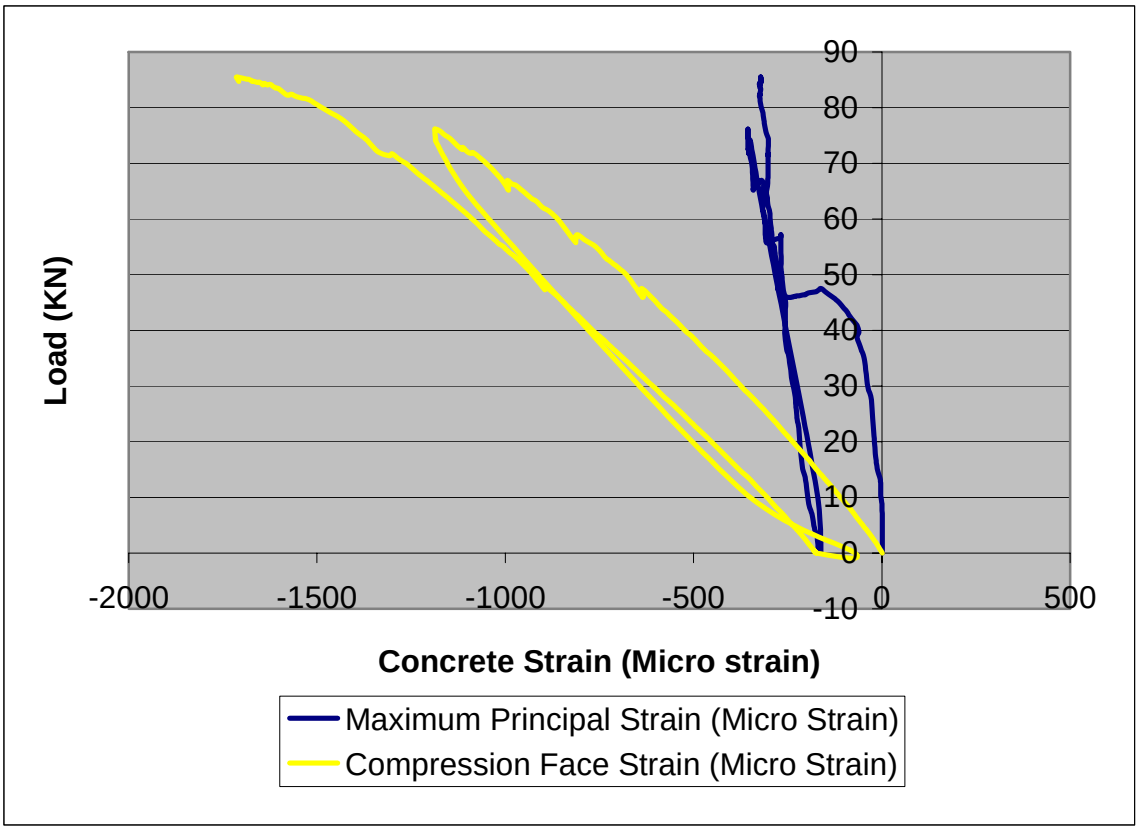

Figure 5.16: Load Vs Concrete Strain Curve for beam B2

Figure 5.16 shows the concrete strain development during the application of loading. For beam 2, channel 16 was used at the top middle section of the beam (i.e. compression face section) and maximum principal strain found in channel 18. During preloading (at 75 KN) the maximum compression strain was found in channel 16 and the concrete strain was 1187 micro strain. Before strengthening the maximum principal strain in channel 18 was 359 micro strain. After the 100 KN external post-tensioning, the concrete strain found in channel 16 was found 71 micro strain and corresponding strain in channel 18 was found 162 micro strain. This is because external post tension force exerts axial compression force which help concrete to gain more strength and hence reduction in the strain value.

After the application of external post tensioned force the maximum strain found in channel 16, which was 1714 micro strain and the negative concrete strain value indicates the top section in compression. Whereas, the maximum principal strain in channel 18 was 322 micro strain.

B3 Beam

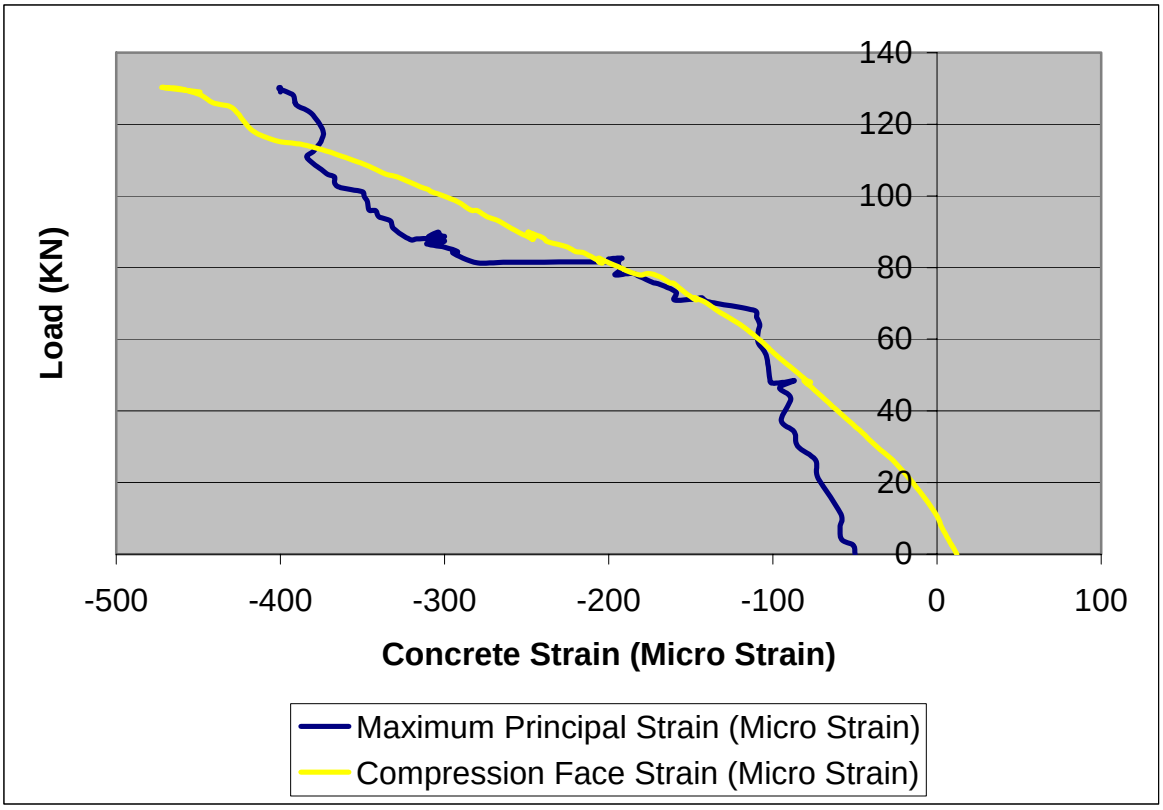

Figure 5.17: Load Vs Concrete Strain Curve for beam B3

Figure 5.17 shows the concrete strain development during the application of loading. For beam 3, channel 13 was used at the top middle section of the beam (i.e. compression face section) and maximum principal strain occurs at channel 20. Due to 100 KN external post-tensioned force the top middle section of the B3 became tensile and as a result channel 13 gave positive strain value prior to loading. This happened due to upward deflection made by post-tension force. The maximum concrete strain was obtained from

channel 13 and it was 472 micro strain and corresponding maximum principal strain was 400 micro strain.

B4 Beam

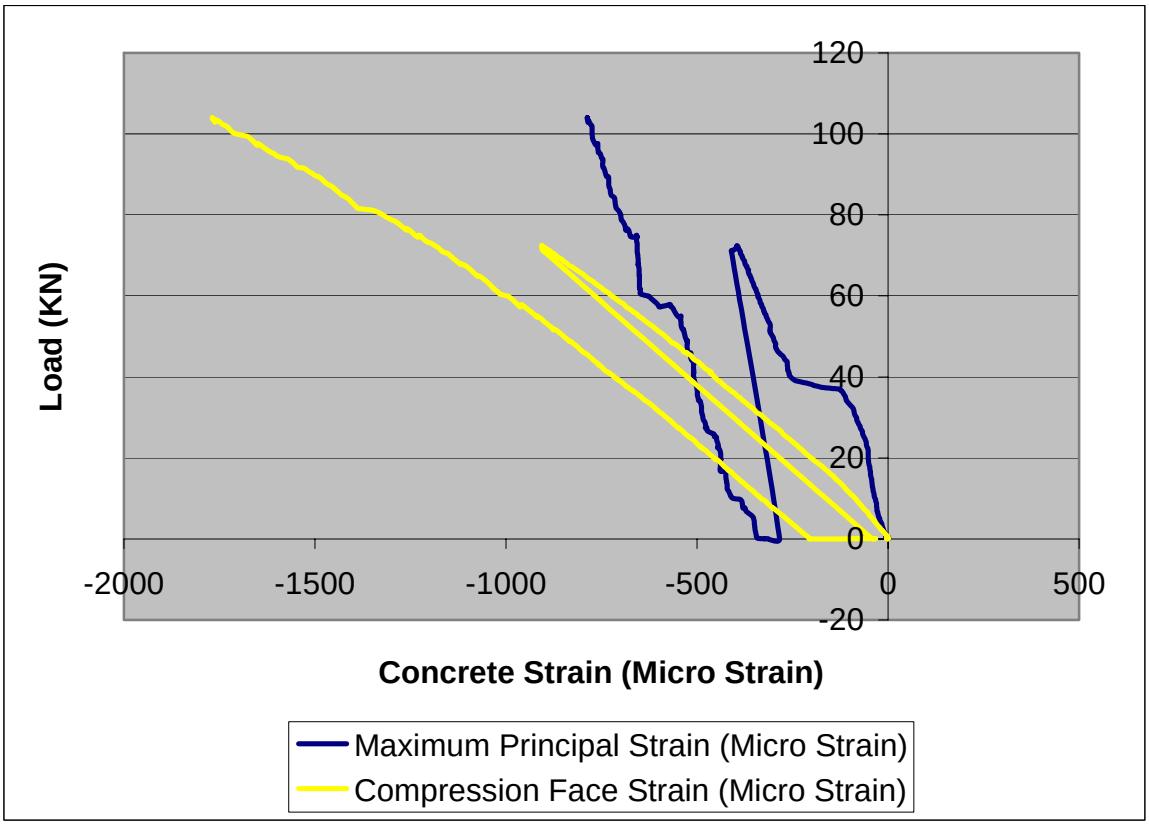

Figure 5.18: Load Vs Concrete Strain Curve for beam B4

For beam 4, channel 13 was used at the top middle section of the beam (i.e. compression face section) and maximum principal strain occurs in channel 11. Figure 5.18 shows the concrete strain development during the application of loading. After preloading the maximum strain (at 72.3 KN) for middle top section was 905 micro strain and after epoxy repairing and 100 KN external post-tension force the concrete strain obtained was 205 micro strain. This reduction of concrete strain is due to axial compression force exerted by the external post-tension force which gives lower concrete strain and increase concrete

strength. At ultimate loading the maximum concrete strain was found 1769 micro strain in compression.

On the other hand, after preloading the maximum principal strain in channel 11 was found 406 micro strain. After epoxy repairing and external post-tension force the concrete strain in channel 11 reduce to 282 micro strain due to post-tension force. After post-tensioning and epoxy repairing the maximum principal strain found was 783 micro strain.

5.5.1 Comparison of concrete strain results for the test beams

The ultimate top concrete section compression for beam B1, B2, B3 and B4 were 2198 micro strain, 1714 micro strain, 472 micro strain and 1769 micro strain respectively. It can be seen from the results that application of external post-tensioning force helps to reduce the ultimate concrete strain of the beams. B2 shows a huge reduction of concrete strain comparing to other three beams. It gives 78.5% less concrete strain comparing to control beam. This means strengthening by only external post-tensioning without preloading have much low concrete strain. Beam B2 gives 19.5% less concrete strain after epoxy treatment and strengthening by post-tensioning comparing to the control beam concrete strain.

From the above analysis, it is apparent that, external post-tensioning with epoxy repairing or without epoxy repairing gives lower concrete strain at ultimate loading. As a result, higher concrete strength, which gives more load bearing capacity of the beam.

5.6 Steel Strain Distribution of Beams

5.6.1 Tensile Reinforcement Strains

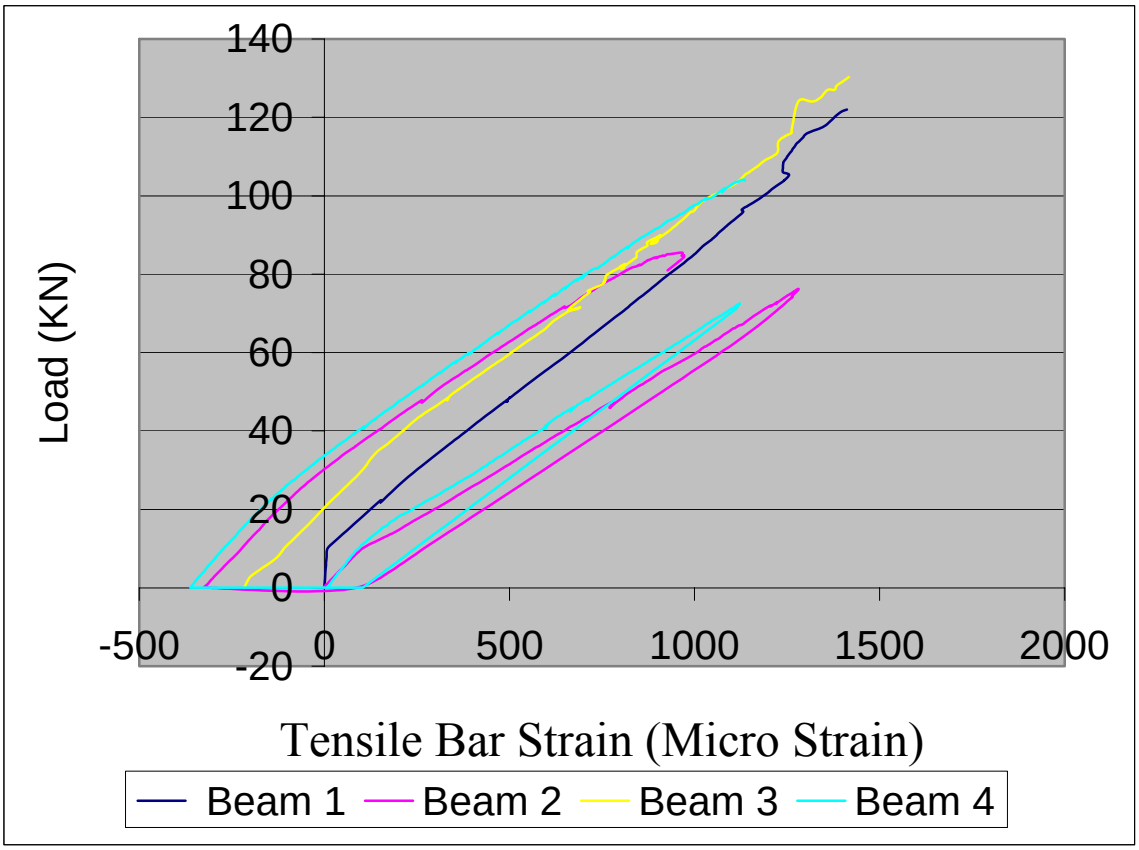

Figure 5.19: Load Vs Tensile bar strain of four beams

Figure 5.19 shows the tensile reinforcement strains for all four specimens. For the measurement of the tensile strain, steel strain gauges were placed in the middle of the beam. From the graph it can be seen that, the tensile strains at no stage yield as the beam failed in shear rather than flexure. The maximum tensile strain was around 1480 micro strain experienced by B3 and B1. Beam B2 and B4 shows the same kind of tensile strain development during preloading. Every beam shows linear development of tensile strain development before and after post-tensioning.

Beam B2 encountered about 1250 micro strain during preloading and it reduces to 120 micro strain after unloading and after application of external post-tensioning force that gives axial compression force and eventually tensile strain experienced a large decrease in tension. The same kind of curve development has been found for beam B4 during preloading and after epoxy repairing and strengthening by external post-tensioning. From the graph it is apparent that, tensile reinforcement encountered compression after application of external post-tensioning force.

5.6.2 Shear Reinforcement Strains

Shear strain development in the beam B1, B2 and B4 have been shown below. The shear strain gauge of B3 beam did not work during loading. Therefore, the shear strain development of B3 has been omitted in this section. For the purpose of shear strain measurement, two steel strain gauges had been attached at the two rear corner of shear stirrups in each beam. At the end of this section the comparison of shear strain in critical section between 3 beams have been described.

B1 Beam

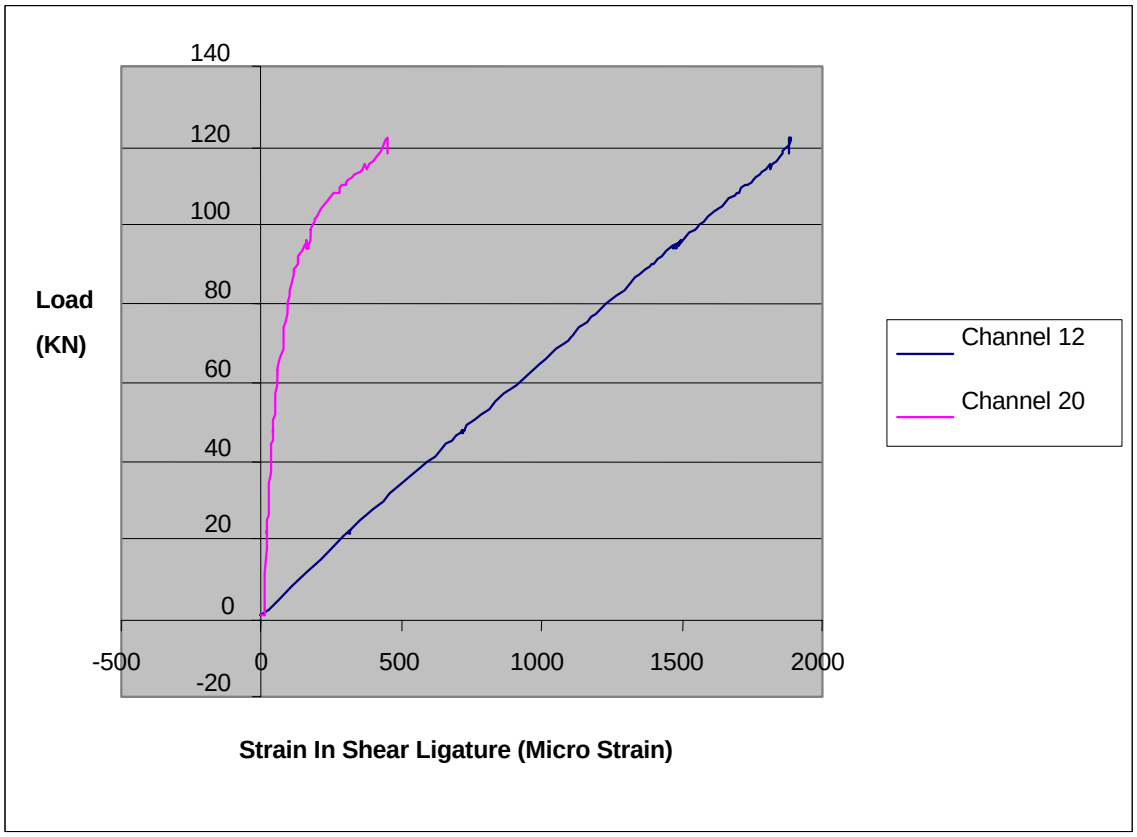

Figure 5.20: Load Vs Shear Steel Strain of Beam B1

Figure 5.20 shows the strain in the stirrup development of B1 beam with the increase of the load. Channel 12 and 20 were used for steel strain gauges. It was mentioned before that in case of B1 there was error during loading. As a result the shear stirrup gained strain prior to final loading, which gives more linear shape of curve for channel 12. Whereas, channel 20 shows different type of shear strain development. This occurs because the crack developed in the channel 12 region during the initial loading and there was no crack initiated on the channel 20 region. At ultimate loading the maximum shear strain gained was 1930 micro strain. Whereas channel 20 experienced only 584 micro strain. As a result shear crack developed in the channel 12 face.

B2 Beam

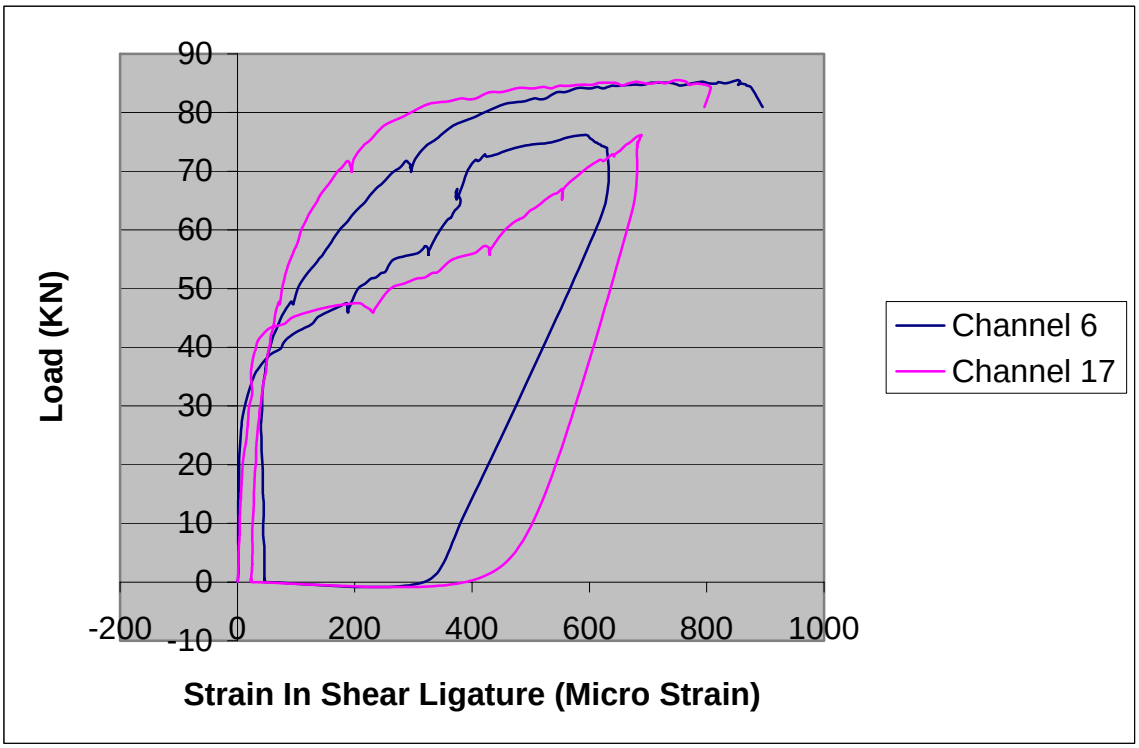

Figure 5.21: Load Vs Shear Steel Strain of Beam 2

Figure 5.21 shows the shear strain experienced by B2 during preloading and after external post-tensioning. Channel 6 and 17 shows almost the same shear strain development. During preloading the strain in the stirrup remains low up to 45 KN. It was mentioned before that the first crack was observed at 45 KN. Figure 5.20 shows that, the strain increases sharply from almost 0με to 600 με for channel 17 and 0 με to 700 micro strain at maximum preloading 75 KN. This is because after the initiations of first crack most of the load carried by the shear stirrup rather than concrete as a result shear stirrup encountered rapid increase in shear strain. During unloading shear strain reduce to 400 micro strain from 700 micro strain for channel 17 and in case of channel 6 it reduces to 350 micro strain from 600 micro strain. After the application of 100 KN external post-tension force, decrease in the shear strain occurred due to the slight recovery of deflection of the beam. As the external post-tensioning exerts axial compression force the shear strain remain near to 0 με up to 50 KN. The strain curve becomes shallower for both

channel 6 and 17 from 50 KN to 75 KN. From this point the strain increases very sharply up to 700 micro strain in case of channel 6 and 800 micro strain in channel 17. B2 beam failed in shear at the maximum loading of 86.3 KN.

B4 Beam

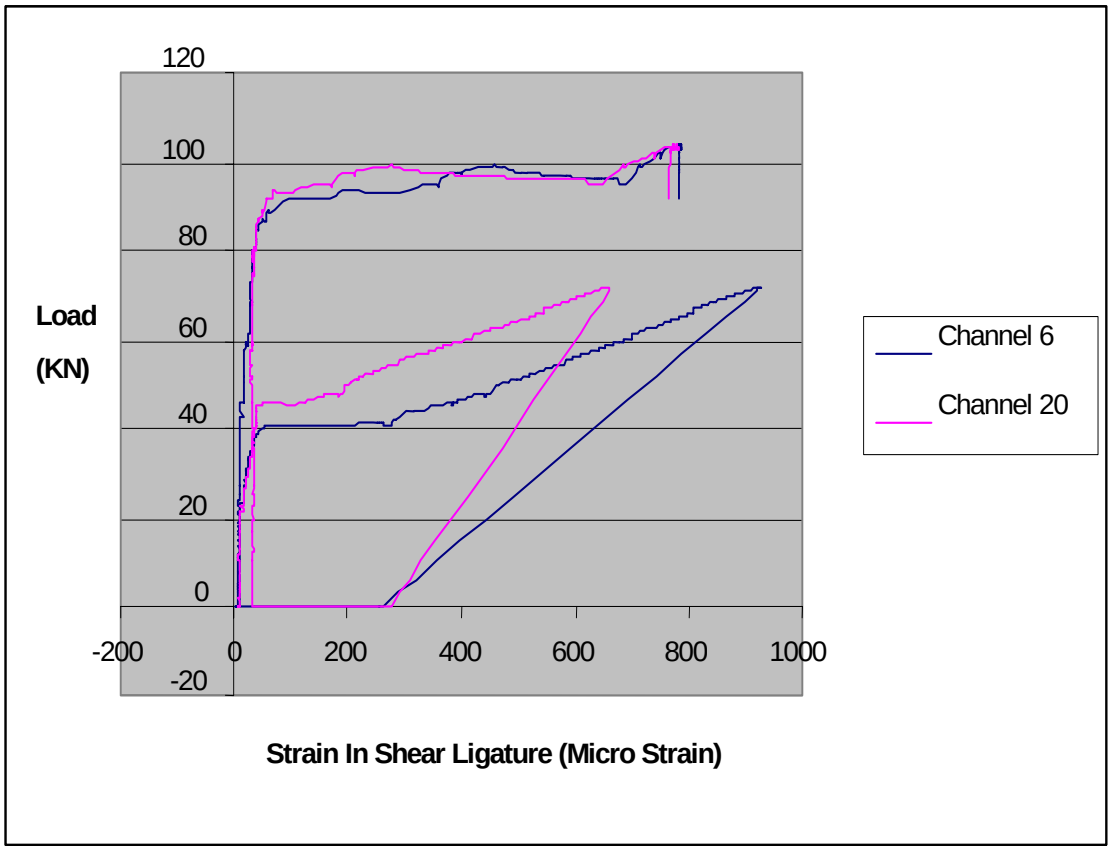

Figure 5.22: Load Vs Shear Steel Strain of Beam B4

In case of B4 channel 6 and 20 had been used to measure the strain development in the shear stirrup. During preloading both channel shows the same shape of curve although the ultimate strain was different. But after the application of epoxy and strengthening by external post-tensioning both channels shows the same strain curve development and this time ultimate strain was almost same. During preloading the maximum strain in channel 6 was 925 micro strain and channel 20 experienced 661 micro strain of shear strain. When the beam unloaded shear strain in both channels reduces to 240 micro strain. After

the epoxy treatment and strengthening by external post-tension force the strain reduces near to 0 micro strain. The shear strain curve of both channel 6 and 20 remain near to 0 micro strain up to 77 KN. As the first shear crack develops at 77 KN the rapid increase in shear strain is apparent after 77 KN of loading due to transformation of load from concrete to shear stirrup and the maximum strain is found 780 micro strain. The corresponding load is 103.95 KN.

Figure 5.23 shows the shear strain of three specimens in the critical section. The ultimate shear strain of B1, B2 and B4 are 1930 micro strain, 800 micro strain and 780 micro strain respectively. It is apparent that B2 and B4 beams encountered lower shear strain before crushing comparing to control beam B4.

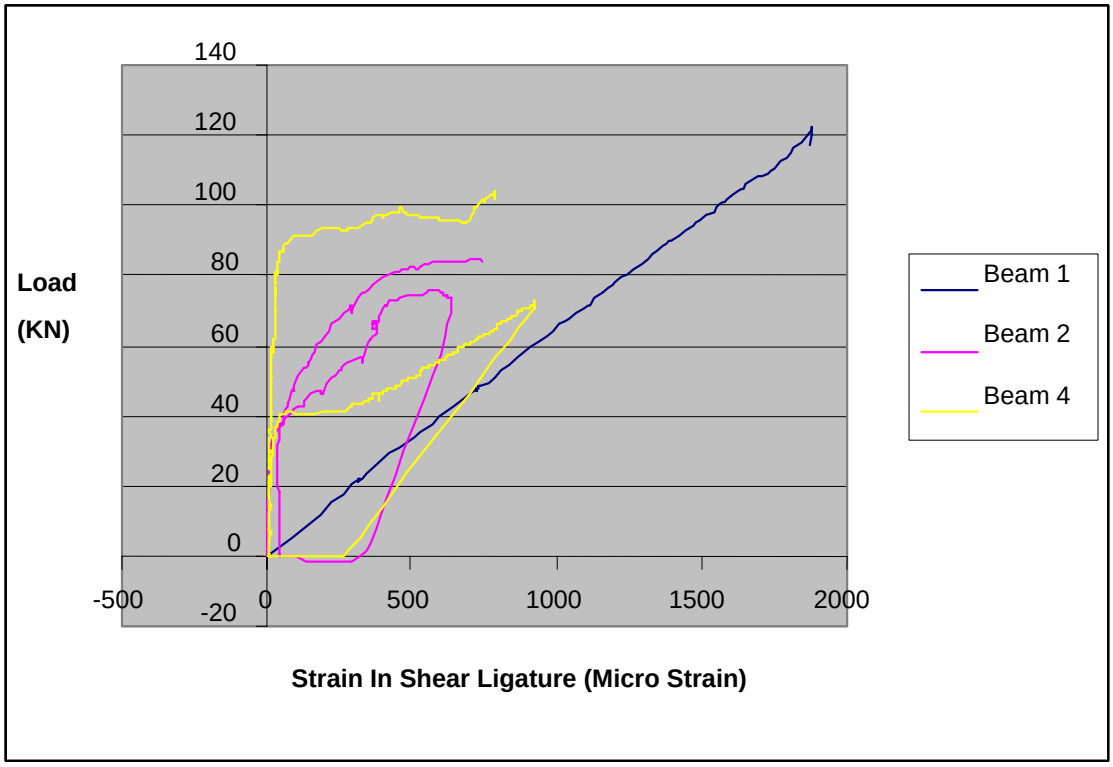

Figure 5.23: Comparison of Shear strain in 3 beams in critical section

It is observed from the graph that, the application of external post-tension force and epoxy reduces the shear strain of the beam stirrup. The shear strain in B2 beam is less than B4 beam; this is because the concrete strength of B2 is higher than B1.

5.7 Stresses in External Rods

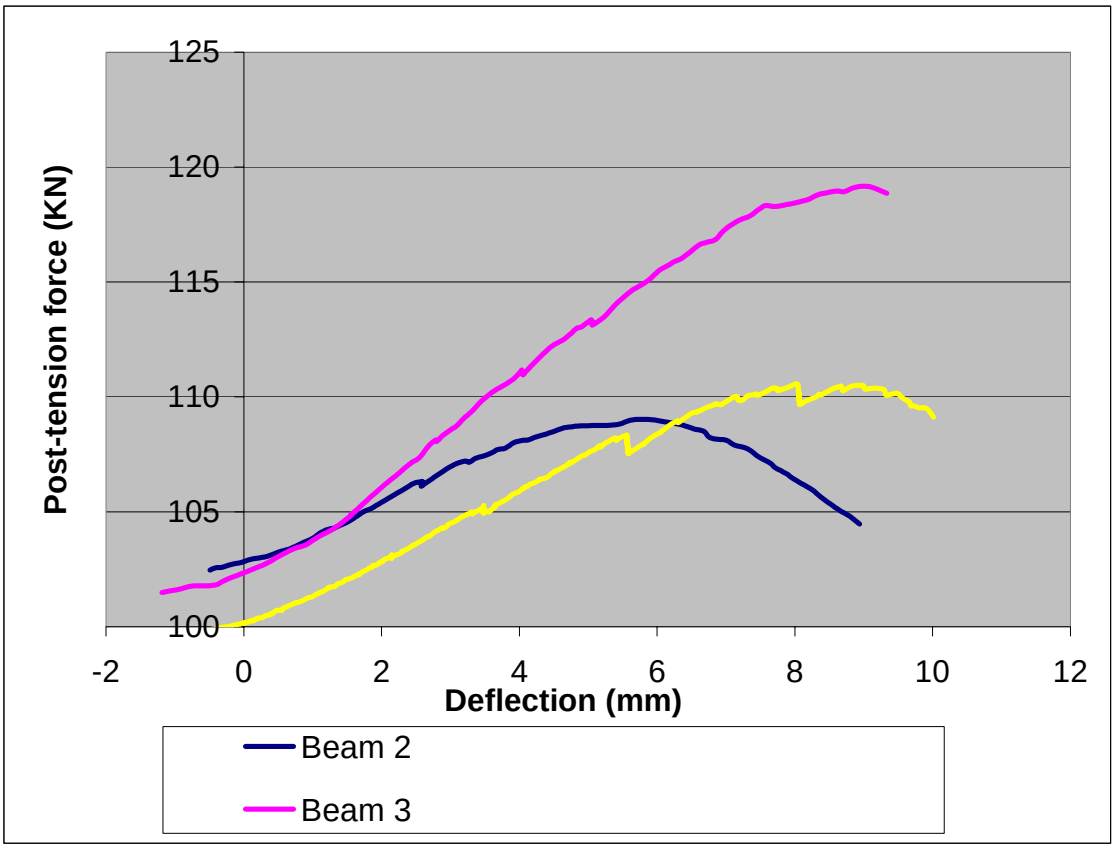

Figure 5.24: Increase in post-tensioning force against deflection

Figure 5.24 shows the effect of deflection during loading of post-tensioning force on B2, B3 and B4 beams. As post-tensioned force produce upward deflection 3 beams encountered negative deflection. From the above graph it is obvious that, with the increase in the deflection of the beam post-tension force increases. This is because when beams deflect during loading, extension in the external rods occurs. These gives change in eccentricity of the external rod and hence increase in post-tensioning force. From the above graph it can be seen that B3 beam shows higher gradient than B2 and B4 beams. This means, increase in tendon forces occurs faster at higher deflections.

Figure 5.25 shows the post-tension force increase with the increase of applied force. From the graph it can be concluded that, with the increase of load the external post-tension force also increases. As the increase in the loading causes increase in the deflection, which gives higher post-tension force.

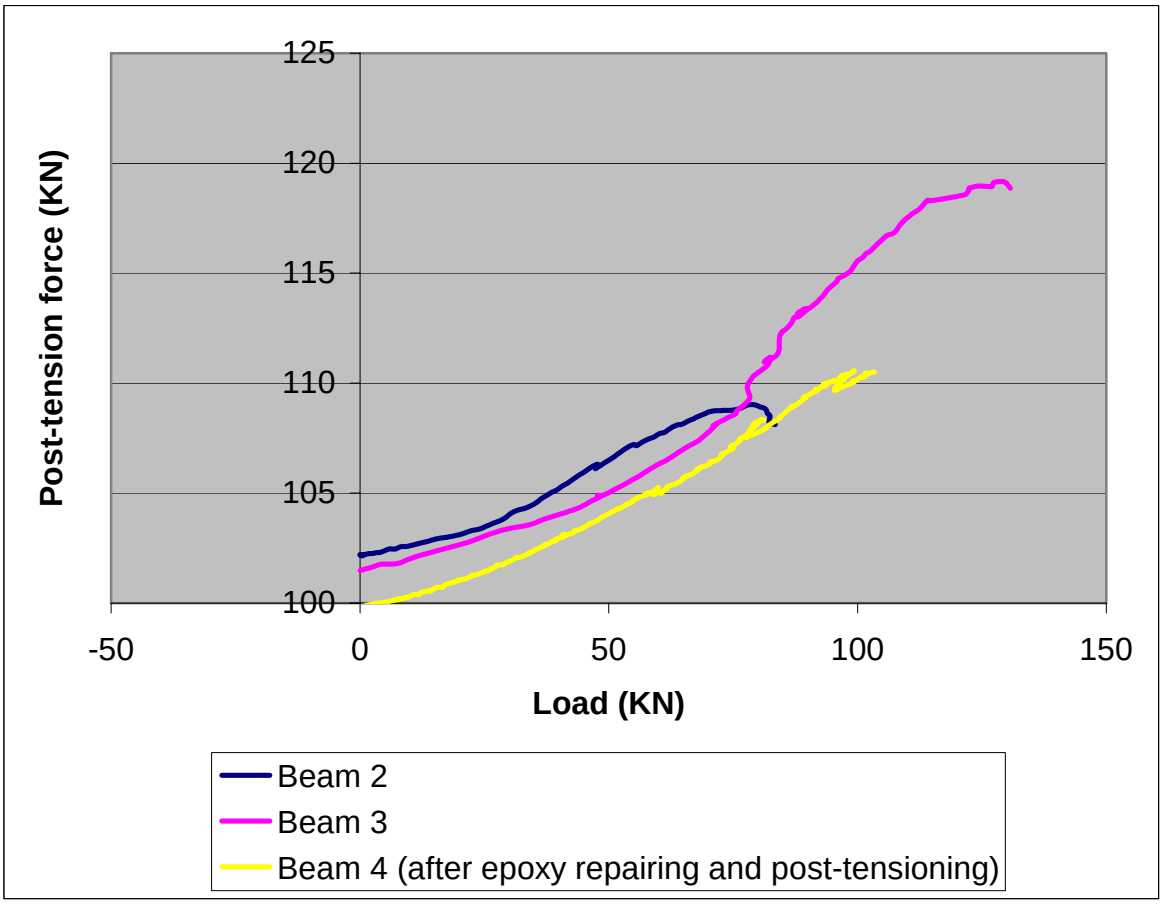

Figure 5.25: Increase in post-tensioning force against applied load

Therefore, for the same initial post-tensioning force, it can be concluded that, higher the deflection of the beam, higher the post-tension force. Below Table 5.3 shows tendon stresses of 3 beams and these results are compared to those predicted using AS3600. From table 5.3 it is clear that, the actual stresses in the external rods is much lower than the predicted stresses. Because the tendon stress according to AS3600 is based on ultimate moment capacity, which is higher load than that encountered due to ultimate shear.

Table 5.3: Comparison of external rod stress

		Predicted	Actual	
Beam No	fpe	fpe	fpe	% Below
	(MPa)	(MPa)	(MPa)	Predicted
2	248.68	332.21	273.05	17.8
3	248.68	332.21	298.42	10.2
4	248.68	332.21	283.5	14.67

5.8. Comparison of Result with result getting from using general formula considering Web-Shear Crack and AS3600 Prediction Equation.

5.8.1 Type of cracking:

Three types of cracking commonly identified in concrete beams at overload. These are flexure cracks; flexure-shear cracks and web shear cracks. Figure 5.25 shows different types of cracking.

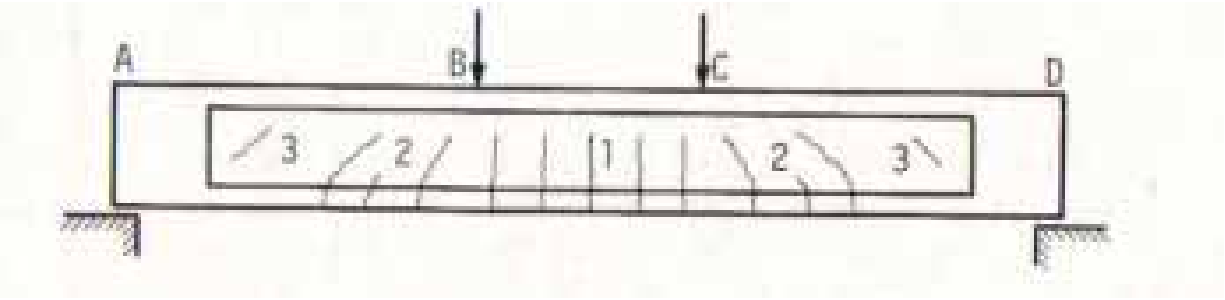

Figure 5.26: Types of cracking (Source: Faulkes et al., 1979)

Here, type 1 represents flexure crack; type 2 represents flexure-shear crack and type 3 represent web-shear crack. In this particular investigation all 4 beams have failed in

shear-compression as failure occurs by crushing of the compressive concrete and it occurs before the full flexural moment capacity.

5.8.2 Calculation of Shear Capacity Using General Formula considering Web-Shear crack:

The general formula for the shear stress in a homogeneous beam is:

$$\tau = (V \times Q)/ (I \times b) \quad (5.11)$$

Where,

V = total shear at the section considered

Q = statical moment about the neutral axis of that of that portion of cross-section lying between a line through the point in question parallel to the neutral axis and nearest face, upper or lower, of the beam

I = moment of inertia of cross section about the neutral axis

b = width of the beam at the given point

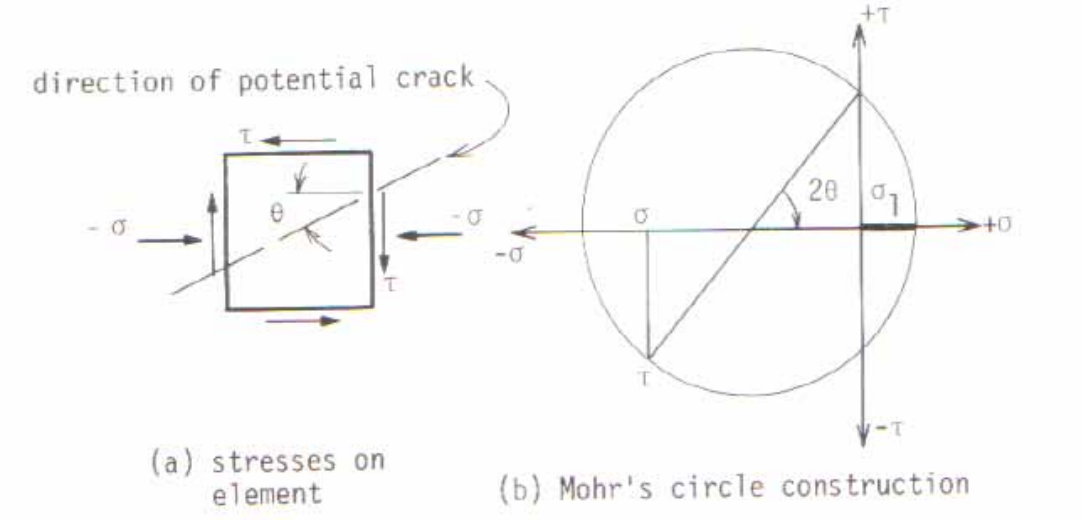

Figure 5.26: Mohr's circle construction for principal stresses.
(Source: Faulkes et al., 1979)

Figure 5.26 describes the Mohr's circle considering potential crack.

From the Mohr's Circle,

Principal tensile stress, $\sigma_1 = ((\sigma/2)^2 + \tau^2)^{0.5} + (\sigma/2)$ (5.12)

Where,

σ = Direct stress

τ = Shear stress

Below the shear capacity calculations of three post-tensioned beams considering web-shear crack have been described.

B2 Beam

Area of the beam, A = 25000 mm^2

Moment of inertia, I = 130.21 x 10^6 mm^4

Self weight of the beam, w = 0.6 KN/m

Prestressing force, P = 100 KN

Concrete strength, f'_c = 24 MPa

Web-shear cracking is assumed to occur when the principal tensile stress reaches 0.33 $(f'_c)^{0.5}$ = 0.33 $(24)^{0.5}$ =1.62 MPa. Near the support the bending moment is very small and the principal tension at the centroidal axis will be greater. Denoting by V the value of the shear force for which the principal tension at the neutral axis is equal to 1.62 MPa,

Therefore,

$$\sigma = - 100 \times 10^3 / 25000 = - 4 \text{ MPa}$$

And,

$$Q = A \times y$$

$$\Rightarrow Q = 25000 \times (D/2 - d_n)$$

$$\Rightarrow Q = 25000 \times (125 - 85.41)$$

$$\Rightarrow Q = 989750 \text{ mm}^3$$

Therefore,

$$\tau = (V \times 989750) / (130.21 \times 10^6 \times 100)$$

$$\Rightarrow \tau = 7.6 \times 10\text{-}5 \text{ V}$$

So,

$$1.62 = ((-4/2)^2 + (7.6 \times 10\text{-}5 \text{ V})^2)^{0.5} + (-4/2)$$

$$\Rightarrow V = 44908 \text{ N}$$

$$\Rightarrow V = 44.908 \text{ KN}$$

So, the total load carrying capacity of the beam after web shear cracking is 44.908 x 2 KN or 89.816 KN.

B3 Beam

Area of the beam, A = 25000 mm^2

Moment of inertia, I = 130.21 x 10^6 mm^4

Self weight of the beam, w = 0.6 KN/m

Prestressing force, P = 100 KN

Concrete strength, f'_c = 36 MPa

Web-shear cracking is assumed to occur when the principal tensile stress reaches 0.33 $(f'_c)^{0.5}$ = 0.33 $(36)^{0.5}$ =1.98 MPa. Near the support the bending moment is very small and the principal tension at the centroidal axis will be greater. Denoting by V the value of the shear force for which the principal tension at the neutral axis is equal to 1.98 MPa,

Therefore,

σ = - 100 x 10^3 / 25000 = - 4 MPa

And,

Q = A x y

$\Rightarrow$ Q = 25000 x $(D/2-d_n)$

$\Rightarrow$ Q = 25000 x (125-85.41)

$\Rightarrow$ Q = 989750 mm^3

Therefore,

τ = (V x 989750)/ (130.21 x 10^6 x 100)

$\Rightarrow$ τ = 7.6 x 10-5 V

so, 1.98 = $((-4/2)^2 + (7.6 \times 10\text{-}5\ V)^2)^{0.5} + (-4/2)$

$\Rightarrow$ V = 51568.205 N

$\Rightarrow$ V = 51.57 KN

So, the total load carrying capacity of the beam considering web-shear cracking is 51.57 x 2 KN or 103.14 KN.

B4 Beam

Area of the beam, A = 25000 mm^2
Moment of inertia, I = 130.21 x 10^6 mm^4
Self weight of the beam, w = 0.6 KN/m
Prestressing force, P = 100 KN
Concrete strength, f'_c = 18 MPa

Web-shear cracking is assumed to occur when the principal tensile stress reaches 0.33 $(f'_c)^{0.5}$ = 0.33 $(18)^{0.5}$ =1.4 MPa. Near the support the bending moment is very small and the principal tension at the centroidal axis will be greater. Denoting by V the value of the shear force for which the principal tension at the neutral axis is equal to 1.4 MPa,

Therefore,

σ = - 100 x 10^3 / 25000 = - 4 MPa

And,

Q = A x y
$\Rightarrow$ Q = 25000 x (D/2-d_n)
$\Rightarrow$ Q = 25000 x (125-85.41)
$\Rightarrow$ Q = 989750 mm^3

Therefore,

τ = (V x 989750)/ (130.21 x 10^6 x 100)
$\Rightarrow$ τ = 7.6 x 10-5 V

So, 1.4 = $((-4/2)^2 + (7.6 \text{ x } 10\text{-}5 \text{ V})^2)^{0.5} + (-4/2)$

$\Rightarrow$ V = 40802.42 N

$\Rightarrow$ V = 40.8 KN

So, the total load carrying capacity of the beam considering web shear crack is 40.8 x 2 KN or 81.6 KN.

5.8.3 Calculation of Shear Strength Using AS3600

B1 Beam

According to AS3600, the ultimate shear strength (V_{uc}) of a reinforced beam, excluding the contribution of shear reinforcement, can be calculated from the following equation:

$$V_{uc} = ß_1\, ß_2\, ß3\, b_v\, d_{st}\, (A_{st}\, f'_c / b_v\, d_{st})^{1/3}$$

Where,

$$ß_1 = 1.1\,(1.6 - d_{st} / 1000) \geq 1.1$$

$\Rightarrow$ $ß_1 = 1.1\,(1.6 - 219 / 1000) \geq 1.1$

$\Rightarrow$ $ß_1 = 1.52 > 1.1$ (ok)

Again, $ß_2 = 1$ (as there is no significant axial tension and compression)

And $ß_3 = 1$;

Therefore,

$$V_{uc} = 1.52 \times 1 \times 1 \times 100 \times 219\,(628.32 \times 25 / 100 \times 219)^{1/3}$$

$\Rightarrow$ $V_{uc} = 29.8$ KN

According to AS3600 Clause 8.2.2 the design shear strength of a beam shall be taken as ϕV_u where

$V_u = V_{uc} + V_{us}$

Where,

V_{us} = Shear resisted by the stirrups

Now calculating the maximum shear strength resisted by the shear reinforcement in accordance to AS3600 Clause 8.2.10:

$V_{us} = (A_{sv}\, f_{sy,f}\, d_{st}/s)\, cot\theta_v$

$A_{sv} = 2(\pi \times 3^2)$

$\Rightarrow A_{sv} = 56.55\ mm^2$

And, $A_{sv,\,min} = 0.35 \times b \times s / f_{sy,f}$

$\Rightarrow A_{sv,\,min} = 0.35 \times 100 \times 250 / 250$

$\Rightarrow A_{sv,\,min} = 35\ mm^2$

Again, $A_{sv,\,max} = b \times s\ (0.2\, f'_c - (V_{uc}/bd_{st})) / (f_{sy,f})$

$\Rightarrow A_{sv,\,max} = 100 \times 250\ (0.2 \times 25 - (29.8/(100 \times 219\ ))) / (250)$

$\Rightarrow A_{sv,\,max} = 499.86\ mm^2$

And,

$\theta_v = 30° + 15°\ [(56.55 - 35)/ (499.86 - 35)]$

$\Rightarrow \theta_v = 30.7° \geq 30°$ (ok)

So, the ultimate shear strength by shear reinforcement in the beam, V_{us}

$V_{us} = (56.55 \times 250 \times 219/250)\, cot 30.7°$

$\Rightarrow V_{us} = 20.86$ KN

So the ultimate shear strength of the rectangular beam is the shear resisted by the concrete at maximum plus the shear resisted by the stirrups:

$$V_u = V_{uc} + V_{us}$$

$$\Rightarrow \quad V_u = 29.8 + 20.86$$

$$\Rightarrow \quad V_u = 50.66 \text{ KN}$$

Therefore, the maximum load can be applied on the beam is 2 x 50.66 or 101.32 KN. (As four point loading is adopted)

Beam 1 was failed in shear compression at 122 KN. It can be seen from the comparison that the predicted shear capacity of the beam is 18.4% less than the tested value. This means AS3600 underestimate the shear capacity of the beam and the tested shear capacity of the beam is moderate comparing to results obtained by using AS3600 formula. The beam was cured and compacted in a controlled environment (i.e. in laboratory) and there was minimal error of detailing of shear reinforcement as well as the spacing of the ligatures was almost accurate. Which are the main reasons for difference results.

B2 Beam

The area of the post-tensioning steel is:

$$A_{pt} = 2(\pi \times 8^2)$$

$$\Rightarrow \quad A_{pt} = 402.12 \text{ mm}^2$$

And concrete strength, f'c = 24 MPa

Using equation 2.13 the decompression moment, M_{dec} can be calculated for the section.

So,

$$M_{dec} = [\, P/A_g + Pey_b / I_g \,]\, I_g / y_b$$

Where,

P = External post-tension force = 100 KN

A_g = area of the rectangular beam = 250 x 100

= 25000 mm2

e = eccentricity = 40 mm

y_b = distance from centroidal axis to bottom fibre

= 125 mm

I_g = second moment of area of the cross-section about the centroidal axis = $bd^3/12$

$\Rightarrow$ I_g = (100 x 250^3) /12

$\Rightarrow$ I_g = 130.21 x 10^6 mm^4

Therefore,

M_{dec} = [(100 x10^3/ 25000) + (100 x 10^3 x 40 x125)/ (130.21 x 10^6)] (130.21 x 10^6)/ 125

= 8.1667 KN-m

Now the shear force (V_{dec}) which would occur at the section when the bending moment at that section was equal to the decompression moment (M_{dec}) can be evaluated using equation:

V_{dec} = *Mdec / (M*/V*)*

[For simply supported conditions and *M*/N** is the ratio of bending moment and shear force at the section under consideration, due to same design loading.]

Here,

M_{dec} = 8.1667 KN-m

*M** = 90.14 KN-m

*V** = 101.6KN

$\Rightarrow$ V_{dec} = 8.1667 / (90.14/101.6)

$\Rightarrow$ V_{dec} = 9.2 KN

And the ultimate contribution of the shear strength by the concrete at ultimate and the external post-tensioning is:

$$V_{uc} = 1.52 \text{ x } 1 \text{ x } 1 \text{ x } 100 \text{ x } 219 \left((628.32 + 402.12)\, 24 / (100 \text{ x} 219)\right)^{1/3} + 9.2 + 0$$

$$\Rightarrow \quad V_{uc} = 43.86 \text{ KN}$$

The total shear capacity of this externally post-tensioned girder from equation 2.11 is:

$$V_u = V_{uc} + V_{us}$$

$$\Rightarrow \quad V_u = 43.86 + 20.72.$$

$$\Rightarrow \quad V_u = 64.58 \text{ KN}$$

So the maximum load carrying capacity of the girder using AS3600 is 64.58 x 2 or 129.16 KN and the actual value achieved through testing was 86.3 KN. The main reason is the shear strength of the specimen was calculated considering no cracks in the beam. But the beam was strengthened by external prestressing after preloading of 75 KN and initiating cracks. The decrease in shear cracks is also due to aggregate interlock, which states that after formation of initial crack some shear force carried by shear stresses in the intact compressive concrete above the cracks and some transfer of shear force occurs by bearing and friction across the jagged faces of the cracks.

B3 Beam

The area of the post-tensioning steel is:

$$A_{pt} = 2(\pi \times 8^2)$$

$$\Rightarrow \quad A_{pt} = 402.12 \text{ mm}^2$$

Concrete strength, $f'c = 36$ MPa

Using equation 2.13 the decompression moment, M_{dec} can be calculated for the section.

So,

$M_{dec} = [\ P/ A_g + Pey_b / I_g\ ]\ I_g/ y_b$

Where,

P = External post-tension force = 100 KN

A_g = area of the rectangular beam = 250 x 100

= 25000 mm2

e = eccentricity = 40 mm

y_b = distance from centroidal axis to bottom fibre

= 125 mm

I_g = second moment of area of the cross-section about the centroidal axis = $bd^3/12$

$\Rightarrow \quad I_g = (100 \text{ x } 250^3) /12$

$\Rightarrow \quad I_g = 130.21 \text{ x } 10^6 \text{ mm}^4$

Therefore,

$M_{dec} = [(100 \text{ x}10^3/ 25000) + (100 \text{ x } 10^3 \text{ x } 40 \text{ x}125)/ (130.21 \text{ x } 10^6)]\ (130.21 \text{ x } 10^6)/ 125$

$= 8.1667$ KN-m

Now the shear force (V_{dec}) which would occur at the section when the bending moment at that section was equal to the decompression moment (M_{dec}) can be evaluated using equation:

$V_{dec} = Mdec / (M^*/V^*)$

[For simply supported conditions and M^*/N^* is the ratio of bending moment and shear force at the section under consideration, due to same design loading.]

Here,

M_{dec} = 8.1667 KN-m

M^* = 114 KN-m

V^* = 110 KN

$\Rightarrow \quad V_{dec} = 8.1667 / (114/110)$

$\Rightarrow \quad V_{dec} = 7.88$ KN

And the ultimate contribution of the shear strength by the concrete at ultimate and the external post-tensioning is:

$V_{uc} = 1.52 \times 1 \times 1 \times 100 \times 219 ((628.32 + 402.12)\ 36 / (100 \times 219))^{1/3} + 7.88 + 0$

$\Rightarrow \quad V_{uc} = 47.56$ KN

The total shear capacity of this externally post-tensioned girder from equation 2.11 is:

$V_u = V_{uc} + V_{us}$

$\Rightarrow \quad V_u = 47.56 + 22$

$\Rightarrow \quad V_u = 69.56$ KN

So the maximum load can be applied on the girder according AS3600 is 69.56 x 2 or 139.12 KN and the actual value achieved through testing was 130.3 KN. The beam was experienced premature failure due to low cover and small section and as a result the load carrying capacity of the beam was reduced.

B4 Beam

The area of the post-tensioning steel is:

$A_{pt} = 2(\pi \times 8^2)$

$\Rightarrow \quad A_{pt} = 402.12\ mm^2$

Concrete strength, $f'c = 18$ MPa

Using equation 2.13 the decompression moment, M_{dec} can be calculated for the section.

So,

$$M_{dec} = [\, P/ A_g + Pey_b / I_g \,] \, I_g / y_b$$

Where,

P = External post-tension force = 100 KN

A_g = area of the rectangular beam = 250 x 100

= 25000 mm2

e = eccentricity = 40 mm

y_b = distance from centroidal axis to bottom fibre

= 125 mm

I_g = second moment of area of the cross-section about the centroidal axis

$= bd^3/12$

$\Rightarrow \quad I_g = (100 \text{ x } 250^3) /12$

$\Rightarrow \quad I_g = 130.21 \text{ x } 10^6 \text{ mm}^4$

Therefore,

$M_{dec} = [(100 \text{ x}10^3/ 25000) + (100 \text{ x } 10^3 \text{ x } 40 \text{ x}125)/ (130.21 \text{ x } 10^6)] (130.21 \text{ x } 10^6)/ 125$

$= 8.1667$ KN-m

And, the shear force (V_{dec}) which would occur at the section when the bending moment at that section was equal to the decompression moment (M_{dec}) can be evaluated using equation:

$$V_{dec} = Mdec / (M^*/V^*)$$

[For simply supported conditions and M^*/N^* is the ratio of bending moment and shear force at the section under consideration, due to same design loading.]

Here,

M_{dec} = 8.1667 KN-m

M^* = 76.24 KN-m

V^* = 91.41 KN

$\Rightarrow \quad V_{dec} = 8.1667 / (76.24/91.41)$

$\Rightarrow \quad V_{dec} = 9.8$ KN

And the ultimate contribution of the shear strength by the concrete at ultimate and the external post-tensioning is:

$V_{uc} = 1.52 \times 1 \times 1 \times 100 \times 219 ((628.32 + 402.12)\ 18 / (100 \times 219))^{1/3} + 9.8 + 0$

$\Rightarrow \quad V_{uc} = 41.29$ KN

The total shear capacity of this externally prestressed girder from equation 2.11 is:

$V_u = V_{uc} + V_{us}$

$\Rightarrow \quad V_u = 41.29 + 19$

$\Rightarrow \quad V_u = 60.29$ KN

So the maximum load can be applied on the girder according to AS3600 is 60.29 x 2 or 120.58 KN and the actual value achieved through testing was 103.95 KN. Due to low cover and small section the B4 beam experienced premature failure and as a result the actual value obtained from testing was much lower than expected value according to AS3600.

5.9 Summary

Table 5.4 shows a summary of predicted values according to AS3600 and general formula and the actual value achieved through testing.

Table 5.4 Summary of predicted values and actual value achieved after testing

Beam No	Post-tension load (KN)	Preload (KN)	Epoxy	Shear Capacity		
				General Formula (KN)	AS 3600 (KN)	Tested Value (KN)
1	0	0	X	X	101.32	122
2	100	75	X	89.816	129.16	86.3
3	100	X	X	103.14	139.12	130.3
4	100	72.3	√	81.6	120.58	103.95

It can be seen from the table that the predicted value of the control beam B1 is much less than predicted value according to AS3600. The main reason is the tested specimen is cured and compacted in controlled environment (i.e. in laboratory). One other aspect is that there is minimal possibility of error during detailing.

It is apparent from the table that after post-tensioning with or without preloading the predicted values according to AS3600 are much higher than ultimate shear capacity of the beams. This means AS3600 over-estimate the shear capacity of the beam after external post-tensioning. Beam B2 gave 33% less strength than predicted strength according to AS3600 and also B3, B4 gave 6.3% and 17.8% less strength respectively.

The result obtained considering the web shear cracking during loading gave much accurate result in case of B2 as it showed web-shear cracking after post-tensioning. Beam B3 was strengthened by post-tensioning without initiating any crack by preloading and therefore gave higher shear strength comparing to predicted value using general formula. In case of B4 beam the web-shear crack was repaired by epoxy, later strengthened with post-tensioning and it showed no existence of cracking during loading. As a result it gave higher ultimate strength than predicted strength using general formula.

5.10 Conclusion

From the above discussion and analysis it can be said that although external post-tensioning with epoxy repairing does not give the same strength as expected but it increases the serviceability reducing the deflection of the beam and above all shear strength of the beam.

Analysing the B2 beam it can be concluded that the effectiveness of the external post-tension force depend largely on the extent of the crack development. Having mentioned that, it was found that B2 beam, gave much less strength after post-tensioning comparing to predicted shear strength with post-tensioning and without post-tensioning.

CHAPTER 6

CONCLUSION

6.1 Achievement of Objectives

By completion of this project all the objectives have been thoroughly achieved. They are given as follows:

- Review the background information relating to epoxy repaired girders shear strengthened with external post-tensioning. Very few information is available concerning strengthening shear capacity of epoxy-repaired girders with external post-tensioning. Therefore available information on epoxy and external post-tensioning has been studied separately. Chapter 1 and 2 gives relevant information about historical development, the related researches had been done in past with some idea about advantages, disadvantages, application and technical features of external post-tensioning and epoxy.

- Design model beams for conducting experimental investigations and calculate the critical external post-tension forces to be used. In Chapter 3 the design of the specimens and the calculations of the external post-tension forces have been derived. The design consideration and selection of the adopted post-tensioning forces have been included in this particular chapter. Moreover, the ultimate shear capacity of the test specimen with and without external post-tension forces has been studied.

- Preparation of designed model beams and testing of specimen. Chapter 4 gives detail information about preparation of designed specimen and description of construction process from the initial formation of reinforcing cage to curing of the

specimens. In addition, it gives brief ideas about the adopted testing process and equipment that have been used during testing.

- Critically evaluate and analyse the data obtained as a result of specimen testing. The results are discussed and analysed in detail in Chapter 5. The results have been compared with the predicted result obtained using AS3600 and formula considering web-shear cracking.

6.2 Conclusion

This particular project was conducted to find the effect of the external post-tension forces on shear strength of girders repaired with epoxy. After the completion of this project it gives some interesting outcomes. As a result, a number of conclusions can be drawn based on this experimental investigation.

From the result obtained after testing, it can be concluded that for the shear strengthening of girders external post-tensioning in combination of epoxy repairing is a useful technique. Crack repairing by epoxy can restore the strength of the beam whereas external post-tension force increases the stiffness and decrease the deflections of the beam. As a result improves the ultimate shear strength capacity of the girders.

Analyzing the test results of B2 beam it can be said that, the effectiveness of the strengthening of beams by post-tension forces depends on the shear crack formation and size of the existing crack. The result obtained from B2 beam is far lower than expected value after strengthening of external post-tensioning and it also gave much lower value comparing to the ultimate strength of the control beam. This proves the point that, crack formation influences the ultimate shear strength of the girder, strengthened with external post-tensioning.

Premature failure occurs in four tested beams due to low cover and small section. The final crack pattern of every beam was similar to each other. The compression and shear

reinforcement opened up after final cracking. From the load Vs crack width diagram it was observed that, crack propagated very rapidly after formation of certain width of fracture. This indicates that, due to low cover and small section crack propagated very quickly and as a result the shear strength capacity of the girders reduced.

Comparing the test results of three external post-tensioned beams with predicted results obtained from AS3600 it is apparent that, AS3600 over-estimate the shear capacity after strengthening. Crack was initiated early and propagated rapidly due to low cover and small section. After the initiation of the crack most of the load is carried by shear reinforcement and thus shear strength reduces. As a result the tested value gives much lower value than predicted results according to AS3600 equation.

6.3 Recommendations for further Studies

This project gave some unexpected results. To investigate the actual reasons for these unanticipated outcome further studies should be carried out in the area of shear strengthening of not only girders but also concrete members on the whole. The recommended further studies are mentioned below:

- The shear strength of the girders was reduced due to premature failure. Section dimension can be increased and adequate cover can be adopted to prevent the premature failure and to check the effect of epoxy repairing on shear strengthened of girders with external post-tensioning.

- More investigations should be carried out to find the actual effect of external post-tensioning technique on the shear strengthening of concrete structures and to verify the tested data with the predicted result according to AS3600.

- Further study should be carried out to check the effect of strengthening on deteriorated structures. B2 beam shows unexpected results after the strengthening

of the beams. The ultimate load after applying external post-tensioning was found much lower than the final load of control beam.

- Further research about shear performance of reinforced concrete sections strengthening with fiber composites can also be carried out to examine new technique for strengthening of deteriorated concrete structure.

- It is suggested that, the concrete strength of all testing specimen should be same or near to each other. The concrete strength influences the shear capacity and the ultimate capacity of the specimens. Therefore, to compare the strength capacity of specimens the same concrete strength specimens gives more accurate results.

REFERENCES:

Burns, N.D., Charney, F.A., & Vines, W.R. 1978, 'Tests of one way Post-tensioned slabs with unbonded Tendons.' *Journal*, Prestressed Concrete Institute, vol. 23, No. 5, September-October, pp. 66-83

Burns, N.H.1990, 'Post-tension force changes in Continuous Beams.' *ASCE Structures Congress Abstracts*, ASCE, New York, pp. 455-456

Burns, N. H., Helwig, T., & Tsujimoto.1991, 'Effective Prestress Force in Continuous Post-tensioned Beams with Unbonded Tendons.' ACI Structural Journal, January-February, vol. 88, No. 1, pp. 84-90

Burns, N.H., & Pierce, D.M. 1967, 'Strength and Behaviour of Prestressed concrete members with Unbonded Tendons.' *Journal*, Prestressed Concrete Institute, vol. 12, No. 5, October, pp. 15-29

Cady, P.D. 1994, 'Sealers for Portland Cement Concrete Highway Facilities.' National Cooperative Highway Research Program Synthesis 209, TRB, *National Research Council*, Washington, DC, pp.

Chabbra, Y.2004, 'Bridge Rehabilitation Techniques.' D S Brown Company, viewed 5th August 2004, <http://www.dsbrown.com>

Celebi, M.1988, 'Research on Epoxy Repaired Reinforced Concrete Beams.' viewed 5th September 2004, <Source: http://www.compendex.com/ASCE/ Journal.html>

David, P.B. 2004, 'Historical Perspective on Prestressed Concrete.' *PCI Journal*, January-February, vol. 49, No. 1, pp. 14-30

Dunker, K.F., Klaiber, F.W., & Sanders, W.W. 1987, 'Methods of Strengthening Existing Highway Bridges.' *NCHRP Research Report No. 293*, Transportation Research Board, Washington, D.C., September, pp. 114

Epoxy, 2001, 'Epoxy Manufacture and Supply, organization.' *Epoxy Manufacturing Incorporation*, viewed 10th April 2004, <http://www.epoxy.com>

Faulkes, K.A., & Warner, R.F. 1979, 'Prestressed Concrete.' *Pitman Publishing Pty Ltd*, Victoria, Australia

French, C.W., Thorp, G.A., & Tsai, W.J.1990, 'Epoxy Repair for Moderate Earthquake Damage.' *ACI Structural Journal*, July-August, vol. 87, No. 4, pp. 416-424

Goldberger, H.W. 1961, 'Corrective Measures Employing Epoxy Resins on Concrete Bridge Decks.' *Highway Research Board*, National Academy of Sciences, National Research Council, vol. 40, Washington, DC, 1961, pp. 489 – 496

Hall, A.S., Faulkes, K.A., Rangan, B.V., & Warner, R.F. 1998, 'Concrete Structures.' *Addison Wesley Longman Australia Pty Limited*, South Melbourne, Australia

Harajli, M. H. 1993, 'Strengthening of Concrete Beams by External Prestressing.' *PCI Journal*, vol. 38, No. 6, pp. 76-88

Harajli, M. H. 1990, 'Effect of Span-Depth Ratio on the Ultimate Steel Stress in Unbonded Prestressed Concrete Members.' *PCI Journal*, vol. 87, No. 3, pp. 204-312

Harajli, M. H., & Hijazi, S.A 1991, 'Evaluation of the Ultimate Steel Stress in Partially Prestressed Concrete Members.' *PCI Journal*, vol. 36, No. 1, pp. 62-82

Harajli, M. H., Khairallah, N., & Nassif, H. 1999, 'Externally Prestressed Members: Evaluation of Second Order Effects.' *ASCE Journal of Structural Engineering*, October, vol. 125, No. 10, pp. 1151-1161

Khalifa, A., Gold, W.J., & Nanni, A. 1998, 'Contribution of Externally bonded FRP to Shear Capacity of RC Flexural members.' Journal of Composites for Construction, vol. 2, No. 4, November, pp. 195-202

Klaiber. F. W, Dunker, K.F., & Sanders, W.W.1989, 'Strengthening of Existing Bridges (simple and continuous span) by post-tensioning.'*ACI SP*, Pros. Int. Symp. A.E Naaman and J. E Breen, Eds. American Concrete Institute (ACI) Detroit, vol. 120, No. 10, pp. 207-228

Miyamoto, A., & Nakamura, H. 1997. 'Application of prestressing technique with external tendons to existing bridge strengthening.' *Proc., Int. Conf. on Rehabilitation and Devel. of Civ. Engrg. Infrastructure Sys*, M. Harajli and A. Naaman, eds, American University of Beirut, Beirut, Lebanon, 2, pp. 242–255.

Muller, J.M. 1980, 'Long Span Concrete Segmental Bridges.' *Annuals of the New York Academy of Sciences*, vol. 352, pp. 123-131

N.A. 2003, CIV3506-Concrete Structures, STUDY BOOK, *Distance Education Center*, USQ, Toowoomba, Australia.

NAHB Research Center. 2002, 'Testing and Assessment of Epoxy Injection Crack Repair For Residential Concrete Stem Walls and Slabs-On-Grade.' Prepared for Consortium of Universities for Research in Earthquake Engineering, July, Richmond, CA

Neale, K.W., & Proulx, J. 1997, 'Proceedings of the 1997 Annual Conference of Canadian Society for Civil Engineering Part 4 (of 7).' *Proceedings-Annual Conference-*

Canadian Society for Civil Engineering, Second Symposium on Applied Mechanics Structures: Seismic Engineering, vol. 4, pp. 428

Pisani, M.A. 1999, ‘ Strengthening by means of External Prestressing.’ *Journal of Bridge Engineering*, May, vol. 4, No. 2, pp. 131-135q

Pisani, M.A., & Nicoli, E. 1996, ‘Beams Prestressed with Unbonded at Ultimate.’ Canadian Journal of Civil Engineering, vol. 23, No. 6, December, pp. 1220-1230

Rabbat, B.G., & Sowlat, K.1987, ‘Testing of Segmental Concrete Girders with External Tendons.’ *PCI Journal*, vol.32, No.2, pp. 86-107

Snelling, G. 2003 ‘The Shear Strengthening of Bridge Headstocks Using External Prestressing’, *Undergraduate Dissertation*, October, University of Southern Queensland (USQ), Australia.

Standards Australia. 2003, ‘Australia Standards for Civil Engineering Students.’ Part 2, Standards Australia International, Australia.

Taiwan Earthquake Report, 1995, ‘Bridge Performance’, viewed 10th September 2004, < http://www.structures.ucsd.edu/taiwaneq.html>

Tan, K.H., Farooq, A., & Ng, C. K. 2001, ‘Behaviour of Simple Span Reinforced Concrete Beams Locally Strengthened with External Tendons’ *ACI Structural Journal*, vol. 98, No. 2, March-April, pp. 174-183

Tan, K.H., & Ng, C. K. 1998, ‘Effect of Shear in Externally Prestressed Beams’ *ACI Structural Journal*, vol. 95, No. 2, March-April, pp. 116-128

Tan, K.H., & Ng, C. K. 1997, 'Effect of Deviators and Tendon Configuration on Behavior of Externally Prestressed Beams.' *ACI Structural Journal*, vol. 94, No. 1, pp. 13-22

VSL, 2000, 'VSL Structural Group', *VSL Strengthening Products*, viewed 5th August 2004, <http://www.vsl.net>

VSL Report. 1999, 'Design Considerations VSL External Tendons examples from practice.' *VSL Report Series*, VSL International Ltd.

Warner, R.F., Rangan, B.V., Hall, A.S. & Faulkes, K.A.1998, Concrete Structures. Addison Wesley Longman Australia Pty Ltd, Melbourne.